



<https://theses.gla.ac.uk/>

Theses Digitisation:

<https://www.gla.ac.uk/myglasgow/research/enlighten/theses/digitisation/>

This is a digitised version of the original print thesis.

Copyright and moral rights for this work are retained by the author

A copy can be downloaded for personal non-commercial research or study,  
without prior permission or charge

This work cannot be reproduced or quoted extensively from without first  
obtaining permission in writing from the author

The content must not be changed in any way or sold commercially in any  
format or medium without the formal permission of the author

When referring to this work, full bibliographic details including the author,  
title, awarding institution and date of the thesis must be given

Enlighten: Theses

<https://theses.gla.ac.uk/>  
[research-enlighten@glasgow.ac.uk](mailto:research-enlighten@glasgow.ac.uk)



**UNIVERSITY**  
*of*  
**GLASGOW**

**Constructing a Recombinant Model of the Human Pyruvate  
Dehydrogenase Complex**

Audrey Elaine Brown BSc.

This thesis is presented for the degree  
Doctor of Philosophy  
May 2002

Institute of Biomedical and Life Sciences  
University of Glasgow

ProQuest Number: 10647102

All rights reserved

INFORMATION TO ALL USERS

The quality of this reproduction is dependent upon the quality of the copy submitted.

In the unlikely event that the author did not send a complete manuscript and there are missing pages, these will be noted. Also, if material had to be removed, a note will indicate the deletion.



ProQuest 10647102

Published by ProQuest LLC (2017). Copyright of the Dissertation is held by the Author.

All rights reserved.

This work is protected against unauthorized copying under Title 17, United States Code  
Microform Edition © ProQuest LLC.

ProQuest LLC.  
789 East Eisenhower Parkway  
P.O. Box 1346  
Ann Arbor, MI 48106 – 1346

## **Acknowledgements**

There has been a multitude of guiding lights and kindred spirits providing support and encouragement throughout my three year descent into madness and mayhem:

A big thank you is first of all due to the boss, Gordon Lindsay, for his endless support, patience and sense of humour, all of which he needed in infinite amounts. I would also like to thank all the girls (and occasional honorary ones!) who have passed through the doors of our lab. They made it a real pleasure to come to work. I am also indebted to Dr Sharon Kelly for her expertise with circular dichroism and Professor Alan Cooper and Mrs Margaret Nutley for doing the ITC experiments. I gratefully acknowledge the BBSRC who funded my PhD.

I am lucky enough to have been blessed with some of the best friends a girl could ever hope to have. And because you lot specifically requested a mention by name here you go: Slevvers, Boga, Susan, Sileas, Colin, Annie, Nik, Alison and Neil. Despite my protestations that I couldn't go out while writing this thing I would like to thank my agents of evil for regularly tempting me off the straight and narrow (yeah, I know it was difficult!).

I owe a huge debt (of money, gratitude, but mostly money...) to my folks. They let me get on with it while I followed my own path but somehow, were always there when I needed them.

Finally, I would like to pay homage to my spiritual home, East End Park. May we one day scale the giddy heights of the top of the Premier League for longer than a fortnight! Jimmy, I salute you.

**“The most exciting phrase to hear in science, the one that heralds new discoveries, is not Eureka! (I found it!) but rather, ‘hmm.... that’s funny....’”**

**Isaac Asimov**

## Abstract

The human pyruvate dehydrogenase complex (PDC) is a large macromolecular assembly involved in the oxidative decarboxylation of pyruvate yielding acetyl CoA as the end product of this reaction, which subsequently enters the tricarboxylic acid (TCA) cycle. PDC is composed of multiple copies of various enzyme subunits, termed E1, E2 and E3. Human PDC also contains an additional component, E3BP, which has evolved in order to bind E3 to the core of the complex.

The individual components of human PDC have now been cloned and overexpressed in *E. coli*. A His-tag has been engineered into the N-terminus of each protein to facilitate the rapid purification of these subunits using affinity chromatography. With the exception of E1, an  $\alpha_2\beta_2$  heterotetramer, all recombinant proteins are soluble and produced in high yield. By using antibodies specific only for lipoylated E2 and E3BP from PDC, and by assaying the catalytically active subunits for activity, it has been found that these proteins are correctly folded and have been produced in active form. The use of a detergent, N-lauroylsarcosine, was required to produce a soluble E1. However, this component is active, as determined by enzymatic assay, under these conditions.

Gel filtration studies have shown that E2 and E3BP must be coexpressed in *E. coli* in order for them to assemble into the stable E2/E3BP core complex that is central to the structure and organisation of human PDC. When these two proteins are expressed individually and then mixed they cannot form a stable core assembly. This suggests that the association between E2 and E3BP occurs in a co-translational manner and presumably requires their initial association as folding intermediates.

Circular dichroism and fluorescence studies have been employed to examine the stability of the independently expressed E3BP. These studies have shown that each domain of E3BP, the N-terminal lipoyl domain, subunit-binding domain and C-terminal inner domain, unfolds at discrete concentrations of GdmCl. This indicates that while each domain is capable of independent folding, they also unfold independently of one another.

In the native complex it is unclear how many E3 dimers are associated with human PDC. Isothermal titration calorimetry was utilised in order to assess the stoichiometry of binding between the recombinant E3BP and E3. These studies were performed using both full-length E3BP and a truncated construct, which consists of the subunit-binding domain expressed as a GST-fusion protein. These results suggest that one E3 dimer binds to two E3BP subunits; thus there would be six E3 dimers present per complex. The association constant for these two proteins was in the nanomolar range, indicative of very tight binding as expected. The binding affinity of E3 to E2 was also assessed using this technique. Truncated constructs of E2, specifically the subunit-binding domain expressed as a GST-fusion protein and the E2 didomain, a His-tagged protein containing the lipoyl domain and the subunit-binding domain of E2, were utilised in these studies. It was found that while E2 preferentially binds E1, it has also retained a residual affinity for the E3 subunit. Binding between E2 and E3 is approx. 100-1000 fold weaker than that between E3 and E3BP. The results described here support previous findings from our laboratory, obtained using an alternative technique, surface plasmon resonance and provide a molecular basis as to why E3BP-deficient patients retain residual PDC activity.

While pursuing the main aim of this research, to reconstitute a recombinant human pyruvate dehydrogenase complex *in vitro*, a number of findings have produced interesting results. The unexpected 2:1 stoichiometry determined for the interaction between E3 and E3BP suggests that E3 dimers may form a network of crossbridges linking pairs of E3BP monomers across the 12 faces of the core. Production of sufficient quantities of active E1 is required in order to investigate whether a similar 2:1 stoichiometry exists between the  $\alpha_2\beta_2$  E1 heterotetramer and the E2 didomain. If this is indeed the case, this introduces a new level of structure into the human pyruvate dehydrogenase complex, which has not been recognised previously.

# Contents

Declaration	I
Acknowledgements	II
Quotation	III
Abstract	IV
Contents table	VII
List of figures	XIV
List of tables	XVIII
Abbreviations	XIX
<b>Chapter 1 Introduction</b>	<b>1</b>
1.1 Multienzyme complexes	2
1.2 2-oxoacid dehydrogenase complexes	2
1.3 Complex organisation	5
1.4 Catalytic mechanism	7
1.5 Pyruvate decarboxylase (E1)	9
1.6 Dihydrolipoamide dehydrogenase (E2)	12
1.6.1 The linker regions	12
1.6.2 The lipoyl domain	14
1.6.2.1 The lipoic acid moiety	14
1.6.2.2 Structure of the lipoyl domain	17
1.6.3 The peripheral subunit-binding domain (P-SBD)	19
1.6.4 The C-terminal domain	21
1.7 E3-binding protein (E3BP)	21
1.8 Dihydrolipoamide dehydrogenase (E3)	23

1.9	Regulation of PDC	25
1.10	Genetic defects of PDC	29
1.11	Primary biliary cirrhosis	31
1.12	Protein targeting	32
1.13	Molecular chaperones	34
1.13.1	The Hsp70 family of molecular chaperones	34
1.13.2	The Hsp60 family of molecular chaperones	35
1.13.4	Mechanism of action of GroEL-Gro-ES	36
1.14	Aims of this thesis	36
<b>Chapter 2 Materials and Methods</b>		<b>39</b>
2.1	Molecular biology materials	40
2.1.1	Enzymes and kits	40
2.1.2	Molecular weight markers	40
2.1.3	Oligonucleotides	40
2.1.4	Bacterial media	40
2.1.5	Bacteria and plasmid vectors	40
2.2	Molecular biology methods	41
2.2.1	Polymerase chain reaction (PCR)	41
2.2.1.2	PCR using <i>Taq</i> DNA polymerase	41
2.2.1.3	PCR using <i>Pfu</i> DNA polymerase	46
2.2.2	Restriction digestion	46
2.2.3	Dephosphorylation of digested plasmid	47
2.2.4	Production of competent cells	47
2.2.5	Transformation of competent bacteria	47

2.2.6	Purification of DNA from bacterial cultures	47
2.2.7	Agarose gel electrophoresis	48
2.2.8	Extraction of DNA from an agarose gel	48
2.2.9	Ligations	49
2.2.10.1	Growth of bacterial cultures for protein induction	49
2.2.10.2	Large scale protein induction	50
2.3	Protein Biochemistry Materials	50
2.3.1	Chemicals	50
2.3.2	Molecular weight markers	50
2.3.3	Photographic materials	50
2.4	Protein Biochemistry Methods	51
2.4.1	Dialysis of protein samples	51
2.4.2	Concentration of protein samples	51
2.4.3	Determination of protein concentration	51
2.4.4	SDS-polyacrylamide gel electrophoresis (SDS-PAGE)	52
2.4.4.1	Tris/glycine discontinuous buffer system	52
2.4.4.2	Sodium phosphate continuous buffer system	53
2.4.5	Immunoblotting using ECL™ chemiluminescence	53
2.4.5.1	Solutions used in immunoblotting	53
2.4.5.2	Immunoblotting protocol	54
2.4.6	Purification of GST-fusion proteins	55
2.4.6.1	Preparation of bacterial extracts	55
2.4.6.2	Column purification	55
2.4.7	Purification of His-tagged proteins	55
2.4.7.1	Preparation of bacterial cell extracts	56

2.4.7.2	Purification of His-tagged proteins	56
2.4.8	TCA precipitation of proteins	57
2.4.9	Purification of pyruvate dehydrogenase from bovine heart	57
2.4.10	Gel filtration	58
2.4.11	Protein crosslinking	58
2.4.12	Solubilisation of inclusion bodies	59
2.4.12.1	Preparation of inclusion bodies	59
2.4.12.2	Solubilisation of inclusion bodies	59
2.4.13	Isothermal titration calorimetry	60
2.4.14	Circular dichroism	60
2.4.15	Fluorimetry	61
2.4.16	Enzyme assays	61
2.4.16.1	Pyruvate dehydrogenase (E1) activity	61
2.4.16.2	Dihydrolipoamide acetyltransferase (E2) activity	61
2.4.16.3	Dihydrolipoamide dehydrogenase (E3) activity	62
2.4.17	Preparation of dihydrolipoamide	62
2.4.18	Densitometric scanning analysis	62
<b>Chapter 3 Molecular cloning and overexpression of the individual components of the human pyruvate dehydrogenase complex</b>		<b>63</b>
3.1	Introduction	64
3.1.1	Aims of this chapter	67
3.1.2	Plasmids	67
3.2	Cloning of the E2, E3 and E3BP components	68
3.2.1	PCR amplification and purification	68

3.2.2	Ligation, transformation and identification of clones	71
3.3	Overexpression of heterologous protein	76
3.4	Coexpression of E2 and E3BP	80
3.4.1	Cloning of E2 and E3BP	80
3.4.2	Overexpression of coexpressed E2 and E3BP	81
3.5	Cloning of the E1 component	81
3.5.1	PCR amplification and purification	83
3.5.2	Product ligation, transformation and clone identification	83
3.5.3	Cotransformation of E1 $\alpha$ and E1 $\beta$	85
3.6	Discussion	88
<b>Chapter 4 Purification of the recombinant enzymes of human</b>		<b>91</b>
<b>PDC</b>		
4.1	Introduction	92
4.1.1	Inclusion bodies	93
4.2	Aims of this chapter	93
4.3	Results	94
4.3.1	Lipoylation states of E2 and E3BP	94
4.4	Purification of recombinant proteins	99
4.4.1	Lysate preparation	99
4.4.2	Purification of crude extracts	99
4.5	Purification of E2	100
4.5.1	Optimisation of purification using ion-exchange chromatography	100
4.5.2	Specific activity of E2	103

4.6	Purification of E3BP	104
4.7	Purification of E3	104
4.8	Purification of coexpressed E2/E3BP	110
4.9	Purification of E1	113
4.9.1	Solubilisation and purification of E1 from inclusion bodies	119
4.9.1.1	Solubilisation of E1 using N-lauroylsarcosine	119
4.10	Discussion	120
<b>Chapter 5 Studies on the independent recombinant E3BP component</b>		<b>125</b>
<b>and the structure and assembly of the recombinant E2/E3BP core</b>		
5.1	Assembly of the structural core of human PDC	126
5.2	E3-binding protein (E3BP)	127
5.3	Aims of this chapter	129
5.4	Results	129
5.4.1	Determining the oligomeric nature of E3BP by gel filtration	129
5.4.2	Crosslinking studies on E3BP	130
5.5	Circular dichroism	131
5.5.1	Circular dichroism studies on the independent recombinant E3BP	133
5.5.2	Secondary structure determination of recombinant E3BP	136
5.6	Protein fluorescence	138
5.6.1	Fluorescence studies on the independent recombinant E3BP	138
5.7	Studies on the E2 and E3BP components of human PDC	142
5.7.1	Gel filtration analysis of the E2 and E3BP components of human PDC	143

5.7.2	Gel filtration analysis of independently expressed E2	143
5.7.3	Gel filtration analysis of the E2/E3BP recombinant core	143
5.7.4	Gel filtration analysis of individually expressed E2 and E3BP, mixed in equal amounts	144
5.8	Densitometric scanning analysis of the recombinant E2/E3BP core	150
5.9	Discussion	153
<b>Chapter 6 Stoichiometry and affinity of E3-E3BP and E3-E2 interactions as measured by isothermal titration calorimetry</b>		<b>157</b>
6.1	Constituents of human PDC	158
6.2	Isothermal titration calorimetry	161
6.3	Aims of this chapter	161
6.4	Results	163
6.4.1	Binding studies using full length mature E3BP	163
6.4.2	Binding studies using truncated constructs of E3BP	167
6.5	Analysis of binding of E3 to E2	171
6.6	Discussion	172
<b>General discussion</b>		<b>182</b>
<b>References</b>		<b>191</b>

## List of figures

1.1	Location of the 2-oxoacid dehydrogenase complexes in cellular metabolism	4
1.2	Structures of the octahedral and icosahedral E2 inner cores of PDC	6
1.3	Reaction scheme for the pyruvate dehydrogenase complex	8
1.4	Three-dimensional structure of E1 from the human branched-chain 2-oxoacid dehydrogenase complex	11
1.5	Domain organisation of the E2 and E3BP components from the 2-oxoacid dehydrogenase complexes	13
1.6	Complementary pathways of protein lipoylation in <i>E. coli</i>	16
1.7	Schematic representation of the three-dimensional structure of the lipoyl domain from <i>B. stearrowthermophilus</i>	18
1.8	Schematic representation of the peripheral subunit-binding domain of E2 from <i>B. stearrowthermophilus</i>	20
1.9	Mechanisms for the metabolic regulation of the pyruvate dehydrogenase complex	28
1.10	Model for a GroEL-GroES-mediated folding reaction	37
2.1a	Map of the expression vector pET-14b	42
2.1b	Map of the expression vector pET-28a	43
2.1c	Map of the pET-11a vector	44
2.1d	Map of the glutathione S-transferase fusion vector, pGEX-2T	45
3.1	Primer sequences for the cloning of each component of the human pyruvate dehydrogenase complex	69
3.2	PCR amplification of E2, E3BP and E3	70

3.3a	Restriction digestion analysis of recombinant E3BP plasmids	73
3.3b	Restriction digestion analysis of recombinant E2 plasmids	74
3.3c	Restriction digestion analysis of recombinant E3 plasmids	75
3.4a	Overexpression of E3BP	77
3.4b	Overexpression of E2	78
3.4c	Overexpression of E3	79
3.5	Overexpression of cotransformed E2 and E3BP	82
3.6	PCR amplification of E1 $\alpha$ and E1 $\beta$	84
3.7	Restriction digestion of recombinant E1 $\alpha$ and E1 $\beta$ plasmids	86
3.8	Coexpression of E1 $\alpha$ and E1 $\beta$	87
4.1a	Western blot of E3BP	96
4.1b	Western blot of E2	97
4.1c	Western blot analysis of cotransformed E2 and E3BP	98
4.2	Purification profile for E2	101
4.3	SDS-PAGE analysis of purified E2 from a metal chelate column	102
4.4	Purification profile for E3BP	105
4.5	SDS-PAGE analysis of the purification of E3BP	106
4.6	Purification profile for E3	108
4.7	SDS-PAGE analysis of the purification of E3	109
4.8	Elution profile for coexpressed E2/E3BP	111
4.9	SDS-PAGE analysis of the purification of E2/E3BP	112
4.10	SDS-PAGE analysis of the purification of the individual recombinant enzymes of human PDC	114
4.11	Solubility studies on the coexpressed E1 $\alpha$ and E1 $\beta$ subunits	116

4.12	Map of the coexpression plasmid, E1	118
5.1	Crosslinking studies on purified recombinant E3BP	132
5.2	Far-UV CD spectra of mature E3BP	134
5.3	Graph showing the % total change in folded protein as a function of GdmCl concentration	135
5.4	Fluorescence spectroscopy of the full length E3BP	140
5.5	Unfolding of E3BP (full-length and didomain) as monitored by the change in fluorescence at 350nm	141
5.6	Gel filtration analysis of recombinant coexpressed E2/E3BP core	145
5.7	SDS-PAGE analysis of coexpressed E2-PDC and E3BP after Superose 6 gel filtration	146
5.8	Gel filtration analysis of individually expressed E2 and E3BP mixed in equal amounts	148
5.9	SDS-PAGE analysis of equal amounts of E2 and E3BP after Superose 6 gel filtration	149
5.10	Resolved native bovine PDC and recombinant E2/E3BP core	152
6.1	Crystal structure of E3 complexed with E2-SBD from <i>B. stearothermophilus</i>	159
6.2	Schematic diagram of an ITC instrument	162
6.3	Titration of E3BP into E3	164
6.4	Titration of E3 into E3BP	166
6.5	Titration of E3 into the subunit-binding domain of E3BP	169
6.6	Titration of E3 into the E2 didomain	173
6.7	Titration of E3 into the subunit-binding domain of E2	174

6.8	Hypothetical model of the proposed binding arrangement between E3 and E3BP, and E1 and E2	178
-----	--	-----

## List of tables

4.1	Purification table for E2	103
4.2	Purification table for E3	107
4.3	Specific activity of E1 solubilised from inclusion bodies	120
4.4	Summary of the yields of individual enzymes cloned and expressed in <i>E. coli</i>	121
5.1	Secondary structure content of the full length recombinant E3BP	137
5.2	Densitometric scanning analysis of recombinant and native E2/E3BP core	151

## ABBREVIATIONS

Amp.	ampicillin
approx.	approximately
APS	ammonium persulphate
BCOADC	branched chain 2-oxoacid dehydrogenase complex
CD	circular dichroism
Da	daltons
DHL	dihydrolipoamide
DTT	dithiothreitol
E1	pyruvate decarboxylase
E2	dihydrolipoamide acetyltransferase
E3	dihydrolipoamide dehydrogenase
E3BP	dihydrolipoamide dehydrogenase-binding protein
EDTA	ethylenediaminetetra-acetate
ECL	enhanced chemiluminescence
FAD	flavin adenine dinucleotide
FPLC	fast protein liquid chromatography
GdmCl	guanidinium chloride
GST	glutathione S-transferase
ITC	isothermal titration calorimetry
LB	Luria broth
min	minutes
OGDC	2-oxoglutarate dehydrogenase complex
PAGE	polyacrylamide gel electrophoresis
PBC	primary biliary cirrhosis

PBS	phosphate buffered saline
PCR	polymerase chain reaction
PDC	pyruvate dehydrogenase complex
PEG	polyethylene glycol
PMSF	phenylmethylsulphonyl fluoride
SDS	sodium dodecyl sulphate
SPR	surface plasmon resonance
TCA cycle	tricarboxylic acid cycle
TEMED	NNN'N'-tetramethylethylenediamine
ThDP	thiamine diphosphate
Tris	2-amino-2-(hydroxymethyl)-1,3-propanediol
UV	ultraviolet
v/v	volume to volume
w/v	weight to volume

# **Chapter 1**

## **Introduction**

## 1.1 Multienzyme complexes

Multienzyme complexes, of which the pyruvate dehydrogenase complex is the most prominent example, are composed of multiple copies of several differing types of protein subunits bound tightly, but noncovalently to each other. These complexes are involved in the sequential catalysis of multistep chemical reactions and provide a unique system for the study of protein-protein interactions in a multifunctional enzyme system. It has also been increasingly recognised that post-translational modification of these complexes and the concept of the “swinging arm” provides an elegant means of channelling substrate between active sites. This idea of the “swinging arm”, first postulated for the 2-oxoacid dehydrogenase multienzyme complexes (Reed, 1974), has since been proposed for other multifunctional enzyme systems including fatty acid synthase and the biotin-dependent enzymes such as pyruvate carboxylase. The structural and biochemical study of these complexes is thus of great interest, not only in examining the importance of protein-protein interactions but also in the study of the mechanisms involved in substrate channelling. The importance of the role played by post-translational modification in the catalytic mechanism of these complexes is also of interest (for review, see Perham 2000).

## 1.2 2-oxoacid dehydrogenase multienzyme complexes

The 2-oxoacid dehydrogenase multienzyme complexes are a family of related complexes that catalyse the key committed steps in carbohydrate and amino acid metabolism. The branched-chain 2-oxoacid dehydrogenase complex (BCOADC) oxidatively decarboxylates the branched chain 2-oxoacids derived by transamination from valine, leucine and isoleucine. Mammalian BCOADC has also been found to be capable of metabolising intermediates involved in the breakdown of the amino acids

threonine and methionine (Jones & Yeaman, 1986). The 2-oxoglutarate dehydrogenase complex (OGDC) acts as an important regulatory enzyme within the tricarboxylic acid (TCA) cycle and oxidatively decarboxylates 2-oxoglutarate to succinyl CoA. The pyruvate dehydrogenase complex (PDC), the focus of this work, oxidatively decarboxylates pyruvate with the concomitant production of acetyl CoA for entry into the tricarboxylic acid cycle. As such, PDC controls the rate of carbon flux into the TCA cycle and so plays a central role in the control of carbohydrate utilisation. Figure 1.1 illustrates diagrammatically the positions of these complexes in cellular metabolism.

This family of complexes share a common architectural design. Each complex is composed of multiple copies of at least 3 enzyme components and consists of a central core, composed of either 24 or 60 E2 subunits, to which are bound multiple E1 and E3 subunits. These E1 and E2 components are distinct for each complex and are encoded by separate genes while the E3 component, at least in mammals, is common to all three complexes and is encoded by a single gene. Exceptions to this rule have been found in *Pseudomonas putida* where three separate genes for E3 have been identified (Palmer *et al*, 1991). Similarly, in pea (*Pisum sativum*) two distinct E3s have been identified. One appears to be specific for the mitochondrial complex while the second is associated with its chloroplastic counterpart (Conner *et al*, 1996). Three distinct mitochondrial isoforms of E3 have also been found in potato (Cook *et al*, 1996) where it is believed that these isoforms may represent tissue- and complex-specific isoforms of the enzyme. Multiple enzymatic forms of E3 have also been reported in *E. coli* (Richarme, 1989).

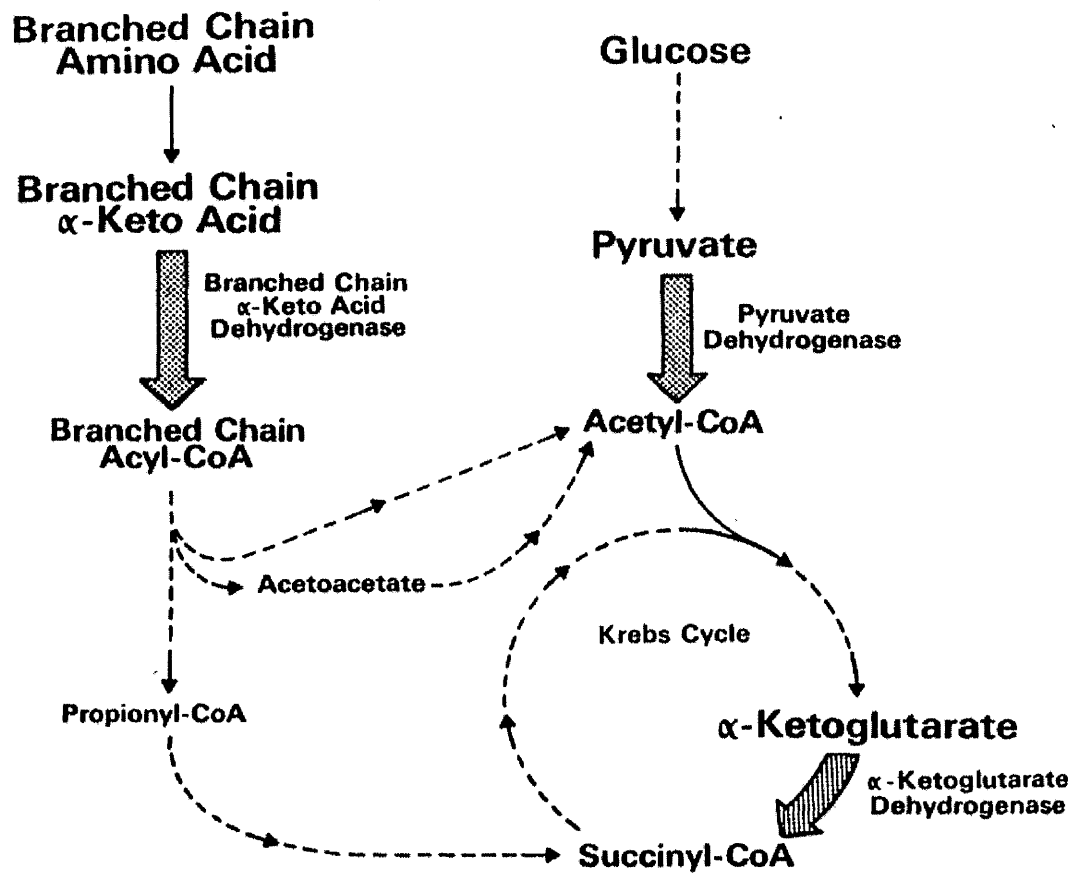


**Figure 1.1** Location of the 2-oxoacid dehydrogenase complexes in cellular metabolism.

( $\alpha$ -keto acid, 2-oxoacid;  $\alpha$ -ketoglutarate, 2-oxoglutarate)

In mammalian and yeast PDC, an additional subunit was identified which was originally termed protein X. This component has since been found to be responsible for binding E3 to the core of the complex and so has been renamed E3-binding protein (E3BP). E3BP has not been identified in PDC from any other sources apart from yeast and mammals and the nematode *Ascaris suum*, nor has it been found in any OGDC or BCOADC complexes.

ref 5?

The multisubunit, multicopy structure of these complexes means that they are among the largest, macromolecular assemblies known, with molecular masses of approx 4-10 million Da.

### 1.3 Complex organisation

The main components of the mammalian pyruvate dehydrogenase complex (PDC) are pyruvate decarboxylase (E1, EC 1.2.4.1), dihydrolipoamide acetyltransferase (E2, EC 2.3.1.12), dihydrolipoamide dehydrogenase (E3, EC 1.8.1.4) and E3-binding protein (E3BP). There are also other associated polypeptides that are involved in the regulation of the complex, namely a specific PDC-associated kinase and phosphatase.

The key to the macromolecular assembly of these complexes lies with the E2 subunit as this enzyme provides the structural core around which the other components assemble. Uniquely, E2 can form one of two structural scaffolds depending on the source of the enzyme. A pentagonal dodecahedral core structure consisting of 60 monomers of E2-PDC noncovalently bound to one another with icosahedral (532) symmetry is found in PDC complexes from mammalian cells and Gram positive bacteria. In Gram negative bacteria and all known OGDCs, and BCOADCs, the E2



**Figure 1.2 Structures of the octahedral and icosahedral E2 inner cores of PDC.**

(Taken from Perham, 2000)

The E2 core from *A. vinelandii* in panel A is shown on its two-, three- and fourfold axes of symmetry.

The icosahedral E2 core from *B. stearothermophilus* is seen in panel B on its two-, three- and fivefold axes of symmetry.

The three different subunits of the basic trimeric unit are shown in different colours.

core exists as a cubic structure with octahedral (432) symmetry. This is formed from the noncovalent assembly of 24 E2 subunits. The other components of these complexes then assemble around this central structural core. Figure 1.2 demonstrates the two types of structural scaffold that can form.

In mammalian PDC up to 30 E1  $\alpha_2\beta_2$  heterotetramers bind noncovalently at the 30 edges of the 60meric E2 core. Evidence from densitometric-scan analyses suggests that 1 E3BP molecule binds in each of the 12 faces of the E2 core while 6-12 E3 homodimers are connected to the complex via E3BP (Sanderson *et al*, 1996a). In OGDC and BCOADC it is believed that 12 E1 molecules bind to the edges of the 24meric cubic structure while an estimated 6 E3 dimers are associated with the 6 faces of these complexes.

#### 1.4 Catalytic Mechanism

The overall reaction catalysed by PDC results in the decarboxylation of pyruvate with the concomitant production of acetyl-CoA, CO<sub>2</sub> and NADH. This is a multistep reaction involving the 3 main components of the complex (Figure 1.3). E1 catalyses a two step reaction and this is the first, and rate-limiting step in the overall catalytic mechanism. E1 has an absolute requirement for the cofactor thiamine diphosphate (ThDP) and Mg<sup>2+</sup>. Pyruvate forms an adduct with the thiazole ring of ThDP and this then undergoes decarboxylation to produce a 2-(1-hydroxyethylidene)-ThDP intermediate. This intermediate undergoes oxidation while the dithiolane ring of the lipoyl moiety on E2 becomes reductively acetylated. This produces the acetyl group and electrons that are transferred, via E2 and E3 respectively, to CoA and NAD<sup>+</sup>. Both of these partial reactions are catalysed by E1. E2 then mediates the transfer of

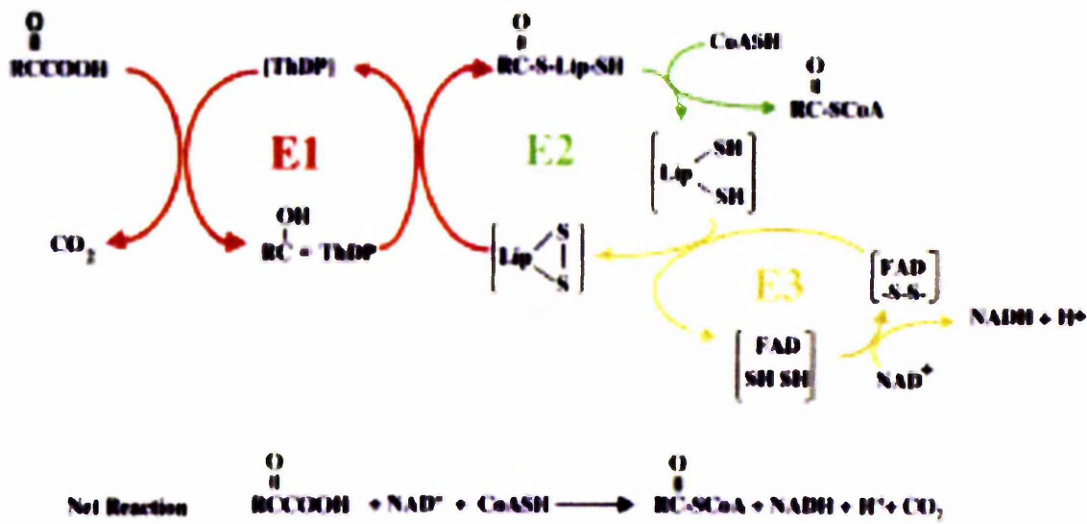


**Figure 1.3 Reaction scheme for the pyruvate dehydrogenase complex**

(Taken from Perham, 2000)

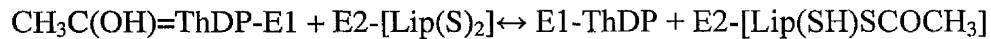
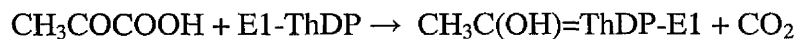
The reactions catalysed by E1 are shown in red, the reaction catalysed by E2 is in green, and that catalysed by E3 is indicated in yellow.

ThDP, thiamine diphosphate.

the acetyl group from its lipoyl moiety to free CoA, thus forming acetyl CoA. E3 reoxidises the reduced lipoyl moiety of E2 thus regenerating the disulphide bridge in the lipoyl group, with  $\text{NAD}^+$  acting as the final electron acceptor.

### 1.5 Pyruvate Decarboxylase (E1)

The E1 subunit of the 2-oxoacid dehydrogenase complexes is a thiamine diphosphate (ThDP)-dependent enzyme which catalyses two successive steps in the overall catalytic mechanism of the complex. It catalyses the decarboxylation of pyruvate to  $\text{CO}_2$  to form the intermediate 2- $\alpha$ -hydroxyethylidene-TPP (HE=TPP) and the reductive acetylation of the lipoyl groups of E2 as shown below.



ThDP-dependent enzymes share a number of common features. Comparison of the 3-dimensional structures of three ThDP-dependent enzymes (yeast pyruvate decarboxylase, yeast transketolase and *Lactobacillus plantarum* pyruvate oxidase) revealed that the ThDP-binding site is located in a deep cleft formed by hydrophobic amino acids at the interface between two subunits (Hawkins *et al*, 1989). This ThDP-binding motif is responsible for the binding of a metal ion that anchors ThDP via its phosphate groups. Subsequent x-ray crystallographic analysis of the heterotetrameric E1 from the BCOADC of *P. putida* (Ævarsson *et al*, 1999) and from human BCOADC (Ævarsson *et al*, 2000) placed the cofactor thiamine diphosphate (ThDP) at the end of a long hydrophobic channel that is capable of accommodating the E2 lipoyl-lysine arm. Similarly, the recently reported crystal structure of the  $\alpha_2$

homodimeric E1 from *E. coli* has confirmed that the catalytic ThDP is found at the bottom of a deep funnel-shaped hole at the interface between the two subunits (Arjunan *et al*, 2002). The functional dimer contains two such catalytic centres. Similarly, mammalian E1-PDC, an  $\alpha_2\beta_2$  heterotetramer, is also known to contain two active centres (Khailova & Korotchkina, 1982).

Relatively little is known about the active sites of mammalian E1-PDC. Chemical modification has previously identified cysteine-62 of the  $\alpha$  subunit (Ali *et al*, 1993) and tryptophan-135 of the  $\beta$  subunit (Ali *et al*, 1995) as being involved in the active site of E1. Site-directed mutagenesis of these two residues has now indicated that they are involved in coenzyme binding and could also be important for the stability of the protein (Korotchkina *et al*, 1999). However, the lack of a 3-dimensional structure of mammalian E1-PDC makes it difficult to predict the exact position of residues located in or near the active site of the protein.

In the octahedral complexes of OGDC and PDC, E1 exists as an  $\alpha_2$  homodimer while in the octahedral BCOADC and the icosahedral PDC complexes, E1 consists of 2 nonidentical subunits forming an  $\alpha_2\beta_2$  heterotetramer. Studies on the heterotetrameric E1 component from *B. stearothersophilus* showed that binding to the peripheral subunit-binding domain of E2 is mediated by the E1 $\beta$  subunit (Lessard *et al*, 1995). Each E1 tetramer is believed to bind only one binding domain, thus the binding site is predicted to lie at or close to the 2-fold axis of symmetry on the  $\beta$  subunits (Wynn *et al*, 1992; Lessard *et al*, 1995).

The structure of human heterotetrameric E1 from BCOADC is shown in Figure 1.4.

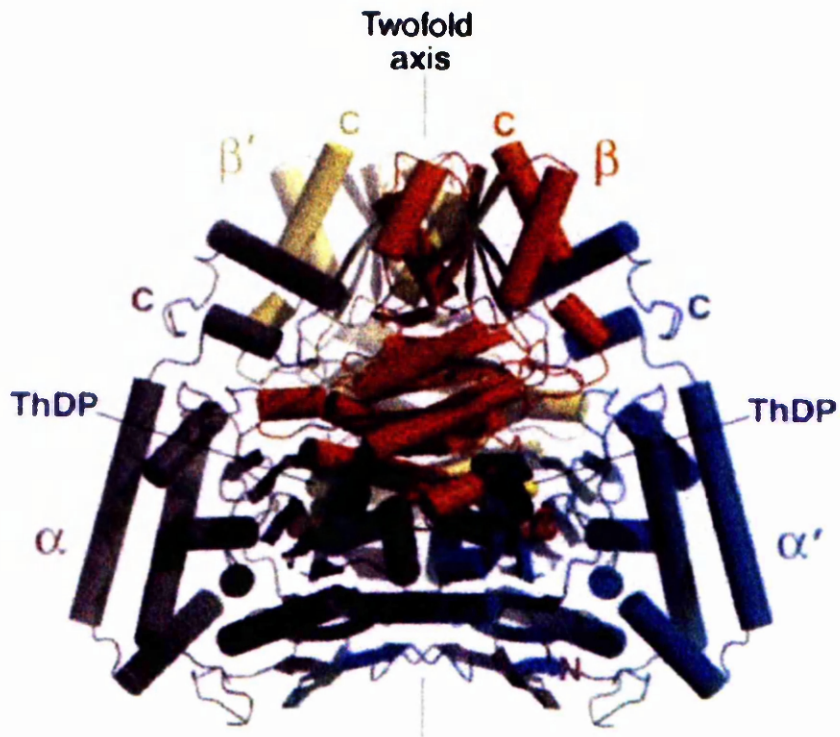


**Figure 1.4 Three-dimensional structure of E1 from the human branched-chain 2-oxoacid dehydrogenase complex**

(From *Ævarsson et al*, 2000)

The crystal structure of heterotetrameric E1 from human BCOADC is shown along its twofold axis of symmetry. Each subunit is shown in a different colour ( $\alpha$  subunits shown in purple and blue,  $\beta$  subunits in red and yellow).

## 1.6 Dihydrolipoamide Acetyltransferase (E2)

## 1.6 Dihydrolipoamide Acetyltransferase (E2)

E2 plays a key role not only in determining the structure and organisation of PDC but also in co-ordinating the sequence of catalytic events within the complex. The E2 polypeptide has a modular organisation consisting of at least three independently folding domains separated by flexible linker regions. Each subunit contains, from the N-terminus, 1-3 highly homologous lipoyl-containing domains which are each about 80 amino acids long followed by a small subunit-binding domain consisting of approximately 40-50 amino acids and, at the C-terminus, a large catalytic inner domain. This inner domain contains the binding sites for E2 involved in the self-assembly of this enzyme into the central core complex as well as the catalytic site for acetyl transfer (Radford *et al*, 1987). In mammals and yeast this central core is formed from multiple copies of both E2 and E3BP. E3BP shares a similar domain organisation to E2 as indicated in Figure 1.5. The C-terminal domain of this protein contains the binding sites for the E2 polypeptide. The number of lipoyl domains present on the E2 polypeptide depends on the source of the enzyme. This ranges from three in the *E. coli* PDC to one in PDC from *B. stearothermophilus* and *S. cerevisiae* and all known OGDCs and BCOADCs. Mammalian PDC contains two lipoyl domains on the E2 polypeptide while E3BP contains a single lipoyl domain.

### 1.6.1 The linker regions

Regions of polypeptide chain approximately 20-30 amino acids in length connect each of these domains. These linker regions are rich in alanine and proline residues and charged amino acids. [<sup>1</sup>H] NMR has shown that these linker regions are highly flexible, a function which is very important in maintaining the catalytic activity of the complex (Perham *et al*, 1981; Green *et al*, 1992). These linker regions provide the

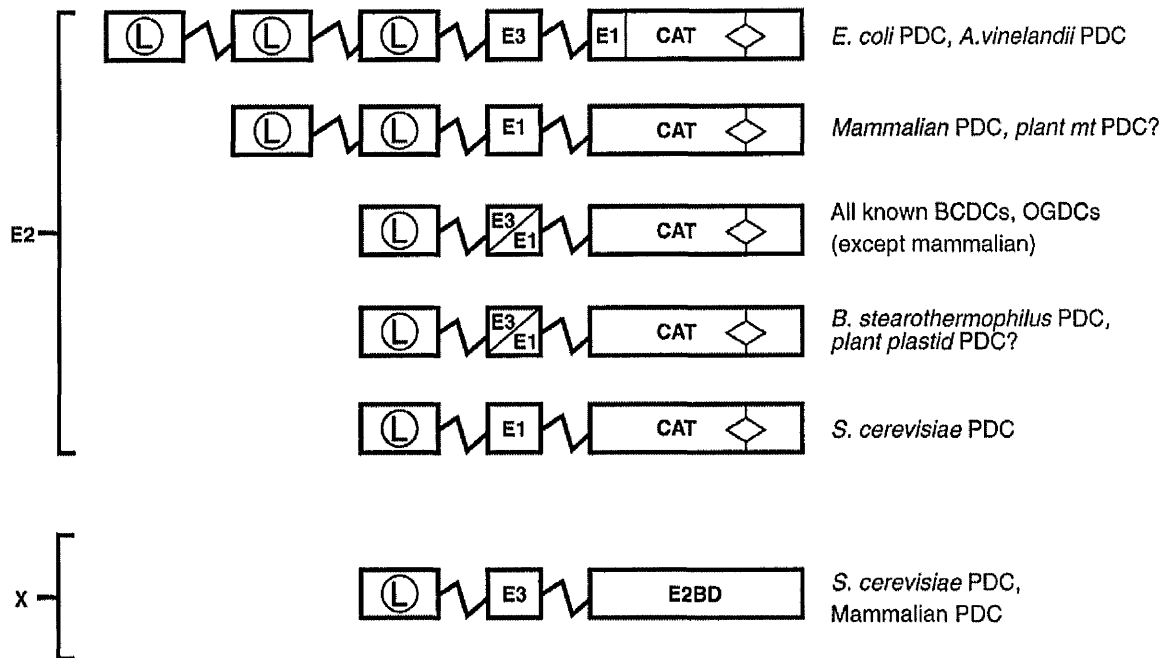


**Figure 1.5 Domain organisation of the E2 and E3BP components from the 2-oxoacid dehydrogenase complexes**

(L), lipoyl domain; E3/E1, E3 and/or E1 binding domain; CAT, C-terminal acetyltransferase domain; E2BD, E2-binding domain; X, E3-binding protein

lipoyl domains with the flexibility they require in order to rotate between the active sites of the 3 catalytically active enzymes. This was demonstrated by making progressive deletions in the linker region of a modified *E. coli* E2 with only one lipoyl domain. It was found that this region must be at least 13 amino acids long for full active site coupling to be maintained. Shorter segments impaired the overall reaction of PDC without unduly affecting the reactions of the individual enzymes (Miles *et al*, 1988).

### **1.6.2 The lipoyl domain**

The lipoyl domain plays a central role in the catalytic mechanism of the 2-oxoacid dehydrogenase complexes and, as such, undergoes two important recognition processes *in vivo*. Each lipoyl domain can be post-translationally modified on a specific lysine residue by the lipoylating enzymes of the cell while recognition of the lipoyl domain by its cognate E1 is a prerequisite for efficient catalysis.

#### **1.6.2.1 The lipoic acid moiety**

Lipoic acid (6,8-thioctic acid or 1,2-dithiolane-3-pentanoic acid) is a sulphur-containing cofactor, which is utilised by the members of the 2-oxoacid dehydrogenase multienzyme complex family. In each lipoyl-containing protein, lipoic acid is attached to a specific lysine residue via an N<sup>6</sup>-amide linkage between its carboxyl terminal and the ε-amino group of the lysine. This amide linkage is flexible, allowing the lipoyl group to shuttle intermediates and reducing equivalents between the active sites of the three catalytically active enzymes.

In *E. coli*, there are believed to be two complementary pathways of protein lipoylation as shown in Figure 1.6. The first pathway (endogenous pathway) of lipoylation requires the product of the *lipB* gene, (lipoyl-[acyl-carrier-protein]-protein-N-lipoyltransferase) which transfers endogenously synthesised lipoate to apoproteins. The biosynthetic pathway by which *E. coli* synthesises lipoate is poorly understood but it has been shown that octanoic acid, 8-thiooctanoic acid and 6-thiooctanoic acid can act as the precursors for lipoate synthesis (Reed & Cronan, 1993). In this pathway the lipoyl group is attached to an acyl carrier protein (ACP) to form lipoyl-ACP (Jordan & Cronan, 1997). The product of the *lipB* gene then transfers the lipoyl moiety to the apoprotein (Morris *et al*, 1995). The second pathway (exogenous pathway) utilises free lipoic acid present in the medium and requires the product of the *lplA* gene, a lipoate-protein ligase (LplA) (Morris *et al*, 1994; Green *et al*, 1995). LplA catalyses the ATP-dependent activation of lipoic acid to lipoyl-AMP and then transfers the activated lipoyl group to the apoprotein with the concomitant release of AMP (Morris *et al*, 1995).

In mammalian cells, the covalent attachment of lipoate to apoprotein occurs in two successive steps and, in contrast to the situation in *E. coli*, requires two separate enzymes. In the first reaction lipoate-activating enzyme acts by promoting the formation of lipoyl-AMP (Tsunoda & Yasunoba, 1967). The second enzyme, lipoyl-AMP:N<sup>ε</sup>-lysine lipoyltransferase (Fujiwara *et al*, 1994; Fujiwara *et al*, 1999), then transfers the lipoyl moiety to the lysine residue of the apoprotein.

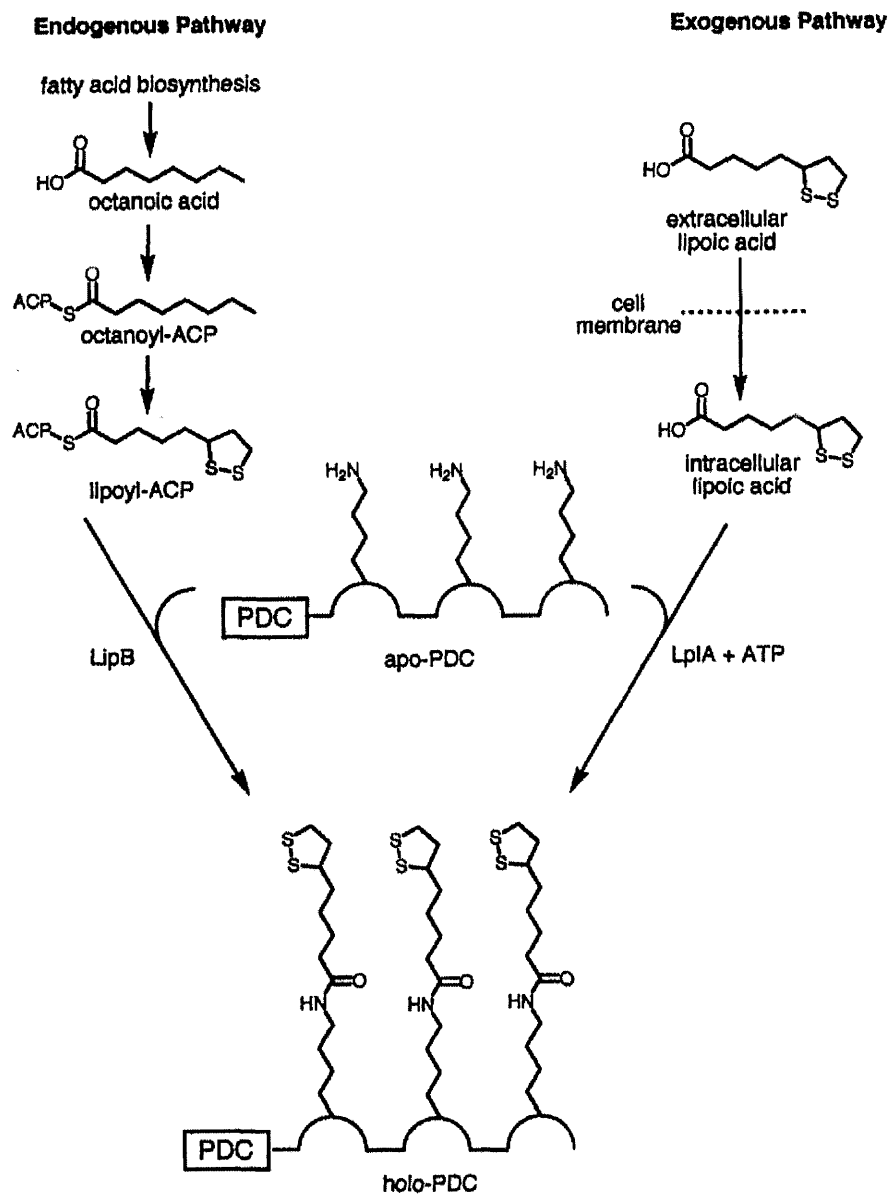


**Figure 1.6 Complementary pathways of protein lipoylation in *E. coli***

(From Miller *et al.*, 2000).

Apo-PDC, unlipoylated protein; Holo-PDC, lipoylated protein

### 1.6.2.2 Structure of the lipoyl domain

The 3-dimensional structure of the lipoyl domain has been solved from a number of sources by means of NMR spectroscopy. The most recently reported structure is that of the inner lipoyl domain of human E2 (Howard *et al*, 1998). Figure 1.7 shows the three-dimensional structure of the lipoyl domain from *B. stearothermophilus*. The overall backbone structure of the lipoyl domain is virtually identical in all species so far examined. It was found that the lipoyl domain consists of two 4-stranded antiparallel  $\beta$ -sheets in the fold of a flattened  $\beta$ -barrel. The lipoylatable lysine residue is located on an exposed type-I  $\beta$ -turn in one of the  $\beta$ -sheets, within a conserved DKA motif. Site-directed mutagenesis of the amino acid residues of this motif and analysis by mass spectrometry have shown that the highly conserved aspartic acid (D) and alanine (A) residues do not appear to be necessary for the recognition of the lipoylatable lysine residue. When these residues were subjected to mutagenesis, the ability of the lysine residue to be lipoylated remained unaffected. The position of the lysine residue itself appears to be the key factor affecting lipoylation. Mutants in which lysine replaced the aspartic acid residue and the lipoylatable lysine residue was mutated to alanine remained unlipoylated, as judged by mass spectrometry. This indicates that the lipoylating enzymes require a precise structural cue in order to initiate lipoylation (Wallis & Perham, 1994).

An additional surface loop on the second  $\beta$ -sheet has also been identified, which lies close in space to the lipoyl-lysine loop, and it is thought that this loop may be involved in the recognition of E2 by its cognate E1 component. In the *B. stearothermophilus* lipoyl domain, it was found that mutagenesis of the residues found in this second surface loop led to virtual complete abolition of the ability of

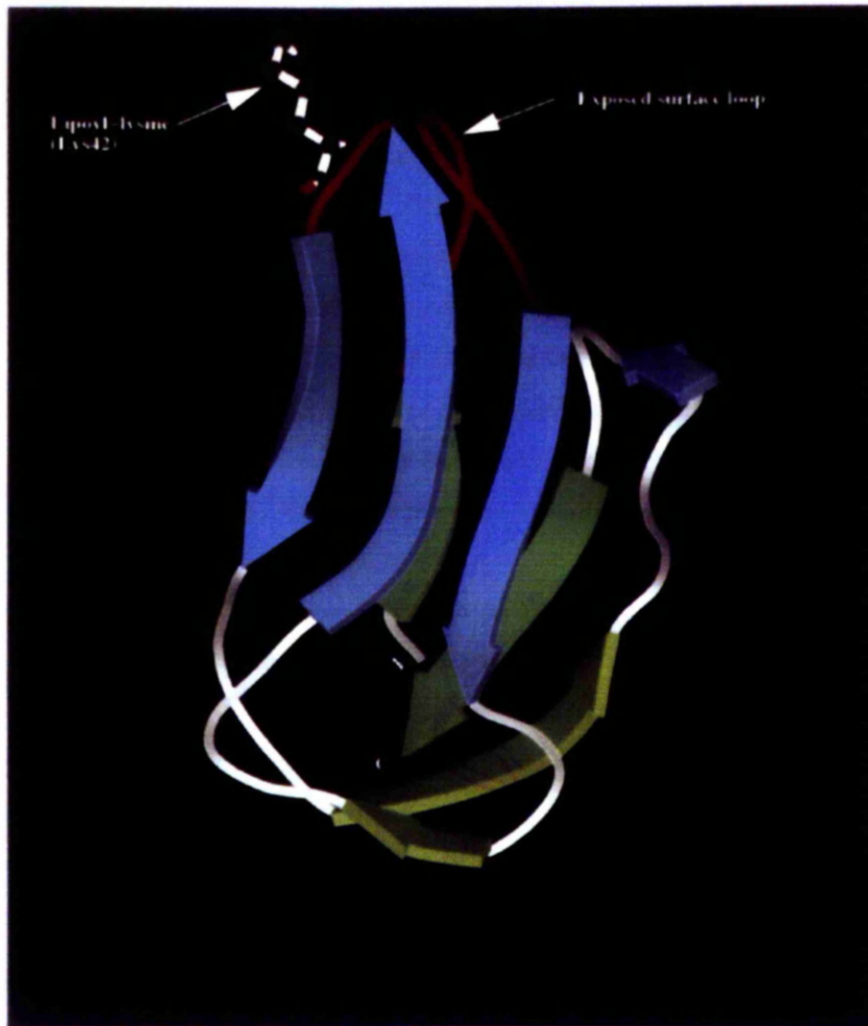


**Figure 1.7 Schematic representation of the three-dimensional structure of the lipoyl domain from *B. stearothermophilus***

The  $\beta$ -sheet containing the lipoyl-lysine residue is shown in blue. The  $\beta$ -sheet coloured green contains the N- and C-terminal residues. The second exposed surface loop is shown in red.

the lipoyl domain to act as a substrate for its cognate E1 component (Wallis *et al*, 1996).

### 1.6.3 The peripheral subunit-binding domain (P-SBD)

The peripheral subunit-binding domain is one of the smallest independently folded protein domains described to date. In human E2-PDC, the primary function of this domain is to bind the E1 component but it has also retained a residual affinity for E3 (McCartney *et al*, 1997). In the bacterial complexes the P-SBD binds both E1 and E3. It has been demonstrated that in the *B. stearotherophilus* PDC, E1 and E3 compete for binding and are capable of displacing each other, suggesting that the overall assembly of the complex may not be strictly symmetrical (Lessard *et al*, 1996).

The 3-dimensional structure of the P-SBD from *B. stearotherophilus* E2-PDC has been solved by means of NMR spectroscopy (Kalia *et al*, 1993) as seen in Figure 1.8. This domain consists of 43 amino acids with 33 of these residues comprising a structured core composed of two  $\alpha$ -helices connected by a loop that contains a short  $3^{10}$  helix. Two highly conserved hydrophilic residues, Asp34 and Thr24 are found buried in the structure and these residues are believed to be crucial in conveying stability to the domain (Spector *et al*, 1998). Sequence comparison of E2 from a variety of organisms has shown that the subunit-binding domain is one of the most conserved parts of the E2 protein. The majority of the conserved residues in this domain are hydrophobic or polar, suggesting that all subunit-binding domains have a similar structure (Russell & Guest, 1991).

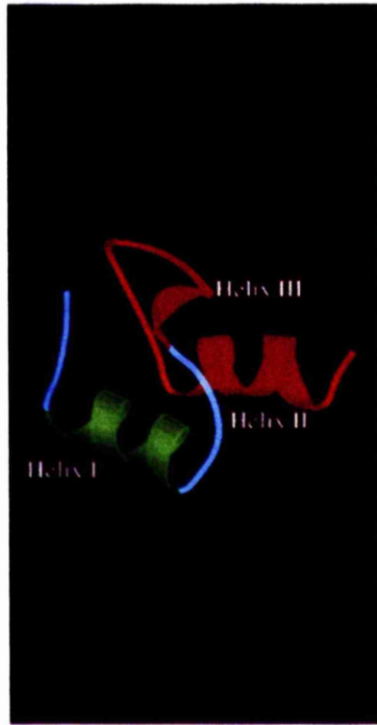


**Figure 1.8 Schematic representation of the peripheral subunit binding domain of E2 from *B. stearrowthermophilus***

#### 1.6.4 The C-terminal domain

The C-terminal domain of E2 houses the acetyltransferase activity of this enzyme and the binding sites which are involved in the self-assembly of E2 into the structural core. Comparison of the amino acid sequences of E2 from *E. coli* and several chloramphenicol acetyltransferases (CATs) revealed 15% sequence homology between these two proteins. This led to the proposal that the C-terminal domain of E2 and CAT were structurally homologous (Guest, 1987). The comparison with CAT also predicted two highly conserved residues, a histidine and an aspartic acid, to be involved with the catalytic mechanism of E2. This prediction was later confirmed when the crystal structure of the cubic core from *A. vinelandii* was solved to 2.6Å resolution (Mattevi *et al*, 1992; Mattevi *et al*, 1993). Comparison of this structure with that of CAT revealed a striking similarity between structures. Like E2, CAT is formed by a tightly associated trimer of identical chains with the catalytic centre, formed by a 30Å long channel, found at the interface between subunits (Leslie, 1990). This structure also confirmed the participation of His-610 (in *A. vinelandii*) in the catalytic mechanism (Mattevi *et al*, 1993b). In E2 the conserved aspartic acid in CAT has been replaced by an asparagine (de Kok *et al*, 1998).

#### 1.7 E3-binding protein (E3BP)

Originally termed protein, or component X this protein is an additional subunit first identified in mammals (DeMarcucci *et al*, 1985; Jilka *et al*, 1986) and then in yeast (Behal *et al*, 1989) of the pyruvate dehydrogenase complex. Gene disruption and mutagenesis studies conducted in *Saccharomyces cerevisiae* indicated that the

subunit-binding domain of protein X was responsible for the high-affinity binding of E3 to the core of the complex (Lawson *et al*, 1991) resulting in it being renamed E3-binding protein (E3BP).

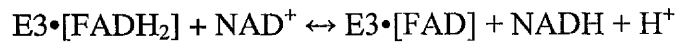
Amino acid sequence analysis of E3BP indicates that this protein has a similar structure to that of E2 as demonstrated previously in Figure 1.5. The E3BP polypeptide consists of a single lipoyl-binding domain, a subunit-binding domain and a larger C-terminal domain. As with E2, these domains are connected by highly flexible linker regions. In all known E2-like proteins with acetyltransferase activity a histidine residue has been identified which is believed to be important in the catalytic activity of the protein. This residue is found in the conserved sequence DHRXXDG in the inner domain. In the corresponding sequence in E3BP (DSRXXDD) the histidine residue has been replaced by a serine (Seyda & Robinson, 2000). No acetyltransferase activity has been detected in E3BP and a catalytic role has not yet been identified for this protein although it has been recognised that the lipoyl domain of E3BP can undergo reductive acetylation in a manner similar to E2. Indeed it has been found that removal of the lipoyl domains of E2 by collagenase treatment resulted in a complex capable of sustaining residual PDC activity at a level of 15-20% compared with wild-type complex. This suggests that the lipoyl domain present on E3BP can, in part, compensate for defective or missing lipoyl domains on E2 (Sanderson *et al*, 1996b). Primary sequence analysis indicates that human E3BP shares greater homology with E2 than with yeast E3BP (Harris *et al*, 1997). It has also been noted that the lipoyl domain of E3BP shares greatest homology with the inner lipoyl domain of E2 (Aral *et al*, 1997).

Complexes deficient in E3BP have been shown to be able to sustain partial PDC activity. Reconstitution studies carried out in this laboratory have shown that reconstituted PDC lacking E3BP is able to sustain residual activity in the presence of a large molar excess of E3. In the presence of stoichiometric amounts of E3, little or no activity was detected (McCartney *et al*, 1997). This is thought to occur because mammalian E2 has retained a residual binding capacity for the E3 component allowing E3 to bind specifically and with low affinity. These results provide support for the discovery of a group of patients with E3BP deficiencies. These patients have no immunologically detectable E3BP but can sustain residual levels of PDC activity approx. 10-20% that of a control group (Marsac *et al*, 1993; Geoffroy *et al*, 1996).

### **1.8 Dihydrolipoamide dehydrogenase (E3)**

E3 is one of a family of enzymes that require FAD for its activity. This family is known as the pyridine nucleotide-disulphide oxidoreductases and includes glutathione reductase and thioredoxin reductase (Mande *et al*, 1996). These enzymes catalyse electron transfer between pyridine nucleotides and disulphide compounds. Of these enzymes, glutathione reductase has been the most extensively studied. The full amino acid sequence and tertiary structure has been elucidated for this protein (Thieme *et al*, 1981) while x-ray diffraction analysis has been employed using purified human glutathione reductase, to confirm the mode of catalysis which has already been postulated from biochemical and spectroscopic studies (Pai & Schulz, 1983). Since E3 has significant sequence homology to glutathione reductase (Otulakowski & Robinson, 1987) a similar catalytic mechanism has been proposed for this protein (Carothers *et al*, 1989; Jentoft *et al*, 1992).

E3 catalyses the reoxidation of the disulphydryl form of the lipoyl moiety attached to the E2 polypeptide. In this reaction electrons are first transferred from the dihydrolipoyl moiety of E2 to the reactive disulphide, then to the FAD cofactor before finally being transferred to  $\text{NAD}^+$  as indicated below.



E3 exists as a dimer of two identical subunits. Each subunit consists of four domains, a FAD-binding domain, the  $\text{NAD}^+$ -binding domain, a central domain and the interface domain. Each subunit also contains a noncovalently bound molecule of FAD, a redox-active disulphide and an  $\text{NAD}^+$ -binding site. Reconstitution studies using the monomeric apoenzymes of E3 from *A. vinelandii* have indicated that the dimeric form of E3 is essential not only for its catalytic activity but also for the interaction with E2 (Schulze *et al*, 1991). This indicates that residues from both E3 monomers form the binding site for E2.

E3 contains two active sites, each of which is formed by the flavin ring of FAD, two cysteine residues from 1 monomer and a histidine residue from the second monomer (Toyoda *et al*, 1998). Site-directed mutagenesis of this histidine residue (His-452 in human E3) results in almost complete abolition of E3 activity (Kim & Patel, 1992). This residue is believed to be important in stabilising the thiolate-anion involved in the charge transfer complex (Liu *et al*, 1995).

E3 is thought to be common to all three 2-oxoacid dehydrogenase multienzyme complexes in eukaryotes. Reconstitution experiments, immunological crossreactivity studies and genetic disorders of E3 which result in simultaneous increases in the levels of pyruvate, branched-chain amino acids and 2-oxoglutarate are three lines of evidence suggesting that this is indeed the case (Pons *et al*, 1988).

### 1.9 Regulation of PDC

Due to its location at an important branch-point in intermediary metabolism, it is of the utmost importance that the activity of the pyruvate dehydrogenase complex is tightly regulated. To date, two separate types of mechanism have been characterised that are involved in the short-term regulation of this complex. The simplest mechanism occurs as a result of end-product inhibition of PDC. The second mechanism, first demonstrated by Linn and coworkers (1969), showed that PDC can be regulated by a phosphorylation/dephosphorylation mechanism which is mediated by PDC-associated kinases and phosphatases.

Feedback inhibition of PDC occurs under metabolic conditions where the levels of NADH and acetyl CoA, the end products of the catalytic mechanism, are elevated. High NADH:NAD<sup>+</sup> and acetyl CoA:CoA ratios enhance the activity of the PDC-associated kinase and hence phosphorylate and inactivate the complex. There is also a reciprocal reduction in phosphatase activity (Pettit *et al*, 1975). Increasing concentrations of pyruvate, ADP and Ca<sup>2+</sup> inhibit the activity of PDC-kinase. Increased Ca<sup>2+</sup> concentrations also enhance the activity of PDC-associated phosphatase (Patel *et al*, 1995).

Direct  
inhibition -

PDC-kinase (PDK, EC 2.7.1.99) is a mitochondrial protein kinase composed of two subunits, an  $\alpha$  subunit of  $M_r$  48000 and a  $\beta$  subunit of  $M_r$  45000 (Stepp et al, 1983). This enzyme is found tightly bound to PDC and is present in very small quantities. It catalyses the phosphorylation of three serine residues present on the E1 $\alpha$  subunit. These are Ser-264, Ser-271 and Ser-203 in the human complex. Phosphorylation at site 1 (Ser-264) was shown to occur in E1 independently. However, phosphorylation of sites 2 (Ser-271) and 3 (Ser-203) also require the presence of E2 (Yeaman *et al*, 1978). In particular it was found that acetyl-CoA-mediated enhancement of kinase activity requires the presence of a lipoate source, preferably the inner lipoyl domain of E2, the catalytic domain of E2 and a peptide substrate (Ravindran *et al*, 1996). Major inactivation of the complex occurs upon phosphorylation of site 1. Each of these sites were found to become phosphorylated at different rates indicating that the rate of phosphorylation is site-specific (Korotchkina & Patel, 1995).

Four isoenzymes of PDK have been identified and characterised, most recently PDK4 (Rowles *et al*, 1996). Each of these isoenzymes has a tissue-specific expression. PDK1 is found mostly in cardiac muscle while PDK2 is found in most tissues. PDK3 appears to be most abundant in testis while PDK4 is predominantly expressed in skeletal muscle and heart (Gudi *et al*, 1995; Bowker-Kinley *et al*, 1998). Each isoenzyme appears to act preferentially at different phosphorylation sites adding a new level of complexity to the regulation of PDC. For example, site 1 seems to be preferentially phosphorylated by PDK2, site 2 by PDK3 while site 3 can only be phosphorylated by PDK1 (Korotchkina & Patel, 2001). It has been proposed that the different PDK isoenzymes may perform specialised roles. PDK1 and 2 may be specialised for short-term or metabolic control of PDC activity, while it has been

postulated that PDK4 may be more adapted to the long-term regulation of PDC under circumstances such as starvation (Bowker-Kinley *et al*, 1998).

PDC-phosphatase (PDP, EC 3.1.3.43) is a mitochondrial protein serine/threonine phosphatase that catalyses the dephosphorylation, and hence activation, of the E1 component of PDC. This enzyme consists of two subunits, a  $Mg^{2+}$ -dependent and  $Ca^{2+}$ -stimulated catalytic subunit and an FAD-containing regulatory subunit. PDP is found loosely associated with the E2 component of PDC and requires an increase in intracellular  $Ca^{2+}$  ion concentration for the activity of the phosphatase to be enhanced. Liu and coworkers (1995b) found that association of PDP with the complex occurs at the inner lipoyl domain on E2. To date, two isoenzymes of PDC-associated phosphatase have been identified. One isoenzyme, PDP1 is found predominantly in muscle while PDP2 is expressed mainly in liver and adipose tissue (Huang *et al*, 1998).

Long-term regulation of PDC by either nutritional or hormonal changes has not been extensively studied but is believed that regulation probably occurs through a variety of mechanisms (Denton *et al*, 1996). The mechanisms by which PDC is regulated are summarised in Figure 1.9.

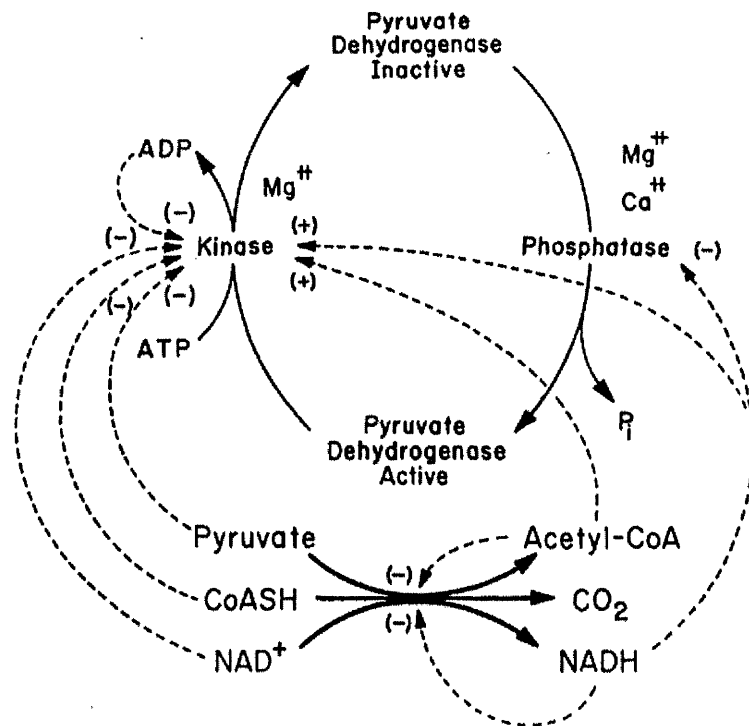


**Figure 1.9 Mechanisms for the metabolic regulation of the pyruvate dehydrogenase complex**

(From Behal, 1993).

### 1.10 Genetic defects of PDC

Human pyruvate dehydrogenase complex deficiency is a potentially severe inborn error of oxidative metabolism. The clinical symptoms of PDC deficiency tend to vary quite markedly but commonly patients present with lactic acidosis and some form of neurological dysfunction. The nature and severity of this dysfunction can vary considerably between patients. PDC deficiency can be caused by mutations in any of the subunits of the complex.

The most common cause of PDC deficiency occurs as a result of a defect in the E1 $\alpha$  subunit (Chun *et al*, 1993). Nearly 80 different point, insertion or deletion mutations have been identified in this component but the nature and severity of the abnormalities caused by these mutations show great variation. This is purported to be because the gene for E1 $\alpha$  has been localised to the short arm of the X chromosome (Brown *et al*, 1989; Szabo *et al*, 1990). In females, the pattern of expression of E1 $\alpha$  is dictated by X-chromosome inactivation and this can account for some of the variation in clinical symptoms. In males only one X chromosome is present so all cells will be affected by the mutation in E1 $\alpha$ . Residual complex activity will, therefore, depend on the severity of the mutation (Lissens *et al*, 2000). A second gene has been identified which also codes for the E1 $\alpha$  subunit. This was localised on chromosome 4 and codes for a testis-specific E1 $\alpha$  (Dahl *et al*, 1990). To date, no mutations have been characterised in this testis-specific gene (Dahl, 1995) nor have any mutations causing PDC deficiency been detected in the E1 $\beta$  subunit. However, patients with a defect in the E1 $\alpha$  component usually also have no detectable, or severely depleted amounts of E1 $\beta$  protein. This is thought to be as a result of an impaired ability of heterotetrameric E1 protein to form (Saijo *et al*, 1996) due to the mutation in the E1 $\alpha$  subunit.

A number of patients with an apparent absence of E3BP as detected by Western blotting have been identified (Robinson *et al*, 1990; Marsac *et al*, 1993; Geoffroy *et al*, 1996; Ling *et al*, 1998). Defects in the E2 component (Robinson *et al*, 1990) and the PDC-phosphatase (Ito *et al*, 1992) have also been detected. The symptoms that these patients present with are generally clinically indistinguishable from those caused by a defect in the E1 $\alpha$  subunit.

A mutation in the E3 subunit results in impaired activity of all the 2-oxoacid dehydrogenase complexes since E3 is an essential component of these complexes. E3 deficiency leads to elevated levels of the 2-oxoacid substrates in plasma and urine (Hong *et al*, 1997; Shany *et al*, 1999). To date, defects in the E3 component are the only identified mutations found in the OGDC complex. Mutations in the E1 and E2 components have not yet been reported (Sheu & Blass, 1999) although OGDC has been implicated in the aetiology of several neurodegenerative diseases (Sheu *et al*, 1994; Gibson *et al*, 1998).

Deficiency in OGDC is associated with a number of neurological disorders. In particular, it has been found that in the brains of patients suffering from Alzheimer's disease there is a pronounced reduction in the activity of OGDC (Sheu *et al*, 1994). Since the substrate of OGDC, 2-oxoglutarate, and glutamate are interconverted in the brain, a deficiency of OGDC would be expected to impair the removal of glutamate, which is a potential neurotoxin. OGDC is also particularly sensitive to the production of free radicals caused under conditions of oxidative stress (Gibson *et al*, 1998) and this can lead to its inactivation. However, the mechanisms by which OGDC is

selectively inactivated by these reactive oxygen species are, as yet, unclear (Gibson *et al*, 2000).

Mammalian BCOADC is encoded by six genetic loci and mutations at any one of these loci can cause a dysfunction in the complex resulting in increased concentrations of the branched-chain amino acids in the blood, tissues and urine of patients. This results in maple syrup urine disease (MSUD) which causes seizures, mental retardation, coma and, in severe cases, death (Chuang *et al*, 1995). As with PDC, most defects in the BCOADC complex appear to be associated with the E1 component (Patel & Harris, 1995).

### **1.11 Primary Biliary Cirrhosis**

Primary biliary cirrhosis (PBC) is a chronic cholestatic autoimmune liver disease causing inflammatory destruction of the intrahepatic biliary epithelial cells lining the intrahepatic bile ducts resulting in cirrhosis and liver failure. It is characterised by a high titre of serum anti-mitochondrial autoantibodies (AMA). The primary target for these autoantibodies was identified as being the E2 component of PDC (Gershwin *et al*, 1987; Yeaman *et al*, 1988). It was also found that these autoantibodies inhibit enzyme function (Van de Water *et al*, 1988). Since the identification of the major autoantigen in this disease, a further five proteins have been detected that cross-react with sera from patients with PBC. PBC sera reacts against the E3-binding protein (Yeaman *et al*, 1988; Surh *et al*, 1989) and cross-reactivity was demonstrated for the E2 components of OGDC and BCOADC (Fussey *et al*, 1988) in a significant number of patients. The 2 subunits of PDC-E1 have also been identified as autoantigens

(Fussey *et al*, 1989). These autoantigens are collectively known as the M2 antigens.

There are currently no reports of antibodies being present to the E3 subunit.

The main immunogenic region on E2, recognised in 95% of patients, has been mapped to the inner lipoyl domain (Fussey *et al*, 1990) with the dominant epitope spanning the lipoic acid binding site. These workers also demonstrated that the lipoyl moiety itself appears to play a role in antibody recognition. Subsequently, an antigen was identified at the plasma membrane of biliary epithelial cells isolated from the livers of patients with PBC, which was postulated to be the E3BP component of PDC (Joplin *et al*, 1997). Further work indicated that both E2-PDC and E3BP are aberrantly expressed at the cell surface of biliary epithelial cells in patients with PBC (Joplin & Gershwin, 1997). The mechanism by which these autoantigens become either up-regulated or aberrantly expressed at the plasma membrane is, as yet, unknown.

### **1.12 Protein targeting**

The fully assembled 2-oxoacid dehydrogenase complexes are found loosely associated with the mitochondrial inner membrane (Maas & Bisswanger, 1990). Since all the components of these complexes are nuclear-encoded, these polypeptides must be targeted to the mitochondrion. Each polypeptide is synthesised as a larger  $M_r$  precursor protein containing an N-terminal leader sequence. These sequences have a number of common features. They tend to be between 20 and 40 amino acids in length, are rich in positive amino acids and are predicted to form amphipathic  $\alpha$ -helices (see Neupert, 1997 for review). After synthesis on cytoplasmic ribosomes these precursor proteins are transported in a loosely folded state to receptor sites on

the mitochondrial outer membrane. The presequence then interacts with the membrane receptor and directs the polypeptide's signal sequence into the translocation channel. The mechanism by which this process occurs is still unclear but in mitochondria, an intact transmembrane electrochemical gradient and ATP is thought to be required (Schatz & Dobberstein, 1996).

Members of the Hsp70 family of molecular chaperones (discussed in section 1.13) are believed to be essential in promoting formation of translocation-competent precursors by binding to them and thus preventing premature aggregation of the polypeptides. This may happen by two means, by binding to the unfolded mature part of the precursor protein, but also perhaps by binding to the presequence itself (Endo *et al*, 1996). This, essentially, would prevent the presequence from interacting with the newly synthesised protein and hence prevent aggregation of the precursor.

The Hsp70 family of proteins has also been implicated in the transport of unfolded polypeptides across the mitochondrial membrane. As the polypeptide chain crosses the membrane, mitochondrial Hsp70, located on the trans side of the inner membrane, interacts with segments of the chain as it enters the matrix of the mitochondrion and, by hydrolysis of ATP, pulls the polypeptide across the membrane. Only when the complete chain has entered the mitochondrial matrix does protein folding take place (Hartl, 1996).

Once the polypeptides have reached their destination in the mitochondrial matrix maturation of the polypeptide occurs by cleavage of the presequence. This allows the

mature protein to begin folding and assembly into its active form. Molecular chaperones are also believed to be required for this process.

### **1.13 Molecular chaperones**

The original definition of a molecular chaperone was that of a group of proteins that mediate the correct assembly of other proteins but are not themselves components of the final functional structures (Ellis *et al*, 1987). More recently, chaperones have been defined as proteins that bind to and stabilise an unfolded conformation of a protein and by controlled binding and release aid its folding, oligomeric assembly or targeting to the correct cellular location (Hartl, 1996). Molecular chaperones occur ubiquitously in both prokaryotes and eukaryotes and are present within organelles as well as in the cytosol. Perhaps the most common molecular chaperones are those belonging to the Hsp70 and Hsp60 families, the heat shock proteins.

#### **1.13.1 The Hsp70 family of molecular chaperones**

The Hsp70 molecular chaperones are a family of highly conserved ATPases that are found in both prokaryotes and in most organelles of eukaryotic cells. Members of this family include the bacterial DnaK. Although they are termed heat shock proteins, they also have essential functions under normal cellular conditions although their expression is up-regulated during times of stress. The basic function of this family of proteins is to bind and release hydrophobic segments of an unfolded polypeptide chain in an ATP-dependent manner. They achieve this with the help of other molecular chaperones such as DnaJ, an Hsp40 member and GrpE, a nucleotide-exchange factor.

### 1.13.2 The Hsp60 family of molecular chaperones

The Hsp60 family of stress proteins (chaperonins) are constitutively expressed and are found mainly in the bacterial cytosol, the stroma of chloroplasts and the mitochondrial matrix. These proteins (GroE) are the major heat-shock proteins in *E. coli*. GroEL is perhaps the best studied of this particular group of proteins. Electron microscopy and x-ray crystallography have shown that GroEL is a large cylindrical complex consisting of 14 subunits arranged in 2 heptameric rings with a central cavity where polypeptide binding and folding occurs (Xu *et al*, 1997).

It is thought that GroEL promotes the productive folding of polypeptides through one of two mechanisms. The first involves the binding of non-native polypeptides in the central cavity of GroEL. This effectively avoids aggregation of proteins and can also allow kinetically trapped intermediates to unfold enabling them to undergo more productive folding pathways. The second mechanism is to promote folding of the polypeptide in the central cavity formed by GroEL and which is capped at one end by GroES (Xu *et al*, 1997). GroEL and GroES function cooperatively to bind and aid unfolded polypeptides to fold into their native conformation. As with the Hsp70 family of molecular chaperones, this process requires ATP.

Unfolded polypeptides interact with GroEL through multiple rounds of ATP hydrolysis-mediated GroES binding and release indicating that folding of polypeptides to their native state requires multiple rounds of folding and structural rearrangement (Mayhew *et al*, 1996).

#### **1.13.4 Mechanism of action of GroEL-GroES**

GroEL and GroES form an asymmetric complex where 1 GroES ring binds one end of the GroEL cylinder. The mechanism of action of GroEL-GroES is shown schematically in Figure 1.10 and described in the legend.

#### **1.14 Aims of this thesis**

Knowledge and understanding of the effects of mutations on the individual subunits of the human pyruvate dehydrogenase complex has been greatly increased in recent years by the generation of cDNAs for each enzyme subunit. This has allowed mutations to be characterised both at the genetic and biochemical level. However, our level of understanding would be greatly enhanced by the generation of a recombinant model of the human pyruvate dehydrogenase complex, which could be used to mimic naturally occurring mutations found at the genetic level. The construction of a recombinant model of human PDC is the central aim of this thesis.

In order to achieve this objective it was first necessary to devise a strategy for the successful cloning and overexpression of the individual subunits of PDC in active form (Chapter 3). Development of a reproducible purification protocol was also required before any studies could be undertaken (Chapter 4).

Studies on the E3-binding protein (E3BP) focus on assessing its stability as an independent entity as examined by circular dichroism and protein fluorescence analysis. Also of great interest is the nature of the association and stoichiometry of binding between E3BP and E2 in order to form the structural core of the complex (Chapter 5).

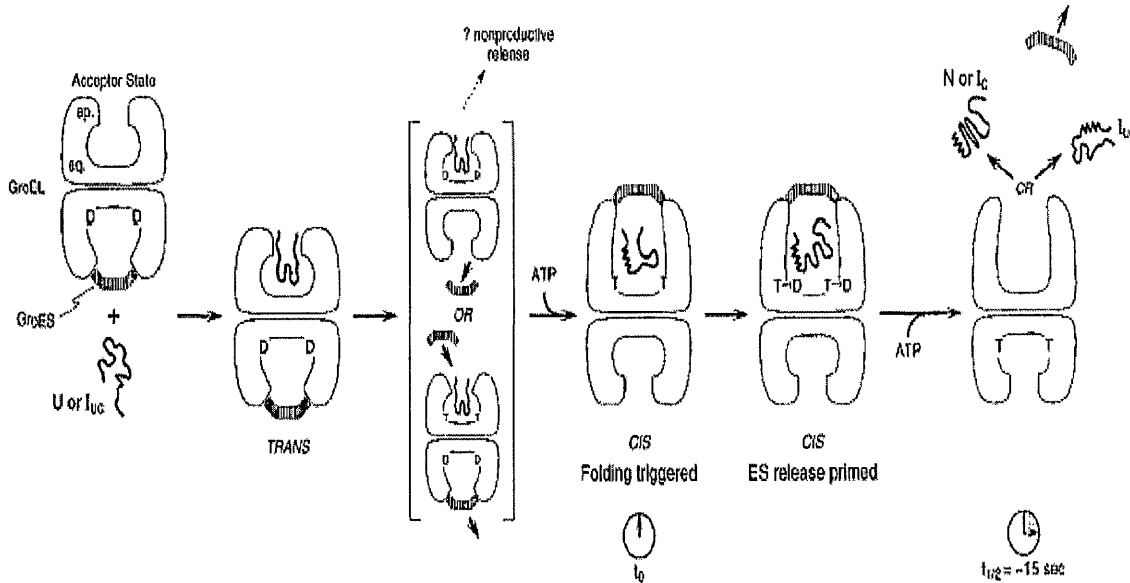


**Figure 1.10 Model for a GroEL-GroES-mediated folding reaction.**

(Taken from Bukau & Horwich, 1998)

The asymmetric GroEL-GroES complex (seen in panel 1) binds unfolded polypeptides or kinetically trapped intermediates to form a trans ternary complex (panel 2). Binding of GroES to the ring containing polypeptide in the presence of ATP (panel 4) initiates release of polypeptide from the binding sites within the cavity thus allowing folding to begin. ATP hydrolysis in the cis ring (panel 5) weakens the interaction between GroEL and GroES so that when ATP binds in the trans ring GroES is released from the complex. This allows the polypeptide to leave the complex.

Binding studies, performed using isothermal titration calorimetry, were also carried out to assess the affinity and stoichiometry of binding between E3BP and E3, and the E2 didomain and E3. A GST construct encoding the subunit-binding domain of E3BP was also utilised in these studies (Chapter 6). This was carried out in order to determine the stoichiometry of binding between E3BP and E3 and thus the number of E3 dimers present in each complex. It was also used to confirm previous work, which showed that E2-PDC has retained a residual ability to bind E3 but the affinity of binding between these two proteins is very much weaker than that between E3 and E3BP (Susan D. Richards, PhD thesis).

This thesis also describes the major difficulty, the purification of soluble E1 in the absence of detergent, and thus the rate-limiting step, in producing a recombinant model of the human pyruvate dehydrogenase complex (Chapter 4).

# **Chapter 2**

## **Materials and Methods**

## **2.1 Molecular Biology Materials**

### **2.1.1 Enzymes and kits**

All restriction enzymes, T4 DNA ligase, calf intestinal alkaline phosphatase, dNTPs and *Taq* DNA polymerase were obtained from Promega or Roche. *Pfu* DNA polymerase was purchased from Stratagene.

The Wizard SV Minipreps DNA Purification System was supplied by Promega while the QIAquick gel extraction kit was purchased from Qiagen.

### **2.1.2 Molecular weight markers**

The 1kb molecular mass DNA markers used in agarose gel electrophoresis were supplied by Promega.

### **2.1.3 Oligonucleotides**

Oligonucleotides were designed in the laboratory and synthesised by Genosys Biotechnologies Ltd. or Life Technologies, Paisley.

### **2.1.4 Bacterial Media**

Cultures were grown in LB (10g bacto-tryptone, 10g NaCl, 5g yeast per litre). Media were autoclaved before use and supplemented with ampicillin (50µg/ml), kanamycin (30µg/ml) or chloramphenicol (34µg/ml) where necessary. Growth media for bacterial cultures were purchased from Oxoid Ltd., Basingstoke.

### **2.1.5 Bacteria and plasmid vectors**

Generally, three strains of *E. coli* were employed. DH5α cells were used for the propagation of plasmid vectors while BL21 (DE3) pLysS or BL21 (DE3) CodonPlus cells (Stratagene) were used for the expression of proteins from plasmids containing the T7 promoter.

The pET vectors were bought from Novagen and pGEX-2T, used for expression of GST-fusion proteins in *E. coli*, was supplied by Pharmacia (see Figures 2.1a-d).

## 2.2 Molecular Biology Methods

### 2.2.1 Polymerase Chain Reaction (PCR)

Polymerase chain reaction (PCR) was performed using either *Taq* DNA polymerase or *Pfu* DNA polymerase.

#### 2.2.1.2 PCR using *Taq* DNA polymerase

PCR was performed on a Perkin Elmer Thermal Cycler in 0.5ml thin-walled PCR tubes. A typical 50 $\mu$ l reaction mix contained Taq buffer, 2mM MgCl<sub>2</sub>, 250 $\mu$ M of each dNTP, 250ng each of the appropriate primers, approximately 100ng of DNA template and 3 units of Taq DNA polymerase. The reaction mix was kept on ice until ready for PCR amplification. A typical reaction cycle consisted of:

Step	Temperature (°C)	Time
1 Denaturation	95	3 min
2 Denaturation	95	30s
3 Annealing	55	30s
4 Extension	72	1 min
Steps 2-4 repeated for 30 cycles.		
5 Extension	72	10 min

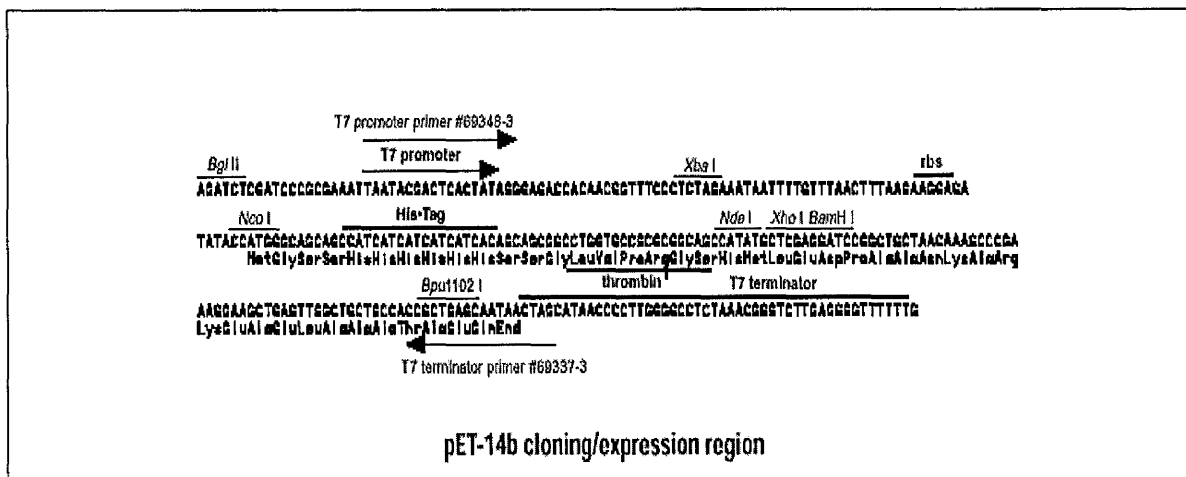
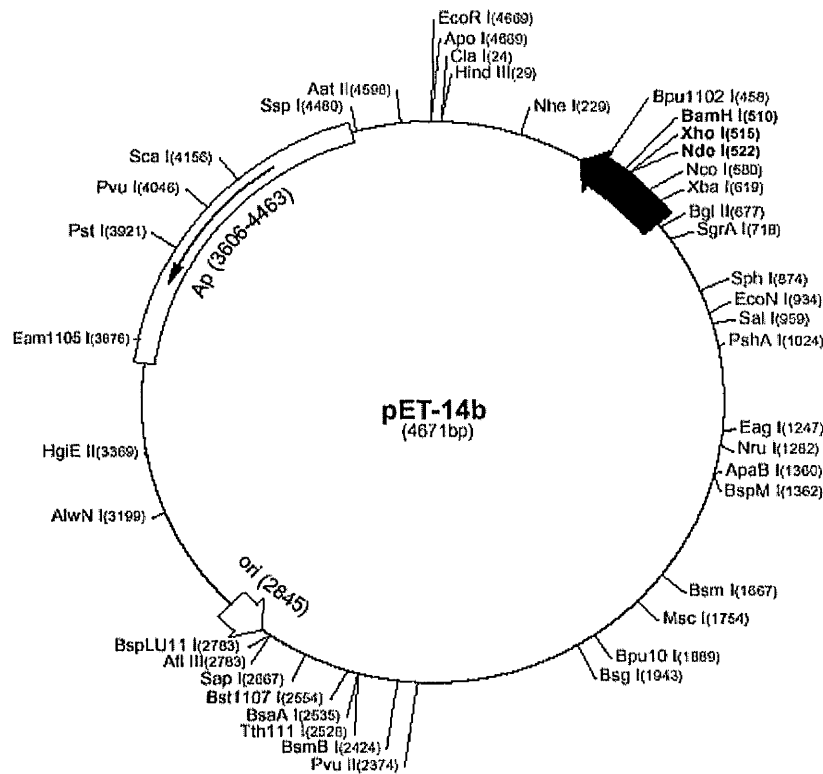


**Fig 2.1a Map of the expression vector pET-14b**

The pET-14 vectors carry an N-terminal His-tag and a BamHI restriction site in the multiple cloning region. The circular map shows the unique sites while the cloning region transcribed by the T7 RNA polymerase is shown below. This plasmid is numbered by the pBR322 convention.



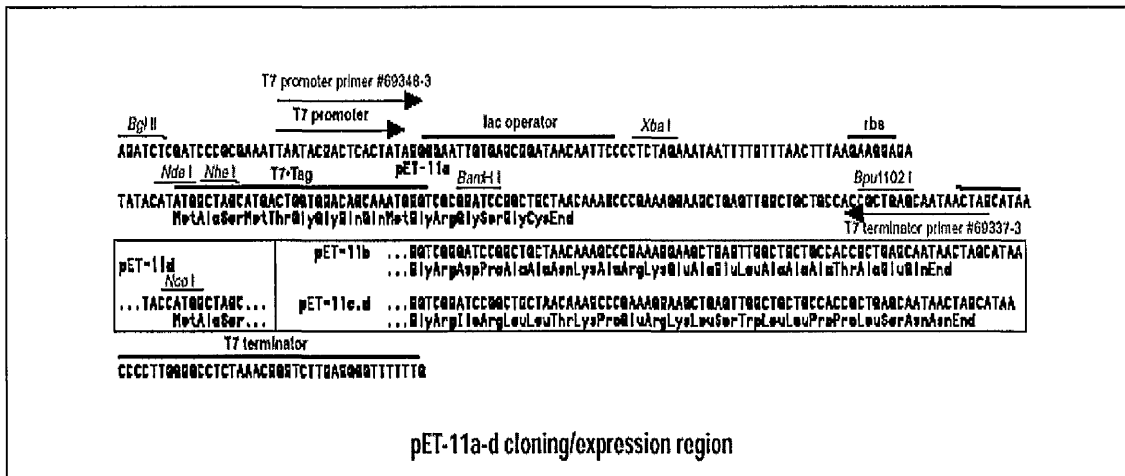
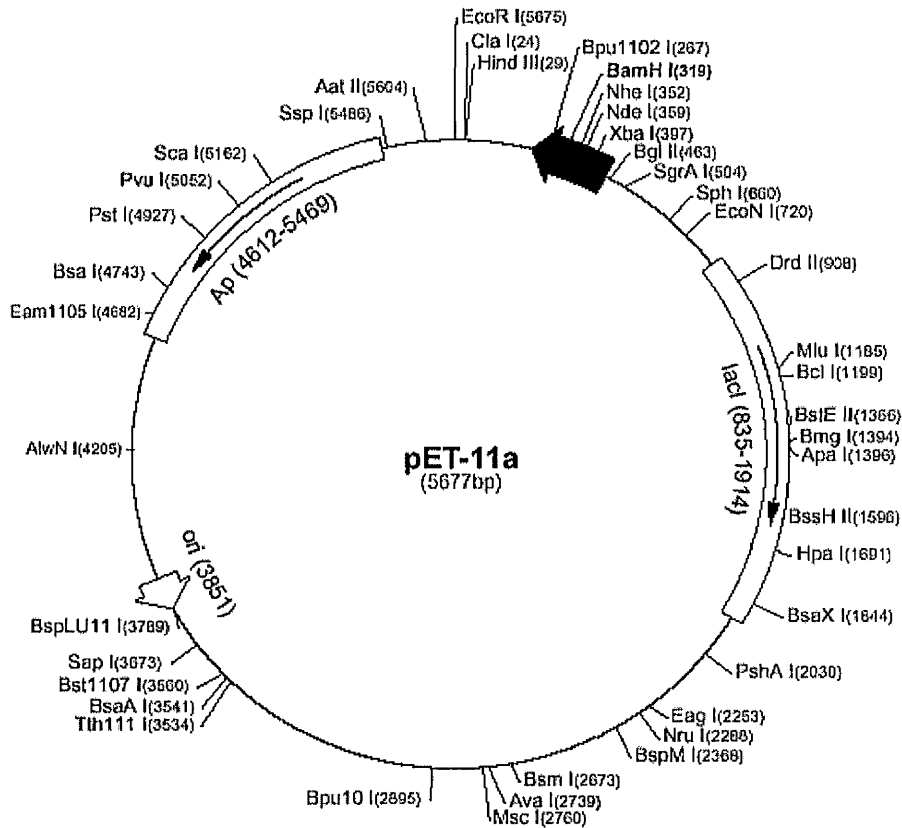
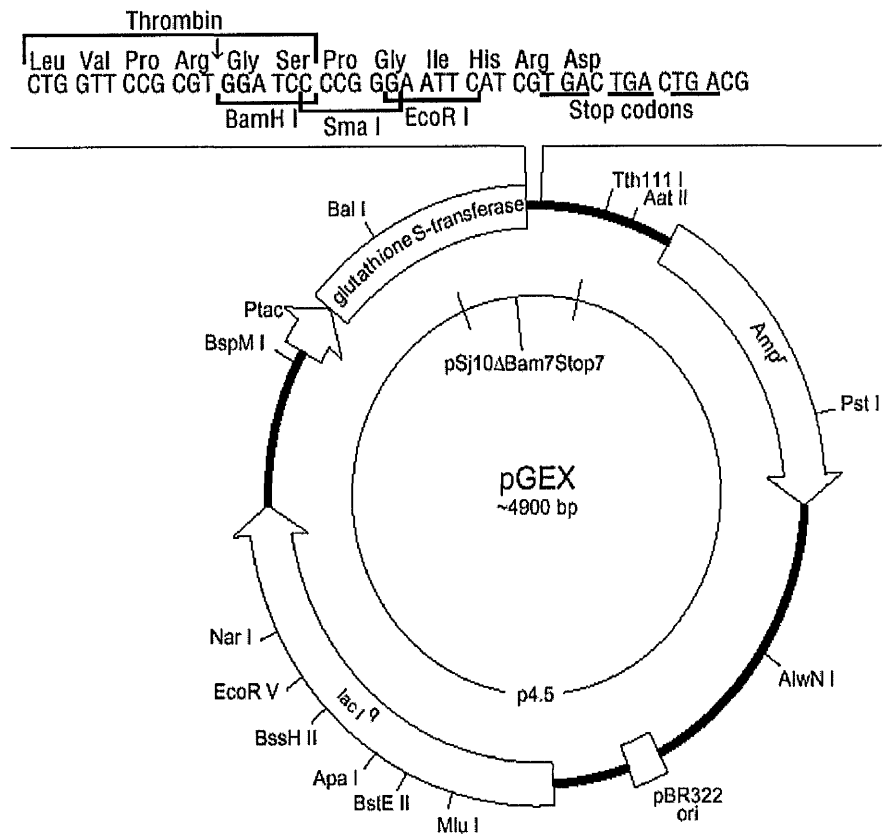


Fig 2.1c Map of the pET-11a vector

The pET-11 vectors carry an N-terminal T7•Tag and BamHI cloning site. Unique sites are shown on the circular map. The cloning/expression region transcribed by T7 RNA polymerase is shown below. pET-11b differs from pET-11a in that it is a 5676bp plasmid. 1bp is subtracted from each site beyond BamHI as position 319.



**Fig 2.1d Map of the glutathione S-transferase fusion vector, pGEX-2T**

The map shows the main features of the multiple cloning site. This vector contains a tac promoter for chemically inducible expression. A thrombin cleavage site is located upstream from the multiple cloning site for cleavage of the target protein from GST.

### 2.2.1.3 PCR using *Pfu* DNA Polymerase

PCR using *Pfu* DNA polymerase was performed as above with the following modifications.

A typical 50 $\mu$ l reaction volume contained 10X reaction buffer (200mM Tris-HCl, 20mM MgSO<sub>4</sub>, 100mM KCl, 100mM (NH<sub>4</sub>)<sub>2</sub>SO<sub>4</sub>, 1% (v/v) Triton X-100, 1mg/ml nuclease-free BSA) at a final concentration of 1X, 250 $\mu$ M of each dNTP, 250ng of the appropriate primers, 100ng of DNA template and 2.5 units of *Pfu* DNA polymerase. Typical cycle parameters were as follows:

Step	Temperature (°C)	Time
1 Denaturation	95	1 min
2 Annealing	55	1 min
3 Extension	72	2 min/kb template DNA
4 Denaturation	95	1 min
Steps 2-4 repeated for 30 cycles		
5 Extension	72	10 min

The quality and quantity of the PCR product obtained was analyzed by agarose gel electrophoresis.

### 2.2.2 Restriction Digestion

Plasmid and PCR products were routinely digested with BamHI before ligation. DNA (15 $\mu$ l) was digested in a reaction mix containing 3 $\mu$ l of BamHI, 3 $\mu$ l of the appropriate enzyme buffer (5mM MgCl<sub>2</sub>, 100mM NaCl, 1mM 2-mercaptoethanol in 10mM Tris-HCl, pH 8.0) in a final volume of 30 $\mu$ l. This was incubated at 37°C for 3h.

### 2.2.3 Dephosphorylation of digested plasmid

Digested vector was dephosphorylated by the addition of 1 unit of calf intestinal alkaline phosphatase. This was incubated at 37°C for 30 min.

### 2.2.4 Production of Competent Cells

Competent cells were made using the rubidium chloride method.

The appropriate bacterial *E. coli* strain was streaked overnight on a minimal LB plate. A single colony was used to inoculate a 5ml overnight culture. This was subcultured into 100ml LB and grown at 37°C with shaking until the culture reached an optical density of 0.48 at 550nm. The culture was then chilled for 5 min before centrifugation at 3000rpm for 10 min at 4°C. The pellet was resuspended in 40ml buffer 1 (100mM rubidium chloride, 10mM calcium chloride, 50mM manganese chloride, 15% (v/v) glycerol in 30mM potassium acetate, pH 5.8). Cells were centrifuged as before and the pellet resuspended in 4ml buffer 2 (75mM calcium chloride, 10mM rubidium chloride, 15% (v/v) glycerol in 10mM MOPS, pH 6.5). The cells, now competent, were divided into aliquots and stored at -80°C.

### 2.2.5 Transformation of competent bacteria

To 50µl of competent bacteria, 1-10ng of DNA was added. The mixture was chilled for 15 min before heat shocking at 42°C for 90s and returning to ice. After 2 min LB medium (450µl ) was added and this was incubated at 37°C with shaking for 45 min. This mix was plated on an LB plate containing the appropriate antibiotic and incubated overnight at 37°C.

### 2.2.6 Purification of DNA from bacterial cultures

DNA was purified from bacterial cultures using the Wizard SV DNA Minipreps kit supplied by Promega. The kit was used as per the manufacturer's instructions. Briefly, a 5ml overnight culture containing the appropriate antibiotic was inoculated with a single colony from an LB-antibiotic plate. This was incubated with shaking at 37°C for not more than 16h. Cells were

pelleted at 10,000rpm for 5 min and resuspended in 250µl Cell Resuspension Solution (50mM Tris-HCl, 10mM EDTA, 100µg/ml RNase A). Cells were lysed by the addition of 250µl Cell Lysis Solution (0.2M NaOH, 1% (w/v) SDS) and incubated for 5 min in the presence of 250µg alkaline protease to inactivate any endonucleases released during cell lysis. 350µl Cell Neutralisation buffer (4.09M GdmHCl, 0.759M potassium acetate, 2.12M glacial acetic acid) was added and the mixture was centrifuged at 10,000rpm for 10 min in a benchtop centrifuge to pellet the cell debris. Supernatant was applied to a spin column and centrifuged briefly to allow the DNA to bind to the membrane of the spin column. The column was washed twice with Column Wash Solution (60mM potassium acetate, 10mM Tris-HCl, 60% (v/v) ethanol). before the DNA was eluted in 70µl nuclease-free water. The quality and quantity of DNA obtained was analysed by agarose gel electrophoresis.

### **2.2.7 Agarose Gel Electrophoresis**

The appropriate amount of agarose was dissolved in 1XTAE (40mM Tris, 1mM EDTA 40mM glacial acetic acid) to give slab agarose gels of the required percentage. Samples for analysis were diluted 5 fold by the addition of loading buffer (0.25% (w/v) bromophenol blue, 0.25% (w/v) xylene cyanol FF, 15% (w/v) Ficoll) before being loaded on the agarose gel. These were run at 100V/250mA for between 40 min to 1h until the dye front was about 1cm from the bottom of the gel. Gels were then stained with a small volume of ethidium bromide before being viewed using a UV transilluminator.

### **2.2.8 Extraction of DNA from an Agarose Gel**

DNA was purified from agarose gels using the QIAquick gel extraction kit (Qiagen) as described in the manufacturer's instruction.

Briefly, DNA was excised from an agarose gel using a sterile scalpel blade. The agarose slice was solubilized at 50°C in the appropriate volume of Buffer QG (as supplied) and 1 gel volume of isopropanol added. This mixture was applied to a spin column and centrifuged for

1 min to allow the DNA to bind to the column. The column was washed with 750 $\mu$ l of Buffer PE containing 80% (v/v) ethanol. Residual ethanol was removed by centrifuging the column for a further 2 min before eluting the DNA in 50 $\mu$ l of Buffer EB (10mM Tris-HCl, pH 8.5). The quantity and quality of DNA obtained was analyzed by agarose gel electrophoresis.

### **2.2.9 Ligations**

In order to clone the insert of interest into the appropriate vector a series of ligation reactions were set up. In each case, 1.5 $\mu$ l of BamHI-digested, dephosphorylated and gel purified vector was mixed with different quantities of BamHI-digested insert, 10X T4 DNA ligase buffer (100mM MgCl<sub>2</sub>, 100mM DTT, 10mM ATP, 300mM Tris-HCl pH 7.8) at a final concentration of 1X and 1U of T4 DNA ligase. These were incubated at room temperature overnight before being transformed into *E. coli* DH5 $\alpha$  competent cells following the standard protocol above. The resulting colonies were then screened to check for the presence of the insert of interest.

#### **2.2.10.1 Growth of bacterial cultures for protein induction**

A single colony was picked from an LB-agar antibiotic plate and grown at 37 $^{\circ}$ C with shaking in 5ml growth media plus antibiotic for 16h. An aliquot was subcultured into 50ml growth media plus antibiotic and incubated at 37 $^{\circ}$ C with shaking until the A<sub>600</sub> was between 0.5-1.0. IPTG (1mM) was then added and the cultures were induced at 30 $^{\circ}$ C for 3h. If lipoic acid supplementation was required this was added to the growth media at the time of induction. Samples were taken at 1h time intervals to check for overexpression. These were pelleted by centrifugation and the pellets resuspended in Laemmli sample buffer (10 $\mu$ l per 0.1 A<sub>600</sub> units). Cells were harvested by centrifugation.

### **2.2.10.2 Large scale protein induction**

A single colony was picked from an LB-agar antibiotic plate and grown at 37°C with shaking in 10ml growth media plus antibiotic for 16h. This was then subcultured into 500ml growth media plus antibiotic and grown at 37°C with shaking until the  $A_{600}$  reached 0.5-1.0. Protein expression was induced by the addition of 1mM IPTG. Lipoic acid (0.2mM) was added at this point if required. Induction typically took place at 30°C for 3h. Samples taken at zero time and 3h were kept for analysis on SDS-PAGE to check that expression had occurred as before. Cells were harvested by centrifugation.

## **2.3 Protein Biochemistry Materials**

### **2.3.1 Chemicals**

Ultra pure imidazole, zinc chloride and the reagents for SDS-PAGE were purchased from BDH Chemicals Ltd., Poole. Ultrapure guanidinium chloride (GdmCl) was supplied by Calbiochem. Polyethylene glycol 6000 (PEG 6000) and Triton X-100 were bought from Fisons, Loughborough.  $NAD^+$ , NADH and acetyl CoA were obtained as sodium salts from Sigma-Aldrich. All other chemicals were of analytical grade or above. Distilled water was of Millipore-Q quality.

### **2.3.2 Molecular weight markers**

Low molecular mass markers for SDS-PAGE were provided by NEB Biolabs.

### **2.3.3 Photographic materials**

Nitrocellulose was purchased from Novagen while the Hyperfilm was obtained from AmershamPharmaciaBiotech, Bucks. The X-Omat-100 processor was supplied by Kodak.

## 2.4 Protein Biochemistry Methods

### 2.4.1 Dialysis of protein samples

Visking tubing was prepared by boiling in 10mM sodium bicarbonate, pH 8.0, 1mM EDTA for 10 min. This was then rinsed in distilled water before being stored in 100% (v/v) ethanol.

Tubing was thoroughly rinsed in distilled water before use.

Dialysis of protein took place at 4°C for several hours using multiple changes of dialysis buffer.

### 2.4.2 Concentration of protein samples

Concentration of proteins took place by one of two methods. After dialysis, protein samples were either concentrated by covering the visking tubing with solid polyethylene glycol-6000 (PEG 6000) and leaving until the required volume of sample was achieved or they were concentrated by centrifugation in a Centricon concentrator (Amicon) according to the manufacturer's instructions.

### 2.4.3 Determination of protein concentration

Protein concentration was determined by one of two methods. The method of Bradford (1976) using the Micro BCA assay system was routinely employed. A standard curve was produced using known concentrations of IgG. The absorbance of the unknown samples were then measured at 595nm and their concentration extrapolated from the standard curve.

For a more accurate determination of protein concentration,  $A_{280}$  measurements were carried out together with amino acid analysis of the protein. The number of tryptophan and tyrosine residues in the protein was determined and the expected  $A_{280}$  of a 1mg/ml solution of the protein calculated by the following equation:

$$\frac{(\text{no. of trp residues} \times 5690) + (\text{no. of tyr residues} \times 1280)}{\text{mol. weight of protein}}$$

A wavelength spectrum was measured for the protein solution from 360-220nm and the absorbance at 280nm noted. The measured  $A_{280}$  was divided by the calculated number to obtain the protein concentration.

## **2.4.4 SDS-polyacrylamide gel electrophoresis (SDS-PAGE)**

### **2.4.4.1 Tris/glycine discontinuous buffer system**

The solutions required for SDS-PAGE were as follows:

Acrylamide solution

29.2% (w/v) acrylamide/0.8% (w/v) bis-acrylamide

Resolving gel buffer (pH 8.8)

0.75M Tris-HCl, 0.2% (w/v) SDS

Stacking gel buffer (pH 6.8)

0.17M Tris-HCl, 0.14% (w/v) SDS

Running buffer (pH 8.3)

0.25M Tris-HCl, 0.95M glycine, 1% (w/v) SDS

10% Tris/glycine gels were routinely prepared. For a 15ml slab gel, acrylamide solution (5ml) and resolving gel buffer (10ml) was mixed with 150 $\mu$ l 10% (w/v) ammonium persulphate and 15 $\mu$ l TEMED. This was poured, overlaid with water and allowed to polymerise for 30 min. Excess liquid was drained and a 5% stacking gel (0.8ml acrylamide, 4.2ml stacking buffer, 60 $\mu$ l 10% (w/v) ammonium persulphate, 6 $\mu$ l TEMED) was poured. The comb was removed just before use and the wells rinsed with distilled water. Samples for analysis on SDS-PAGE were resuspended in Laemmli sample buffer (2% (w/v) SDS, 10% (w/v) sucrose, 62.5mM Tris-HCl, pH 6.8, Pyronin Y dye). DTT (1mM) was added prior to boiling for 5 min to ensure that all proteins were denatured. A portion of each sample (10 $\mu$ l)

was loaded on the gel along with low molecular mass markers. Gels were run using the Atto mini gel kit system at 400V/100mA for 1h or until the dye front was about 1cm from the bottom of the gel.

Gels were then stained (0.1% (w/v) Coomassie Brilliant Blue, 10% (v/v) acetic acid, 50% (v/v) methanol) for 1h and destained in 10% (v/v) acetic acid, 10% (v/v) methanol overnight.

#### **2.4.4.2 Sodium phosphate continuous buffer system**

Solutions required for SDS-PAGE were as above with the following exception:

Sodium phosphate gel buffer (pH 7.0)

17.7mM NaH<sub>2</sub>PO<sub>4</sub>·2H<sub>2</sub>O

6.95mM Na<sub>2</sub>HPO<sub>4</sub>

Sodium phosphate gels (6%) were prepared by mixing the acrylamide (3ml) and sodium phosphate buffer (12ml) with 0.2% (w/v) SDS, 150µl 10% (w/v) ammonium persulphate and 15µl TEMED. This was poured, the comb inserted and the gel allowed to polymerise. For the tank buffer, sodium phosphate buffer and dH<sub>2</sub>O were mixed in a 1:1 ratio and 0.2% (w/v) SDS added. Samples for analysis on the continuous buffer system were resuspended in Laemmli buffer as above and DTT (1mM) added before boiling for 5 min. Gels were run at 400V/50mA before being stained and destained as described above.

#### **2.4.5 Immunoblotting using ECL<sup>TM</sup> chemiluminescence**

##### **2.4.5.1 Solutions used in immunoblotting**

Transfer buffer (10X) per litre

30.3g Tris, 144g glycine, 2g SDS

Blocking solution

20mM Tris-HCl, pH 7.2, 15mM NaCl, 5% (w/v) non-fat milk, 5% (v/v) normal donkey serum, 0.2% (v/v) Tween 20

**Primary antibody solution**

20mM Tris-HCl, pH 7.2, 1% (w/v) non-fat milk, 1% (v/v) normal donkey serum, 0.1% (v/v)

Tween 20,

1:2500 dilution of primary antibody

**Wash solution**

20mM Tris-HCl, pH 7.2, 15mM NaCl, 1% (w/v) non-fat milk, 1% (v/v) normal donkey

serum

**Secondary antibody solution**

20mM Tris-HCl, pH 7.2, 150mM NaCl, 1% (w/v) non-fat milk, 1% (v/v) Tween 20,

1:1000 dilution secondary antibody

**2.4.5.2 Immunoblotting protocol**

SDS-PAGE analysis was performed as described in section 2.4.4. Proteins were then transferred to nitrocellulose overnight using transfer buffer at a concentration of 1X plus 20% (v/v) methanol. Transfer took place electrophoretically using the BioRAD immunoblotting tank at 400V/45mA overnight. The efficiency of protein transfer was checked by staining the nitrocellulose with the non-fixative dye Ponceau S. This was then washed off and the non-specific binding sites were blocked by immersing the nitrocellulose in blocking solution for 1h at room temperature with shaking. The membrane was incubated in diluted primary antibody solution at room temperature for 1h and then washed extensively with 4 changes of wash solution before incubation in the secondary antibody solution, a horseradish peroxidase (HRP)-labelled antibody, for a further 60 min. The nitrocellulose was washed 4 times and excess buffer drained from the membrane before detection.

Equal quantities of ECL solution 1 and ECL solution 2 were added to the membrane,

incubated for 1 min and then drained. In the dark room autoradiography film was placed over the membrane and exposed for 15s before developing the film using a Kodak X-Omat-100 processor.

#### **2.4.6 Purification of GST-fusion proteins**

GST-fusion proteins were purified on a glutathione Sepharose 4B column.

##### **2.4.6.1 Preparation of bacterial extracts**

The pellet from a 50ml bacterial cell culture was resuspended in 3.5ml PBS (140mM NaCl, 2.7mM KCl, 10mM NaHPO<sub>4</sub>, 1.8mM KH<sub>2</sub>PO<sub>4</sub>, pH 7.3) and sonicated in 10s bursts on ice to disrupt the cells. Triton X-100 (1% v/v) was added and the extract mixed with gentle agitation for 30 min to aid solubilisation of the protein. The supernatant was clarified by centrifugation at 10,000rpm for 15 min at 4°C.

##### **2.4.6.2 Column purification**

Clarified supernatant was applied to a 2x1cm glutathione Sepharose 4B column and the matrix washed extensively with PBS. To elute the target protein, the column was incubated in 2ml glutathione elution buffer (10mM reduced glutathione in 50mM Tris-HCl, pH 8) for 10 min. Eluted protein was collected in 1ml fractions. Column elution was repeated 4 times. Samples of the sonicate, supernatant, pellet and the collected fractions were analyzed using SDS-PAGE as before.

#### **2.4.7 Purification of His-tagged proteins**

For purifying His-tagged proteins the BioCAD Perfusion Chromatography System (PE BioSystems) was employed.

### 2.4.7.1 Preparation of bacterial cell extracts

Bacterial cell extracts were prepared by disrupting the cells under high pressure using a French Pressure cell. Pellets from bacterial cell cultures were resuspended in an appropriate volume of starting buffer (1M NaCl, 0.5mM imidazole in 20mM potassium phosphate, pH 8). Cells were disrupted by passing the extract through the French Press at 950psi. Several passes were made and protease inhibitors were added to prevent degradation of protein. The supernatant was clarified by centrifugation at 10,000rpm for 15 min.

### 2.4.7.2 Purification of His-tagged proteins

His-tagged proteins were purified using a POROS metal chelate column (PE BioSystems). The column was prepared by loading the imidoacetate binding sites with zinc ions (0.1M ZnCl<sub>2</sub>, pH 4.5-5) for 25 column volumes and then washing with distilled water followed by 0.5M NaCl to remove any excess metal ions. The column was then washed with 5 column volumes of elution buffer (1M NaCl, 500mM imidazole in 20mM potassium phosphate, pH 6). Finally the column was equilibrated with starting buffer (1M NaCl, 0.5mM imidazole, 20mM potassium phosphate, pH 8) before use.

Clarified supernatant was loaded on to the column in 5ml increments. After extensive washing of the column in starting buffer bound his-tagged protein was eluted in a linear imidazole gradient and 2ml fractions collected. Elution of the protein was monitored by measuring the absorbance at 280nm. After all protein had eluted, the column was regenerated by washing it with 15 column volumes of stripping buffer (50mM EDTA, 1M NaCl).

The appropriate fractions were precipitated with TCA (trichloroacetic acid) and analyzed on 10% SDS polyacrylamide gels.

### 2.4.8 TCA precipitation of proteins

Protein fractions were subjected to TCA precipitation before analysis by SDS-PAGE. TCA (10% v/v) was added to aliquots of protein fractions and incubated at 4°C for 30 min. Samples were centrifuged at 10,000rpm for 15 min at 4°C and the pellets washed with 500µl ice cold acetone. Samples were centrifuged as before and the pellets allowed to air dry before resuspending them in 20µl Laemmli sample buffer. These were then subjected to SDS-PAGE analysis.

### 2.4.9 Purification of pyruvate dehydrogenase from bovine heart

Isolation of the complexes from bovine heart were performed at 4°C following the standard protocol (Stanley & Perham, 1980) with the modifications described here. To 600g of diced heart tissue, two volumes of ice cold extraction buffer (50mM MOPS, pH 7.0, 3% (v/v) Triton X-100, 2.7mM EDTA, 0.1mM DTT, 1mM PMSF, 1mM benzamide, 0.2% (v/v) anti-foam A) was added. After homogenising for 5 min, the volume was made up to 2l with more buffer and clarified at 10,000g for 20 min. The pH of the supernatant was adjusted to 6.45 using 10% (v/v) acetic acid and the first PEG precipitation performed by the addition of 0.12 volumes of 35% (w/v) PEG. This was stirred on ice for 30 min before being pelleted at 18,000g for 15 min. The pellets were resuspended by homogenisation in 400ml of 1% (v/v) Triton X-100 buffer (as above with the addition of 1.5µM leupeptin) and the pH adjusted to 6.8, before clarification at 25,000g for 40 min.

The resulting supernatant was filtered through layers of muslin before adding 0.013 vol of 1M MgCl<sub>2</sub> and 0.05 vol 1M sodium phosphate buffer (pH 6.3). The pH was maintained at 6.8 by the addition of 0.5M NaOH. 10% (v/v) acetic acid was used to readjust the pH to 6.45 before adding another 0.12 vol of 35% (w/v) PEG and stirring the supernatant on ice for 30 min. After clarification at 25,000g for 10 min, the complexes were resuspended by homogenisation in 160ml of 1% (v/v) Triton X-100 buffer (pH 6.8) with the addition of fresh

solutions of 1mM PMSF, 1mM benzamidine, 1 $\mu$ M leupeptin and 0.5% (v/v) rat serum. This was stored at 4°C overnight.

The following day, re-homogenisation took place before clarifying the supernatant at 25,000g for 1h. The pH of the supernatant was adjusted to 6.45 by the addition of 10% (v/v) acetic acid and a third PEG precipitation step performed. 0.04-0.06 vol of 35% (w/v) PEG was added and stirred for 30 min on ice. Centrifugation at 25,000g for 10 min allows OGDC, insoluble at the PEG concentration used in this step, to be separated from PDC, which remains in the supernatant. PDC can then be pelleted by ultracentrifugation at 200,000g for 2.5h. Both PDC and OGDC were resuspended in 1% (v/v) Triton X-100 buffer and stored at 4°C.

#### **2.4.10 Gel filtration**

Purified proteins were dialysed into 50mM potassium phosphate, pH 7.2 containing 150mM NaCl, 1mM DTT before being applied to a gel filtration column. Gel filtration was performed on a Superose 6 (HR 10/30) column attached to a Pharmacia FPLC system. The column was equilibrated in 2 column volumes of 50mM potassium phosphate, pH 7.2, 150mM NaCl, 1mM DTT at a flow rate of 0.5ml/min. A protein sample, typically 500 $\mu$ l, was loaded onto the column and the absorbance at 280nm monitored. Peak fractions were collected, subjected to TCA precipitation and analysed by SDS-PAGE as described above.

#### **2.4.11 Protein crosslinking**

Proteins dialysed in 50mM potassium phosphate, pH 7.2 were subjected to crosslinking with 25% (w/v) glutaraldehyde, a non-specific crosslinker. The protein/glutaraldehyde mixture was incubated on ice for 2 min before 2mM NaBH<sub>4</sub> was added. This was incubated for 20 min before the reaction was terminated by the addition of 10% (w/v) sodium deoxycholate. Crosslinked proteins were precipitated with 100% (w/v) TCA as described in section 2.3.8,

dissolved in Laemmli sample buffer and analysed on a 6% sodium phosphate-buffered SDS-polyacrylamide gel.

#### **2.4.12 Solubilization of inclusion bodies**

The following method is adapted from the Protein Folding kit (Novagen).

##### **2.4.12.1 Preparation of inclusion bodies**

After induction in *E. coli* and expression of the desired protein, the cells were pelleted as normal and resuspended in 0.1 culture volume of IB wash buffer (10mM EDTA, 1% (v/v) Triton X-100 in 20mM Tris-HCl, pH 7.5). Cells were disrupted by passage through a French press and insoluble material pelleted by centrifugation at 10,000rpm for 15 min at 4°C. The pellet was then washed a further twice in IB wash buffer.

##### **2.4.12.2 Solubilization of inclusion bodies**

Inclusion bodies were resuspended in 50mM potassium phosphate, pH 7.5 at a concentration of 10-20 mg/ml and supplemented with an appropriate amount of 30% (v/v) N-lauroylsarcosine to give the desired concentration of detergent in the buffer, typically 0.1-2%. This was incubated at room temperature for 30 min with agitation before clarifying any insoluble material by centrifugation at 10,000rpm for 15 min at 4°C. The supernatant was subjected to dialysis into 50mM potassium phosphate, pH 7.5 in order to remove the detergent from the protein preparation. Samples of the dialysed material were taken for analysis by SDS-PAGE and activity assays.

### **2.4.13 Isothermal titration calorimetry (ITC)**

Isothermal titration calorimetry experiments were conducted on a VP-ITC microcalorimeter (MicroCal Inc., Northampton, MA, USA).

The proteins to be studied were purified as described previously and extensively dialysed into 100mM potassium phosphate pH 7.2 in the same container to minimise any buffer mismatch which can affect the subsequent titration.

One protein (approximately 10 $\mu$ M) was placed in the ITC cell while the second protein, at a concentration of at least 150 $\mu$ M was loaded into the syringe of the microcalorimeter. In a typical ITC experiment automatic injection of protein (10 $\mu$ l) from the syringe into the ITC cell occurs every 3 minutes and a complete experiment usually requires 26 injections. The heat of binding between the 2 proteins is measured directly by the microcalorimeter and the data obtained analysed using Origin software (OriginLab Corporation). For a more detailed explanation refer to chapter 6. These experiments were performed by Mrs Margaret Nutley in the laboratory of Professor Alan Cooper, Glasgow University. Analyses of the data were performed by Professor Alan Cooper.

### **2.4.14 Circular dichroism**

Circular dichroism experiments were performed on a JASCO J-600 spectropolarimeter. Purified E3BP (0.4mg/ml in 150mM sodium fluoride, 50mM potassium phosphate, pH 7.2), was incubated in varying concentrations of guanidinium chloride (0-6M) either for 15 min or overnight before monitoring the change in absorbance in both the near- and far-UV regions of the spectrum. All CD spectra were measured by Dr. Sharon M. Kelly in the laboratory of Professor Nick Price at Glasgow University.

### 2.4.15 Fluorimetry

Fluorescence analysis of E3BP was performed on a Perkin Elmer LS 50B fluorimeter. Purified E3BP (0.4mg/ml in 150mM sodium fluoride, 50mM potassium phosphate, pH 7.2,) was incubated in varying concentration of GdmCl (0-6M) for 15 min at room temperature. The sample was excited at 295nm and the emission spectrum recorded from 310-400nm. Three spectra were recorded for each sample. The data presented in this thesis represent the average of 3 spectra.

### 2.4.16 Enzyme assays

All enzyme assays were performed on a Shimadzu UV-2101 PC uv-vis scanning spectrophotometer. Activities were expressed as U/ml, where one unit (U) of enzyme catalyses the conversion of 1 $\mu$ mol of substrate to product per minute under the specified conditions.

#### 2.4.16.1 Pyruvate dehydrogenase (E1) activity

E1 activity was measured by following the reduction of 2,6-dichlorophenolindophenol (DCPIP) to its colourless form at 600nm. Purified E1 (5-50 $\mu$ g) was added to a cuvette containing 670 $\mu$ l of solution A (3mM NAD<sup>+</sup>, 2mM MgCl<sub>2</sub>, 0.2mM ThDP in 50mM potassium phosphate, pH 7.6) and 14 $\mu$ l of DCPIP, prewarmed to 30°C. The reduction of DCPIP was initiated by the addition of 14 $\mu$ l of solution C (100mM pyruvate). The molar extinction coefficient of DCPIP is 22000 M<sup>-1</sup>cm<sup>-1</sup>.

#### 2.4.16.2 Dihydrolipoamide acetyltransferase (E2) activity

E2 activity was measured by monitoring the formation of acetyldihydrolipoamide at 232nm {Yang *et al*, 1997}. The assay mixture, containing 30mM Tris-HCl, pH 7.4, 1mM acetyl phosphate, 1mM dihydrolipoamide, 20 $\mu$ M CoA and 2 units of phosphotransacetylase were added to a quartz cuvette and the absorbance allowed to settle for 10-15s. The E2 source was then added and the increase in absorbance monitored for 45s at 30°C.

E2 activity is expressed as change in absorbance/min since the extinction coefficient of the immediate product, 8-acetyl-dihydrolipoamide has not been determined accurately.

#### **2.4.16.3 Dihydrolipoamide dehydrogenase (E3) activity**

E3 activity was measured by the formation of NADH from the oxidation of dihydrolipoamide at 30°C. The E3 source was added to a cuvette containing 670µl solution A (3mM NAD<sup>+</sup>, 2mM MgCl<sub>2</sub>, 0.2mM ThDP in 50mM potassium phosphate, pH 7.5) and 20µl dihydrolipoamide (2mM). E3 activity was determined from the increase in absorbance at 340nm. The molar extinction coefficient of NADH was taken to be 6220 M<sup>-1</sup>cm<sup>-1</sup>.

#### **2.4.17 Preparation of dihydrolipoamide**

Dihydrolipoamide was prepared in the laboratory from DL-lipoamide. 60mg of DL-lipoamide was dissolved in 1.2ml of 1M potassium phosphate, pH 8.0, 50% (v/v) ethanol. Addition of 2.4ml of freshly prepared 5% (w/v) sodium borohydride in 10mM NaOH resulted in the reduction of DL-lipoamide to dihydrolipoamide. The reaction was terminated after 10 minutes by the addition of 1.2ml of 3M HCl which neutralises the reaction and destroys any excess reducing agent. The dihydrolipoamide was then extracted into toluene (3x3ml) and, after solvent evaporation under nitrogen, it was stored at -20°C as a white solid.

#### **2.18 Densitometric scanning analysis**

Densitometry was performed on purified recombinant E2/E3BP core and native bovine PDC. Purified protein was resolved by electrophoresis on 10% SDS-PAGE. Gels were stained with Coomassie Brilliant Blue and subjected to densitometric scanning using an Agfa Duoscan gel scanner and ImageQuant version 5.0 software.

## **Chapter 3**

### **Molecular cloning and overexpression of the individual components of the human pyruvate dehydrogenase complex**

### 3.1 Introduction

Significant progress has been made in recent years regarding the elucidation of the structure and function of the individual components of the 2-oxoacid dehydrogenase complexes, in particular those of the pyruvate dehydrogenase complex. However, most of these structural studies have been carried out on the bacterial enzymes and the mammalian PDC, OGDC and BCOADC remain relatively poorly characterised at the atomic level.

Structural information is now available for most of the components of PDC from a number of sources. To date, the 3D-structure of the N-terminal lipoyl domain of PDC-E2 from *A. vinelandii* (Berg *et al*, 1997), *B. stearrowthermophilus* (Dardel *et al*, 1993) and *E. coli* (Green *et al*, 1995b) has been determined by NMR spectroscopy. More recently, this technique was also adopted to determine the 3-dimensional structure of the inner lipoyl domain of PDC-E2 from the human complex (Howard *et al*, 1998). The structure of the peripheral subunit-binding domain of E2 from *B. stearrowthermophilus* (Kalia *et al*, 1993) has also been determined by NMR spectroscopy. The production of truncated constructs encoding the C-terminal domain of E2 from *A. vinelandii* has resulted in the crystal structure of the cubic core being solved to 2.6Å resolution (Mattevi *et al*, 1992; Mattevi *et al*, 1993). The 3D-structure of the 60meric truncated E2 core from *S. cerevisiae* has been modelled at low resolution by means of electron microscopy and image reconstruction (Stoops *et al*, 1992). A similar technique has been adopted to determine the structure of the truncated 60meric core complexed with E3BP at low resolution (Stoops *et al*, 1997). These studies revealed that E3BP was located inside the E2 core with the binding site for E3BP predicted to lie near the inner tip of the E2 trimer.

The E3 components from *A. vinelandii* (Schierbeek *et al*, 1989; Mattevi *et al*, 1991) and *S. cerevisiae* (Toyoda *et al*, 1998) have been successfully crystallised and their structures determined to 2.2Å and 2.7Å resolution respectively. Comparison of this last eukaryotic structure with that of prokaryotic E3 shows that both enzymes have the same basic tertiary structure despite low amino acid homology. The crystal structure of E3 from *B. stearothermophilus* complexed with the subunit-binding domain of E2 has also been solved (Mande *et al*, 1996). The first E3 crystals from a mammalian source, porcine heart, has recently been reported (Toyoda *et al*, 1998b) but as yet, limited structural information is available.

The crystal structure of an  $\alpha_2\beta_2$  heterotetrameric E1 from the BCOADC of *P. putida* represented the first published structure of a heterotetrameric E1 component (Ævarsson *et al*, 1999). A second E1 component, that of the human BCOADC, has also been solved by x-ray crystallography to 2.7Å resolution (Ævarsson *et al*, 2000). In addition, the structure of the  $\alpha_2$  homodimeric E1 from *E. coli* has been determined (Arjunan *et al*, 2002). Crystals have recently been obtained for human PDC-E1 (Ciszak *et al*, 2001) but structural information is not yet available.

Some of the problems associated with studying the 2-oxoacid dehydrogenase complexes result from difficulties in obtaining well-ordered crystals for structural determination. This is thought to be due to the flexibility of the polypeptide chains, in particular the swinging arm of these complexes and the linker regions separating the individual domains of the E2 and E3BP components. Understanding of the roles that the individual domains play in the structure and function of these complexes has been greatly enhanced by the ability to express these domains as individual entities. Not only has this allowed functional studies to be

undertaken, but the three-dimensional structures of a number of domains has now been solved from a variety of organisms, as described above. A more specific problem is that in the native state, E3BP and E2 form a very tightly associated core assembly and can only be separated in the presence of chaotropic agents, such as GdmCl. Reconstitution studies of PDC from bovine heart have shown that under these separation conditions reconstitution of the E2/E3BP core is problematic. Rapid dilution to remove the denaturant has been shown to be incompatible with reintegration of E3BP into the core complex while removing denaturant by slow dialysis results in an E2/E3BP core which is partially depleted in E3BP. However this depleted core can sustain about 30-40% of native PDC activity (McCartney *et al*, 1997).

*not full length*  
The full length cDNA for mammalian E2 was first cloned by Gershwin and coworkers (1987) from a rat liver library as an unidentified antigen which is recognised in the autoimmune disease primary biliary cirrhosis. Detailed analysis of the predicted protein sequence of this unknown antigen subsequently identified it as the E2 component of the mammalian pyruvate dehydrogenase complex (Yeaman *et al*, 1988). The cDNA for the human E2 was then sequenced and cloned (Coppel *et al*, 1988). The individual domains of human E2, specifically the inner and outer lipoyl domains, have been successfully overexpressed as GST fusion proteins in *E. coli* (Quinn *et al*, 1993; Liu *et al*, 1995). More recent studies on the full length mature recombinant human E2 have shown that, in addition to assembling into the dodecahedral structure observed in the native complex, it can also bind the E1 component and support the function of the PDC-associated kinase and phosphatase (Yang *et al*, 1997). However, these investigators were unable to successfully express a recombinant E3BP protein in the absence of E2. In yeast, it was found that recombinant E3BP was sensitive to proteolysis when expressed independently. However, when E3BP was coexpressed with E3 to form a stable E3BP/E3 subcomplex it was found that E3 seemed to confer some protection

against proteolysis on the E3BP component (Maeng *et al*, 1994). This subcomplex was then purified to near-homogeneity before separating the E3BP and E3 components by chromatography in the presence of 5M urea. Human E3 has been cloned and overexpressed as a His-tagged protein by Liu and coworkers (1995) while, most recently, the molecular cloning and overexpression of human E3BP has been reported (Palmer *et al*, 1999; Lee *et al*, 2001).

The E1 component of the human pyruvate dehydrogenase complex (Korotchkina *et al*, 1995) and of both the bovine (Davie *et al*, 1992) and *B. stearothermophilus* branched chain 2-oxoacid dehydrogenase complexes (Lessard & Perham, 1994) have been cloned previously. The composition of the E1 components from these complexes are similar with both existing as  $\alpha_2\beta_2$  heterotetramers. It was found that the correct assembly of the branched chain 2-oxoacid dehydrogenase complex E1 in *E. coli* relies on the presence of additional molecular chaperones GroEL and GroES (Chuang *et al*, 1999). In contrast, successful production of PDC-E1 did not require additional molecular chaperones indicating that the chaperonins naturally present in *E. coli* were sufficient to promote proper folding and assembly of the  $\alpha_2\beta_2$  heterotetramer (Korotchkina *et al*, 1995).

### 3.1.1 Aims of this chapter

- To describe the strategy used to clone the individual components of human PDC.
- To overexpress these recombinant proteins in *E. coli* in active form.

### 3.1.2 Plasmids

The plasmids used for the cloning of the individual components of human PDC were obtained from a variety of sources. pHUMIT contains the full length sequence for mature E2 and was kindly provided by Dr M.E. Gershwin, Division of Rheumatology and Clinical

Immunology, University of California, Davis. Plasmids containing the genes for E3 and E1 $\beta$  were a kind gift from Dr Brian Robinson, Department of Pediatrics and Biochemistry, University of Toronto, Canada. Dr Garry Brown, Department of Biochemistry, University of Oxford, donated the plasmid containing the cDNA for E1 $\alpha$  and the plasmid containing the full length sequence for human E3BP (Genbank accession number H58032) was kindly provided by Dr Bernard Aral, Department of Medicine, Necker Hospital for Sick Children, Paris.

## **3.2 Cloning of the E2, E3 and E3BP components**

### **3.2.1 PCR amplification and purification**

The cDNA sequences for all the enzyme components of human PDC have previously been published (Coppel *et al*, (1988) (E2), Harris *et al*, (1997) (E3BP), Dahl *et al*, (1987) (E1 $\alpha$ ), Chun *et al*, (1990) (E1 $\beta$ ), Pons *et al*, (1988) (E3)) and so this allowed the design of specific primers to be used in PCR. Primers were designed to the 5' region upstream of the start of each mature protein and to the 3' region downstream of the STOP codon of the full length sequence. All primers were designed with BamHI sites to facilitate cloning into the chosen expression vector (see Figure 3.1 for primer sequences).

PCR reactions were generally performed using *Pfu* DNA polymerase (Stratagene) as this enzyme has the lowest error rate of the thermostable DNA polymerases. *Pfu* DNA polymerase has a five-fold lower rate of base misincorporation than *Taq* DNA polymerase due to its 3'-5' exonuclease proofreading activity. Conditions for PCR were as described in Materials and Methods. Samples of each PCR reaction, typically 5 $\mu$ l, were electrophoresed on a 1.5% (w/v) TAE agarose gel. Figure 3.2 illustrates the PCR products obtained. The lack of DNA in the control lanes where water replaced the DNA template shows that there are no contaminants present in the PCR mixture. The presence of minor PCR products in some reactions may be due to the occurrence of non-specific priming events in early cycles.

**E3 forward:**

5'-TC TGA GGA TCC CGC AGA TCA GCC GAT T-3'

**E3 reverse:**

5'-TAA TCT GGA TCC TCA AAA GTT GAT TGA TTT GCC-3'

**E2 forward:**

5'-CGC CGC GGA TCC CAG TCT TCC CCC G-3'

**E2 reverse:**

5'-TTC TTG GGA TCC TTA CAA CAA CAT AGT GAT AGG-3'

**E3BP forward:**

5'-CAG TGG GGA TCC GGG TGA TCC CAT TAA G-3'

**E3BP reverse:**

5'-TAT CTT GGA TCC CTA GGC AAG TCG G-3'

**E1 $\alpha$  forward:**

5'-GCA TCC GGA TCC TTT TGC AAA TGA TGC TAC ATT TG-3'

**E1 $\alpha$  reverse:**

5'-CTT CTC GGA TCC TTA ACT GAC TGA CTT AAA CTT G-3'

**E1 $\beta$  forward:**

5'-GCG CCG GGA TCC GCT GCA GGT GAC AGT TCG-3'

**E1 $\beta$  reverse:**

5'-G ATA TTC AAG GGA TCC CTA AAT ATT TAA TG-3'

**Figure 3.1 Primer sequences for the cloning of each component of the human pyruvate dehydrogenase complex.**

The BamHI sites are underlined in each case.

**Figure 3.2 PCR amplification of E2 (panel A), E3BP (panel B) and E3 (panel C)**

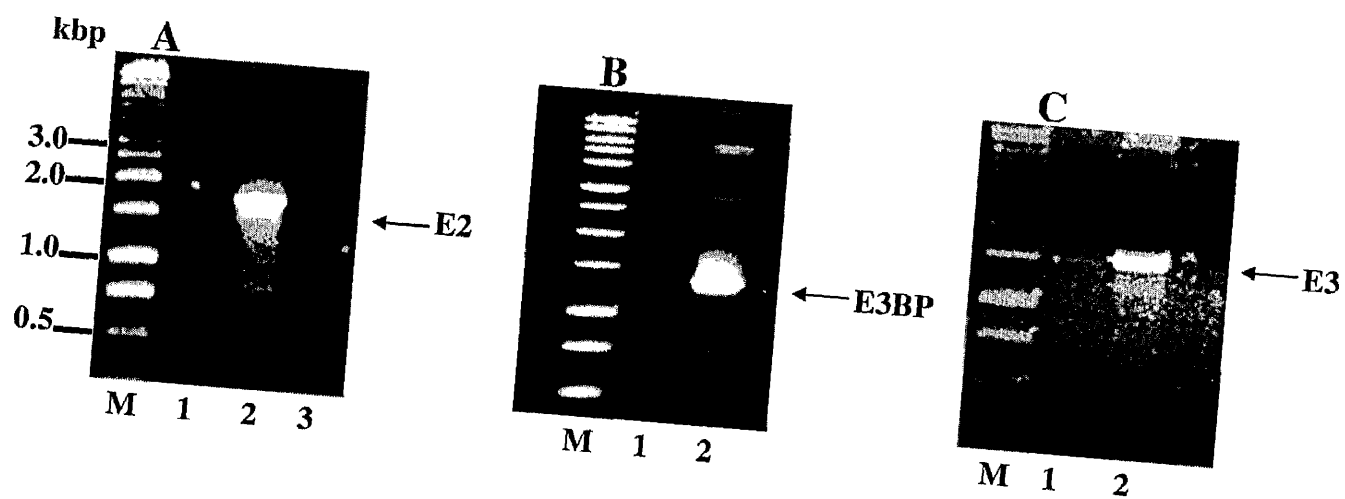
PCR reactions were run on 1.5% agarose gels and stained with ethidium bromide before visualising on a UV transilluminator.

M: 1 kb ladder, 1: negative control (no template DNA added), 2: PCR product

**Panel A:** E2 was amplified from pHUMIT, a plasmid which contains the full length, mature sequence for E2. A strong PCR product was obtained at an approximate size of 1.8kb in lane 2. No PCR product was obtained in lane 3 using diluted template DNA.

**Panel B:** E3BP was amplified from a plasmid donated by Dr B. Aral (Paris). A band at the expected size of 1.5kb is seen.

**Panel C:** Amplification of E3 took place from a plasmid obtained from Dr B. Robinson (Canada). A PCR product at the expected size of 1.5kb was obtained.



In each case, the major product was excised from an agarose gel, under UV light, using a sterile scalpel. The DNA was then purified using the QIAquick gel extraction kit (Qiagen) as described in Materials and Methods. An aliquot of the purified DNA was electrophoresed on a 1.5% (w/v) agarose gel to check the quality and quantity of the DNA obtained (data not shown).

### **3.2.2 Ligation, transformation and identification of clones**

The expression plasmid pET-14b (Novagen) was chosen as a suitable vector in which to clone E2, E3 and E3BP for a number of reasons. The pET vectors provide a convenient strategy for the cloning of DNA as they contain unique restriction sites in their multiple cloning region. In addition, pET-14b contains an N-terminal 6 Histidine-tag which provides a means of conveniently and economically purifying the protein of interest using a metal affinity column. This vector also confers ampicillin resistance on the cloned product.

BamHI was chosen as a suitable restriction site for the cloning of each enzyme since analysis of the individual gene sequences, using GeneJockey software, indicated that there were no BamHI restriction sites present in any of the genes.

Both the vector and PCR product were subjected to restriction digestion by BamHI to generate cohesive ends for ligation. The vector was also treated with calf intestinal alkaline phosphatase (1U/ $\mu$ l) to remove the phosphate groups exposed by digestion and so prevent self-ligation of the vector. This step helps reduce the effort required to screen ampicillin-resistant colonies obtained after transformation.

After digestion, both vector and PCR product were purified using the QIAquick gel extraction kit (Qiagen) and DNA was eluted in 30 $\mu$ l elution buffer. Samples (5 $\mu$ l) of each

were electrophoresed on a 1.5% (w/v) TAE agarose gel to check the quantity of DNA obtained. This was also used to assess the vector:insert ratio required for the ligation reactions. For ligations to be successful a high insert:vector ratio is usually required. A series of ligation reactions were set up with varying ratios of insert:vector (usually from 3:1 to 10:1) and a control reaction containing no insert.

These were left overnight at room temperature and transformed into competent *E. coli* DH5 $\alpha$  cells the following day. The transformations were plated on LB-agar plates supplemented with 50 $\mu$ g/ml ampicillin and incubated at 37 $^{\circ}$ C overnight.

Colonies were selected and cultured overnight in LB media supplemented with ampicillin (50 $\mu$ g/ml) at 37 $^{\circ}$ C. Plasmid isolations were performed using the Wizard SV Minipreps kit (Promega) and DNA was eluted in 70 $\mu$ l nuclease-free water. Samples, typically 5 $\mu$ l, were electrophoresed on a 1% (w/v) TAE agarose gel, along with wild-type pET-14b in order to identify clones containing the insert of interest.

Clones, possibly containing insert, were subjected to restriction digestion with BamHI to assess if an insert of the appropriate size was present. Those clones which were shown to contain insert were then subjected to digestion with a suitable restriction enzyme, selected for its ability to cleave both the vector and also in the actual insert itself. This analysis was performed in order to check the orientation of the insert. For E3BP and E3, the enzyme used was BglII, while E2 was digested with PstI. Figures 3.3a-c show the results of these digestions. For E3BP, out of the six clones examined, four were successfully digested with BamHI. Of these four clones only one, E3BP/6-14b, contains the insert in the correct orientation. In the case of E2, of the six clones digested with BamHI three of these, E2/1, E2/7 and E2/8-14b were in the correct orientation. Only one of the three possible E3 clones, E3/3-14b, was inserted correctly.

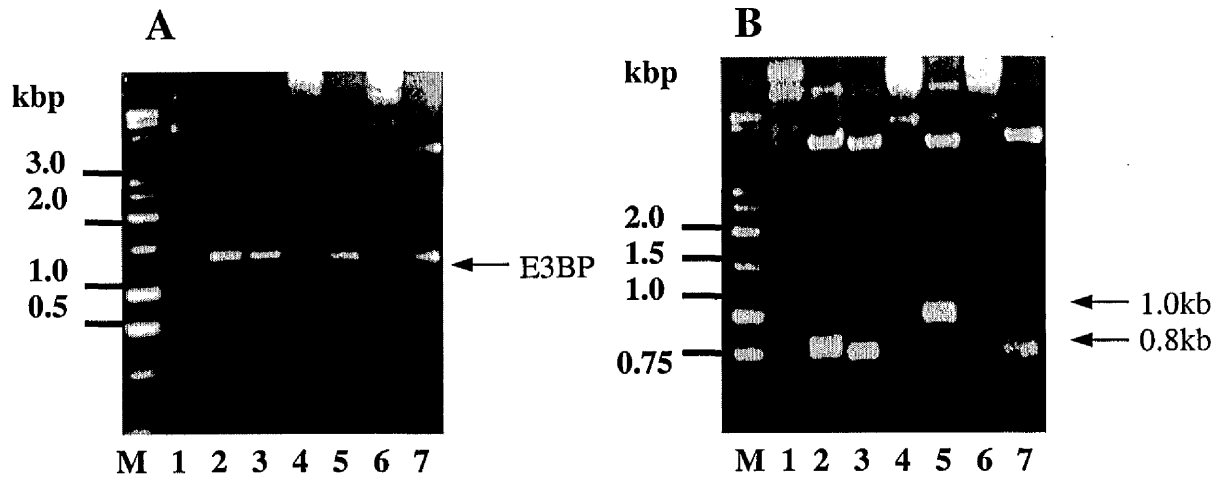
### **Figure 3.3a Restriction digestion analysis of recombinant E3BP plasmids**

Clones containing insert were subjected to restriction digestion by BamHI (panel A) or BglII (panel B). Samples of each digest were analysed on 1.5% agarose gels which were then stained with ethidium bromide and viewed under UV transillumination.

M: 1kb ladder

**Panel A:** BamHI digestion of the seven clones possibly containing insert show that a band of the expected size (1.5kb) is present in lanes 2, 3, 5 and 7.

**Panel B:** BglII restriction digestion of the same seven clones show that out of the four clones which definitely contain insert, clone number 6 (in lane 5) has E3BP inserted in the correct orientation as indicated by the predicted sizes of the fragments. For a clone containing insert in the correct orientation a digestion product 1kb in size was predicted while a band of approximate size 0.8kb was expected for clones containing insert in the wrong orientation.



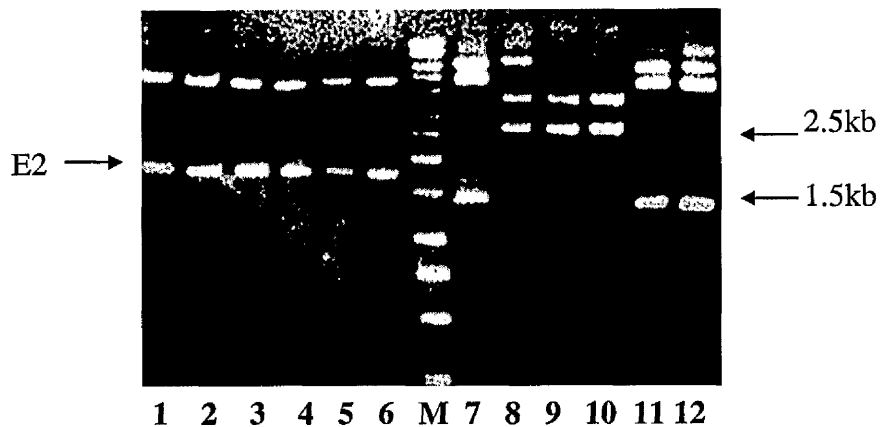


**Figure 3.3b Restriction digestion analysis of recombinant E2 plasmids.**

Six possible E2 clones were subjected to restriction digestion and analysed on a 1.5% agarose gel as before.

M: 1kb ladder, lanes 1-6: BamHI digestion, lanes 7-12: PstI digestion.

All six clones were digested with BamHI and a band of the expected size (1.8kb) was present in each case as seen in lanes 1-6.

PstI digestion resulted in 2 different banding patterns emerging depending on the orientation of the insert. For clones containing insert in the correct orientation a band of approx 1.5kb in size was predicted. In the wrong orientation, digestion with PstI results in a product of 2.5kb. This digestion shows that the samples in lanes 7, 11 and 12 contain E2 that is inserted in the correct orientation.

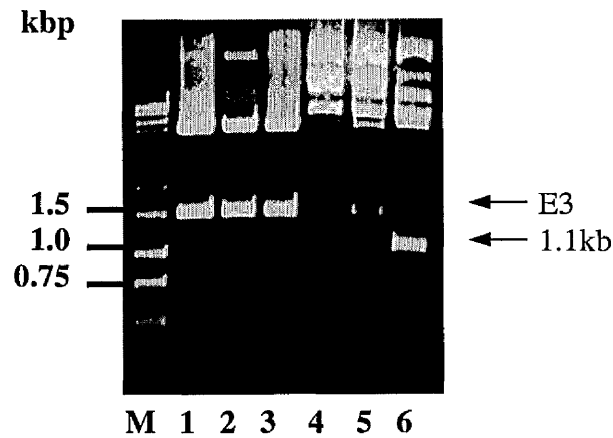


**Figure 3.3c Restriction digestion analysis of recombinant E3 plasmids**

E3 clones were digested with BamHI or BglII and analysed on a 1.5% TAE agarose gel as before.

M: 1kb ladder, lanes 1-3: BamHI digestion, lanes 4-6: BglII digestions.

The three possible E3 clones all contain a band of the correct size (1.5kb) which digested out with BamHI.

The BglII digestion was predicted to produce a band of 1.1kb if the insert was present in the correct orientation and a band of 1.5kb if present in the wrong orientation. This digestion shows that, of these three clones, only one contains the insert in the correct orientation as seen in lane 6.

From these digestions, the clones containing insert in the correct orientation were transformed into competent *E. coli* BL21 CodonPlus cells (Stratagene) for overexpression of the proteins of interest.

### 3.3 Overexpression of heterologous protein

After transforming the relevant clones into *E. coli* BL21 CodonPlus cells, small-scale protein inductions were performed. An aliquot of an overnight culture, supplemented with ampicillin (50µg/ml) was subcultured into a fresh 50ml culture and grown, with shaking, at 37°C. Once the optical density of the culture at 600nm reached 0.5, expression of protein was induced by the addition of IPTG (1mM). Inductions were usually carried out at 30°C. Samples were taken at hourly time intervals, pelleted by centrifugation, resuspended in an appropriate volume of Laemmli sample buffer and analysed by 10% SDS-PAGE. Figures 3.4a-c show the results of each induction. All 3 proteins were successfully overexpressed using this system.

Perhaps the most encouraging result was the successful cloning and overexpression of E3BP as an individual protein in the absence of E2, as described previously by Palmer *et al* (1999). Assuming that the recombinant protein is soluble this means that structural studies of this protein, independent of E2, are now possible.

All proteins cloned so far have been described as being expressed in BL21(DE3) CodonPlus cells. Each recombinant protein was also overexpressed in *E. coli* BL21(DE3) pLysS cells. However, it was found that expression of heterologous protein using the CodonPlus strain of *E. coli* was often more effective than in the more usual pLysS cells (data not shown). This is perhaps because CodonPlus cells contain extra copies of several tRNA species which encode codons which are rarely used in *E. coli* but tend to be more abundant in the organisms from which the heterologous protein is derived. These are the arginine codons AGA and AGG, the isoleucine codon AUA and the leucine codon CUA. The availability of these codons can allow high-level expression of heterologous protein that is poorly expressed in conventional

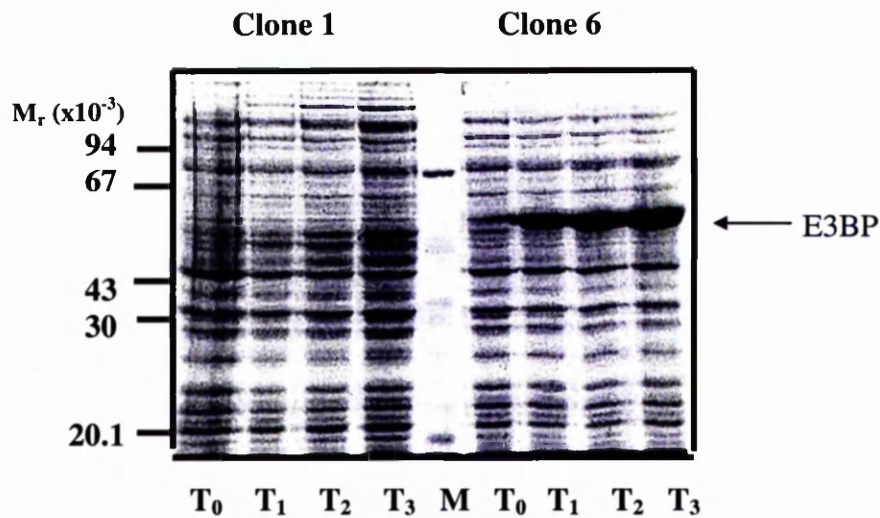


**Figure 3.4a Overexpression of E3BP**

Clone 6, containing E3BP in the correct orientation, and clone 1, which contains the insert in the wrong orientation, were transformed into competent BL21 (DE3) pLysS CodonPlus cells for protein expression. Samples were taken at 1h time intervals after induction of protein with 1mM IPTG.

M: low molecular mass markers, T<sub>0</sub>: sample taken just before induction with IPTG, T<sub>1</sub>, T<sub>2</sub> and T<sub>3</sub> represent samples taken 1, 2 and 3h after induction of recombinant protein.

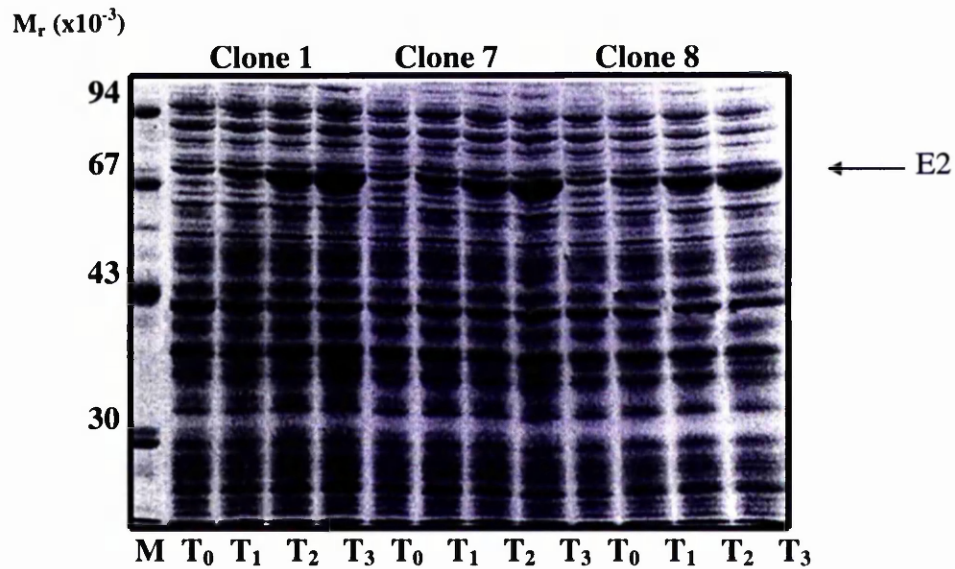


### Figure 3.4b Overexpression of E2

The three clones containing E2 inserted in the correct orientation were transformed into competent BL21 (DE3) pLysS CodonPlus bacteria. Small scale protein inductions were carried out in LB media, at 30°C as described previously.

M: low molecular mass markers, T<sub>0</sub>: sample taken just before addition of 1mM IPTG, T<sub>1</sub>, T<sub>2</sub> and T<sub>3</sub> represent samples taken at 1, 2 and 3h after induction.

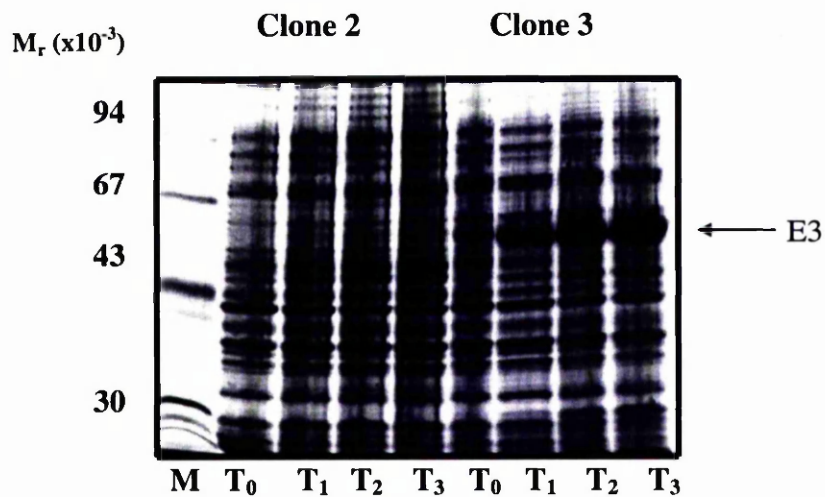


**Figure 3.4c Overexpression of E3**

Clone 2 and clone 3 containing the cDNA for mature E3 in the incorrect and correct orientation were transformed into competent BL21 (DE3) pLysS CodonPlus bacteria for protein expression. Small scale protein inductions were carried out in LB media at 30°C.

M: low molecular mass markers, T<sub>0</sub>: sample taken just before the addition of 1mM IPTG, T<sub>1</sub>, T<sub>2</sub> and T<sub>3</sub> represent samples taken 1, 2 and 3h after induction.

BL21 strains. The optimisation of expression of these recombinant proteins in CodonPlus cells meant that the whole process could be scaled up. Large-scale protein induction was then routinely employed in order to produce large quantities of recombinant protein for purification and subsequent analysis.

### **3.4 Coexpression of E2 and E3BP**

As noted previously, native E3BP is only found tightly associated with E2 and together, these two proteins form the structural core of human PDC. Since native E2 and E3BP can only be separated under strongly denaturing conditions this makes E3BP difficult to study as an independent protein. Obtaining a plasmid containing the full length sequence for E3BP allowed us to attempt to clone a recombinant E3BP as described above. However it was unclear if this recombinant protein would be correctly folded. Another important point to take into consideration was the association of E3BP with E2. It may be that these two proteins form the structural core through association as folding intermediates and it is unclear if they can form a stable complex in a post-translational manner. For this reason it was decided to coexpress E2 and E3BP in the same *E. coli* cells in the hope of circumventing this possible difficulty. This should hopefully allow E2 and E3BP to form the core complex in a co-translational manner.

#### **3.4.1 Cloning of E2 and E3BP**

In order to coexpress E2 and E3BP it was necessary to clone them into plasmids containing different antibiotic resistance markers. To this end, pET-11b was employed as the vector in which to clone E2 and pET-28b was used for cloning E3BP. pET-11b is an ampicillin-resistant vector and does not contain a His-tag while pET-28b confers kanamycin resistance and includes an N-terminal His-tag. Cloning of the individual genes into the relevant plasmids was performed as described previously using BamHI as the restriction enzyme for each vector. After ligation and transformation, clones containing insert were identified by agarose gel electrophoresis. These were then subjected to restriction digestion using BamHI

and either BglII (E3BP) or PstI (E2) to check for the presence of insert and its orientation as described previously. Clones containing insert in the correct orientation were then transformed, individually, into competent *E. coli* BL21 CodonPlus cells to check for overexpression.

### 3.4.2 Overexpression of coexpressed E2 and E3BP

Once it was established that both clones could express protein, they were cotransformed into *E. coli* cells. DNA (1-10ng) from E2-11b and E3BP-28b were added to the same competent *E. coli* BL21 CodonPlus cells and transformed as normal. The mixture was then plated on double antibiotic resistance plates and incubated overnight. Any colonies obtained would, therefore, be expected to contain both plasmids.

Small-scale protein induction was then carried out as previously described in 50ml LB media. After the addition of IPTG (1mM), induction was monitored by removing samples of the culture at zero time and 3h after induction. These samples were pelleted by centrifugation, resuspended in an appropriate volume of Laemmli sample buffer and analysed by 10% SDS-PAGE. Figure 3.5 shows the results of the induction. As can be clearly seen, high levels of expression were obtained for both proteins. This process could now be scaled up to produce milligram quantities of protein for purification and analysis.

### 3.5 Cloning of the E1 component

The E1 component of human PDC contains both an  $\alpha$  subunit and a  $\beta$  subunit, with two copies of each present in E1, forming an  $\alpha_2\beta_2$  heterotetramer. As the two subunits are encoded by separate genes it was necessary to coexpress the two subunits in a manner similar to the coexpression of E2 and E3BP.

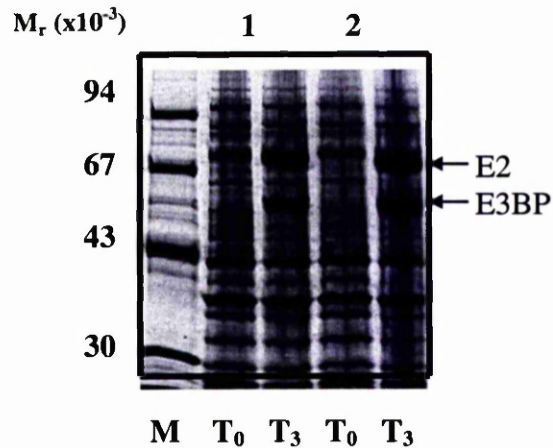


**Figure 3.5 Overexpression of cotransformed E2 and E3BP**

Recombinant pET-11b and pET-28b plasmids containing the coding regions for mature human E2 and E3BP were cotransformed into competent BL21 (DE3) pLysS CodonPlus cells and overexpressed in LB growth media at 30°C. Expression of protein was induced by the addition of 1mM IPTG.

M: low molecular mass markers, T<sub>0</sub>: sample taken just before addition of IPTG, T<sub>3</sub>: sample taken 3h after induction with IPTG.

Two separate colonies were induced for overexpression.

### 3.5.1 PCR amplification and purification

PCR amplifications of E1 $\alpha$  and E1 $\beta$  were carried out as described previously using the primers shown in Figure 3.1. Successful PCR of E1 $\beta$  proved very difficult to achieve using *Pfu* DNA polymerase. The reasons for this are unclear. The conditions for the PCR reaction, such as the annealing temperature, were systematically altered but with no success. Heating the primers to 95°C for 5 min before adding them to the PCR mix also had no effect and the addition of 10% (v/v) glycerol, known to improve the yield of amplification products, or 10% (v/v) DMSO, thought to improve the denaturation of GC-rich DNA, similarly met with no success. Finally, by using the Expand High Fidelity PCR system (Boehringer Mannheim), the PCR proved successful and strong bands of the expected size for E1 $\beta$  were obtained. The Expand system consists of both the *Taq* and *Pwo* DNA polymerases and has a 3-fold increased fidelity of DNA synthesis compared to *Taq* DNA polymerase alone. This is due to the 3'-5' exonuclease proofreading activity of *Pwo* DNA polymerase. PCR of the E1 $\alpha$  gene proved less problematic and was performed using *Pfu* DNA polymerase. The PCR products obtained can be seen in Figure 3.6.

### 3.5.2 Product ligation, transformation and clone identification

Both the PCR products and the relevant vectors, pET-28b and pET-11b, were digested with BamHI in preparation for ligation. The plasmids were also treated with calf intestinal alkaline phosphatase (1U/ $\mu$ l) to remove the 5'-phosphate groups generated by restriction digestion. A number of ligation reactions were set up with different ratios of insert:vector and these were left at room temperature overnight. They were then transformed into competent *E. coli* DH5 $\alpha$  cells and plated on LB agar plates supplemented with the appropriate antibiotic for incubation at 37°C overnight. E1 $\alpha$  was ligated into pET-28b while E1 $\beta$  was cloned into pET-11b.

Colonies obtained from the transformation of the ligation reactions were selected and incubated in 5ml LB plus antibiotic overnight. Minipreps were performed using the Wizard

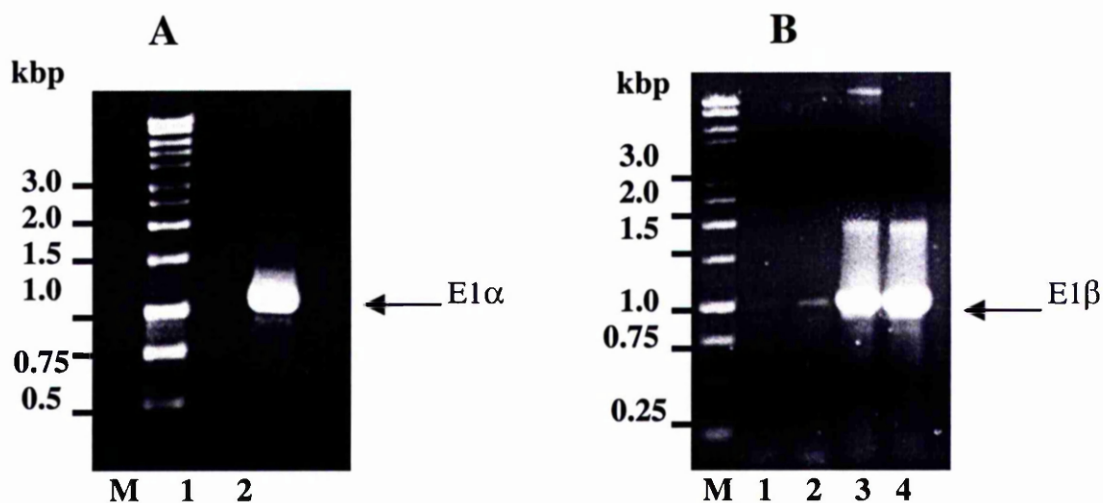


**Figure 3.6 PCR amplification of E1 $\alpha$  (panel A) and E1 $\beta$  (panel B).**

Samples of each PCR were electrophoresed on 1.5% (w/v) TAE agarose gels, stained with ethidium bromide and viewed under UV transillumination.

M: 1kb ladder, 1: negative control (no template DNA added), 2-4: PCR product.

**Panel A:** A strong PCR product of E1 $\alpha$ , at the expected size of about 1.2kb was obtained.

**Panel B:** PCR of E1 $\beta$  was performed using the Expand High Fidelity system. A low yield of PCR product was obtained using the concentrated plasmid for E1 $\beta$  (lane 2). Diluting the template DNA by a factor of 10 resulted in a strong PCR product being obtained at the expected size of 1.1kb (lanes 3 and 4).

SV Minipreps kit as before and DNA was eluted in 70 $\mu$ l nuclease-free water. Samples from each miniprep were electrophoresed on a 1% (w/v) TAE agarose gel along with wild-type pET-28b and pET-11b to assess which, if any, colonies were likely to contain insert. Possible candidates were subjected to restriction digestion by BamHI, to check that the insert could be digested out of the vector, and then with a second enzyme to check the orientation of the insert. For E1 $\alpha$ , this enzyme was BglII while E1 $\beta$  was digested with PstI. Figure 3.7 shows the results of these digestions.

From these digestions it can be seen that one E1 $\alpha$  clone, E1 $\alpha$ /5-28b, and 3 E1 $\beta$  colonies, designated E1 $\beta$ /1, 2 and 3-11b are inserted in the correct orientation and should produce protein after induction with IPTG. These clones were transformed, individually, into BL21 (DE3) pLysS CodonPlus cells to check for overexpression of protein.

Small scale protein induction for each clone was carried out as normal in 50ml LB media. Overexpression of protein was induced by the addition of IPTG (1mM) and protein induction followed by removing samples at zero time and then 3h after addition of IPTG. Both proteins overexpressed strongly (data not shown).

### 3.5.3 Cotransformation of E1 $\alpha$ and E1 $\beta$

Once it was established that both clones were capable of overexpressing protein of the expected size, these clones were cotransformed into BL21 (DE3) pLysS CodonPlus competent cells in a manner similar to that described for the cotransformation of E2 and E3BP (section 3.4.2). The transformations were plated on double antibiotic resistance plates so that any colonies obtained would contain both plasmids.

Small scale protein induction was again carried out in LB media containing both ampicillin (50 $\mu$ g/ml) and kanamycin (30 $\mu$ g/ml) and induction of protein followed by removing samples at zero time and 3h after induction with IPTG (1mM). Induction of protein was monitored at

### **Figure 3.7 Restriction digestion of recombinant E1 $\alpha$ and E1 $\beta$ plasmids**

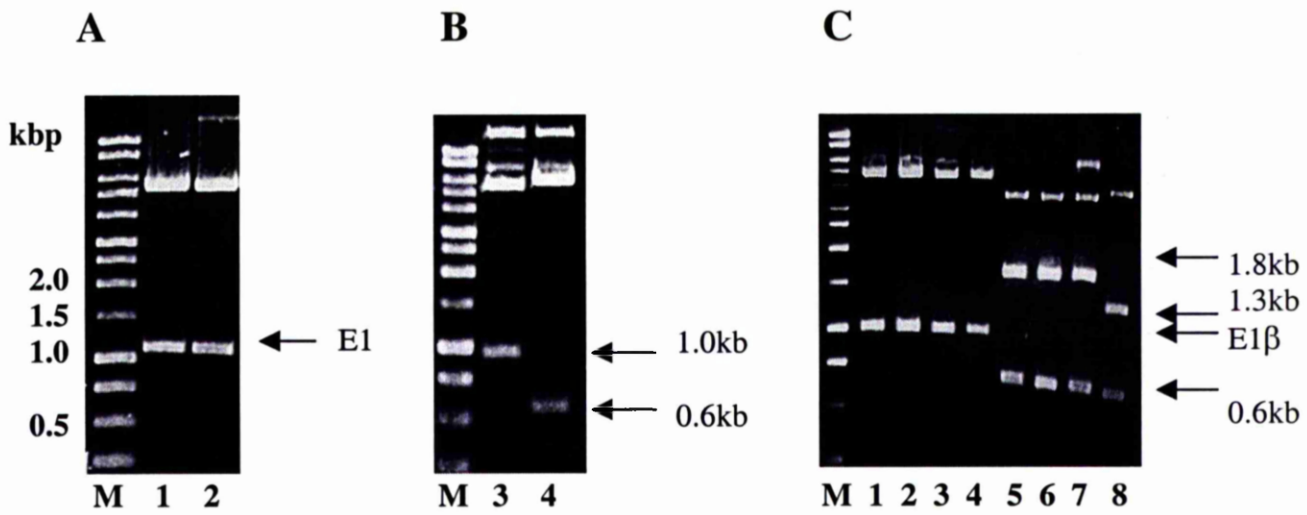
Clones containing either E1 $\alpha$  or E1 $\beta$  were subjected to restriction digestion with BamHI to check for the presence of insert and then with a second enzyme to check the orientation of the insert. Samples of each digest were electrophoresed on 1.5% (w/v) TAE agarose gels, stained with ethidium bromide and visualised using a UV transilluminator.

**Panel A:** BamHI digestion of two possible E1 $\alpha$  clones show that insert is indeed present in both clones.

**Panel B:** Digestion of the two E1 $\alpha$  clones with BglII were predicted to result in a band of 1kb for a clone with the insert in the correct orientation and 0.6kb for a clone containing insert in the wrong orientation. This analysis shows that clone 1 contains the insert in the correct orientation while the second clone contains the gene in the wrong orientation.

**Panel C:** Digestion of four possible clones containing E1 $\beta$  with BamHI (lanes 1-4) indicates that all four contain the insert while digestion of these clones with PstI (lanes 5-8) show that all but one of these clones contain the gene inserted in the correct orientation. The predicted sizes for an insert in the correct orientation was 1.8kb while in the wrong orientation, a digestion product at 1.3kb was expected. An additional digestion product at 0.6kb was also observed.

M: 1kb ladder



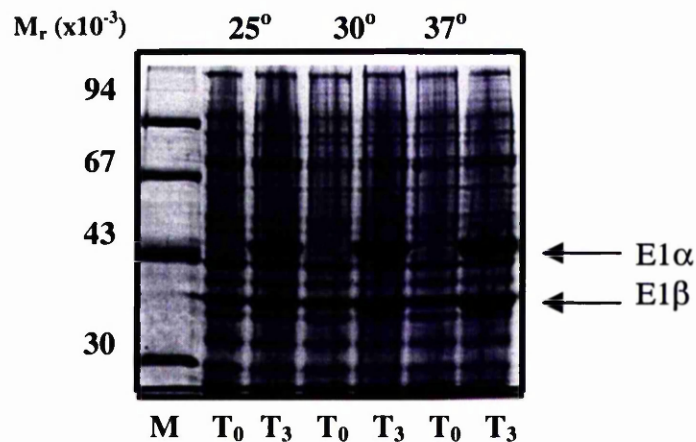


**Figure 3.8 Coexpression of E1 $\alpha$  and E1 $\beta$**

E1 $\alpha$  and E1 $\beta$  were coexpressed in *E. coli* BL21 CodonPlus cells by induction with 1mM IPTG. Induction of protein was performed at 3 different temperatures, 25°, 30° and 37°. Samples were removed at time 0 and 3h after induction for analysis on 15% SDS-PAGE. High levels of overexpression of both subunits occurred at all three temperatures.

3 different temperatures, 25°C, 30°C and 37°C, since it has been noted that investigators who have previously cloned E1 from both PDC (Korotchkina *et al*, 1995) and BCOADC (Davie *et al*, 1992) have found that the solubility of recombinant E1 was increased at lower temperatures. Samples were electrophoresed on a 15% SDS-PAGE gel. From Figure 3.8, it can be seen that cotransformation of E1 $\alpha$  and E1 $\beta$  proved successful with both proteins overexpressing to a significant degree. Overexpressing these constructs at the different temperatures results in similar levels of protein expression although it is possible that protein expression is improved slightly at 37°C. However it is possible that the solubility of these subunits will be affected at the different temperatures.

### 3.6 Discussion

In this chapter the cloning strategy has been described that has allowed us to achieve the successful and reproducible overexpression of the individual components of the human pyruvate dehydrogenase complex in *E. coli*. However the question remains as to whether these proteins have been produced in active form. These proteins have all been cloned and overexpressed in *E. coli* previously by other researchers.

Human E3 has previously been cloned in both its mature and precursor forms (Kim *et al*, 1991). Both proteins were shown to be active although the precursor form was less catalytically efficient than mature E3. This is perhaps not surprising given the additional amino acids present at the N-terminus of the precursor protein. The precursor E3 was also less soluble than the mature protein. Optimum expression was found to occur at 30°C. Human E3 has also been cloned as a His-tagged fusion protein (Liu *et al*, 1995). Human E3BP has been previously overexpressed both in a subcomplex with E2 (Harris *et al*, 1997) and on its own (Palmer *et al*, 1999; Lee *et al*, 2001). While Lee and coworkers (2001) purified a recombinant His-tagged E3BP they failed to show that this protein was active. Recombinant E3BP cloned into the pET-14b vector in a manner similar to that described here was shown to react with the sera of patients suffering from primary biliary cirrhosis, indicating that E3BP

was correctly folded (Palmer *et al*, 1999). This protein was induced at 30°C for 3h. The E2/E3BP subcomplex described by Harris and coworkers (1997) was shown to be able to spontaneously reconstitute the pyruvate dehydrogenase complex in the presence of native E3 and recombinant E1. In this case cells were cultured at room temperature after the addition of 0.4mM IPTG for 20-24h before harvesting. Conditions for the expression of a recombinant His-tagged E2 were found to be optimum at 30°C for 3h in BL21 (DE3) pLysS (Palmer *et al*, 1999). Other investigators found that proteolytic cleavage of recombinant E2 was a problem and minimised this by inducing expression at 27°C (Yang *et al*, 1997).

E1 from both PDC and BCOADC has been cloned and expressed in *E. coli* previously. In general two strategies have been employed in order to produce recombinant active E1. In *B. stearothermophilus*, it was shown that a functional PDC-E1 could be obtained by disrupting mixtures of cells containing the separately expressed E1 $\alpha$  and E1 $\beta$  subunits (Lessard & Perham, 1994). E1 produced in this manner was able to assemble into active heterotetramers *in vitro*. In contrast bovine BCOADC-E1 and human PDC-E1 were expressed by subcloning the genes for both the  $\alpha$  and  $\beta$  subunits into the same expression plasmid. BCOADC-E1 was expressed as a maltose-binding protein (MBP) fusion protein and protein expression was induced at 24°C for 24h. It was found that association of active recombinant bovine BCOADC-E1 relied on coexpression of both subunits in *E. coli* (Davie *et al*, 1992). A similar method was used to express a recombinant human PDC-E1. Both subunits were subcloned into the same expression vector as a His-tagged fusion protein. Optimal expression took place at 25°C overnight (Korotchkina *et al*, 1995). These investigators also showed that when expressed individually neither E1 $\alpha$  nor E1 $\beta$  had any catalytic activity. In this chapter E1 was produced by cotransforming the individually cloned subunits into *E. coli*. This strategy was viewed as being the most straightforward, having proved successful for E2/E3BP.

One of the problems faced by investigators when cloning a recombinant protein is the possibility that, when expressed in *E. coli*, or indeed any other foreign host, the protein may

be insoluble. High level expression of recombinant protein, such as that described in this chapter, can often result in aggregation and accumulation of the protein in inclusion bodies. Preliminary studies of the constructs described herein have indicated that all recombinant proteins, with the exception of the E1 component, are soluble. In general, it appears that 30°C is the optimal induction temperature for the production of a high yield of soluble protein for each construct.

In order to assess whether the recombinant proteins have been produced in active form a number of investigative tools are at our disposal. Enzymatic assays have been developed for the E1, E2 and E3 components of the complex. Immunoblotting techniques can also be utilised employing a monoclonal antibody which is highly specific for lipoylated E2 and E3BP of PDC. This antibody does not recognise the unlipoylated forms of these proteins. Preliminary studies using Western blot analysis have indicated that both E2 and E3BP have, at the very least, correctly folded N-terminal lipoyl domains. This is very encouraging in terms of the recombinant proteins being produced in active form. Again, this is discussed in more detail in chapter 4.

## **Chapter 4**

### **Purification of the recombinant enzymes of human PDC**

## 4.1 Introduction

In order to conduct studies on the structural and functional characteristics of a protein it is usually necessary to first purify the target protein. Protein purification from a native source is often the most time consuming part of any experiment. Lengthy protocols are employed using several types of chromatography in order to achieve purification of the protein to near-homogeneity. Purification of recombinantly expressed protein in bacteria is normally less problematic.

The main advantage in using fusion vectors such as glutathione S-transferase (GST) as opposed to conventional expression vectors is that the recombinant protein can be purified using a highly specific, affinity chromatography step. Glutathione S-transferase is a protein of  $M_r$  value 26kDa and, in general, is preferentially used as a fusion protein for smaller proteins, or individual domains of proteins, which may not be stable as independent entities. It can also be used for proteins that are insoluble since, in the majority of cases, proteins expressed as a fusion with GST show enhanced solubility and can be purified under non-denaturing conditions. GST fusion proteins can be purified very easily by adsorption of the lysate to a glutathione Sepharose column. After thoroughly washing the matrix to remove any unbound protein the GST-tagged protein can be specifically eluted from the column with glutathione. In a similar vein, the pET-14 expression vector encodes six histidine residues, which can be attached to either the N- or C-terminus of the recombinant protein and acts as a convenient means of purifying the target protein. Recombinant proteins containing a Histidine-tag can be purified using the same principles as for GST-fusion proteins. However, this is only possible provided that the recombinant protein is soluble. It is not uncommon for heterologously expressed proteins to form inclusion bodies in the host cell.

### 4.1.1 Inclusion bodies

Inclusion bodies consist mainly of recombinant proteins that have accumulated in the cell and are densely packed together. There are several reasons which can account for the formation of inclusion bodies. Some recombinant proteins depend on post-translational modification for full biological activity, for example phosphorylation or glycosylation. This is often carried out by specialised enzyme systems that may not be present in the host cell. The folded structure of the recombinant protein may not be adapted to the conditions in the host cell or, most simply, the polypeptides may be overproduced to such an extent that the physiological solubility limit is exceeded. Finally, *in vivo* there are a number of additional protein factors present such as molecular chaperones that assist in protein folding but in the host cell, the level and specificity of these factors may differ (Lilie *et al*, 1998).

Since inclusion bodies consist mainly of recombinant protein a high yield of protein can be obtained and this can be isolated with relative ease. However, the problem arises when trying to solubilise and refold the recombinant protein. Refolding is the most difficult part of isolating protein from inclusion bodies and the yield of correctly folded, active protein is usually very low (Misawa & Kumagai, 1999).

### 4.2 Aims of this chapter

- To examine the lipoylation states of E2 and E3BP
- To describe the use of a BioCAD Sprint Perfusion Chromatography System for the purification of His-tagged proteins
- To show that these enzymes have been purified in active form
- To show that, when coexpressed E2/E3BP is purified, the two enzymes coelute suggesting that they have formed a stable complex.
- To describe the solubilisation and purification of active E1 from inclusion bodies.

## 4.3 Results

### 4.3.1. Lipoylation states of E2 and E3BP

After successfully overexpressing the individual components of human PDC the next step was to demonstrate that the recombinant proteins were soluble and biologically active. A convenient method for establishing that the N-terminal domains of both E2 and E3BP are correctly folded is to utilise the fact that both these proteins contain highly conserved lipoyl domains at their N-termini that contain lipoylatable lysine residues.

Lipoylating enzymes in *E. coli* are capable of recognising a specific motif, aspartic acid, lysine, alanine (DKA) which is present on the lipoyl domains of E2 and E3BP. This conserved motif is found at the tip of an exposed type-I  $\beta$ -turn in the three-dimensional structure of the lipoyl domain. The lipoyl group is attached in an amide linkage to the N<sup>6</sup>-amino group of this lysine residue. This lipoyl attachment can only occur if the apodomain is properly folded. Mutation of the conserved residues on either side of the lysine residue does not appear to affect the ability of the lipoylating machinery to recognise the lysine residue but if the lysine residue itself is moved one position to the left or right it is unable to be lipoylated. This suggests that there may in fact be a precise structural cue that is recognised by the lipoylating machinery of the cell as opposed to a conserved sequence motif (Wallis & Perham, 1994).

In the bacterial system used here, overexpression of lipoylatable proteins results in both lipoylated and unlipoylated forms being produced. The most likely explanation is that overexpression of the recombinant protein is so strong that the lipoylating machinery of the cell is unable to modify all the expressed protein (Quinn *et al*, 1993; Green *et al*, 1995). The best estimates suggested that in these studies the ratio between lipoylated and unlipoylated proteins under these growth conditions was approx 50:50. Addition of exogenous lipolate to the growth media during protein induction allows the recombinant protein to become more fully lipoylated.

The lipoylatable proteins, E2-PDC and E3BP can be detected using a monoclonal antibody, a kind donation from Prof. Freda K. Stevenson at Southampton University. Two antibodies, designated PD1 and PD2, were available which are specific only for the lipoylated (holoenzyme) form of these proteins (Potter *et al*, 2001). Protein inductions, of E2, E3BP and cotransformed E2/E3BP were performed as normal in LB growth media. Exogenous lipoate was added to the media on induction of protein with 1mM IPTG and overexpression of protein carried out as described previously. Samples were taken at zero time and at 3h after induction for analysis on SDS-PAGE. Cultures grown in the absence, and in the presence, of exogenous lipoate were then subjected to Western blotting using the monoclonal antibody specific for the lipoylated E2 and E3BP as the primary antibody. Figures 4.1a-c show the results of these immunoblots.

In each case, a substantial enhancement of the lipoylation is seen when the cultures are grown in the presence of exogenous lipoate. However, the level of enhancement seems to vary quite significantly from sample to sample. This is particularly pronounced in the coexpressed E2/E3BP cultures where markedly enhanced lipoylation of E2 is observed with little difference seen in the lipoylation of E3BP. This is in contrast to the individually expressed proteins where E3BP shows a 2-3 fold enhancement in lipoylation while the effect of exogenous lipoic acid on E2 is somewhat less pronounced. They also show that the lipoyl ligase enzyme in *E. coli* is capable of at least partially lipoylating these proteins indicating that these domains are correctly folded. These results are particularly encouraging in terms of the proper folding of the independent E3BP component. When expressed alone, a substantial enhancement in lipoylation is observed in the presence of exogenous lipoate compared to the control lane. This suggests that, at the very least, the N-terminal domain of E3BP is correctly folded. A similar conclusion can be drawn for the individually expressed E2 and also the coexpressed E2/E3BP proteins.

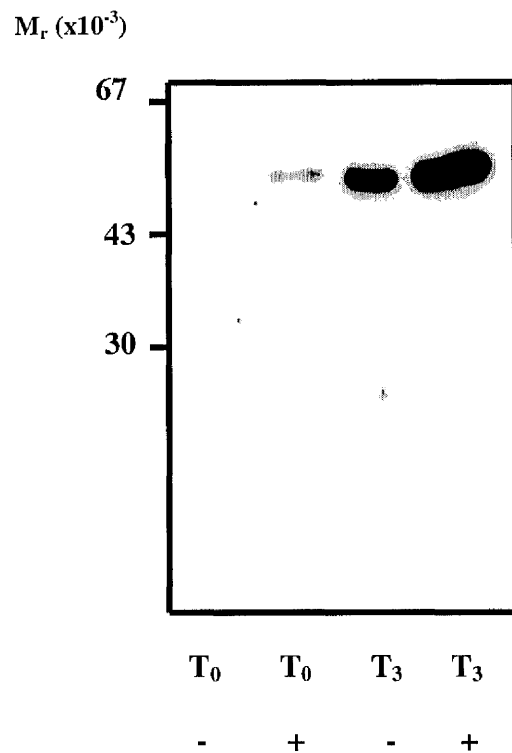


**Figure 4.1a Western blot analysis of E3BP**

Cultures grown in the absence (-) or presence (+) of exogenous lipoate were subjected to Western blotting using a monoclonal antibody (PD2) specific for lipoylated protein at time 0 and 3h after induction.

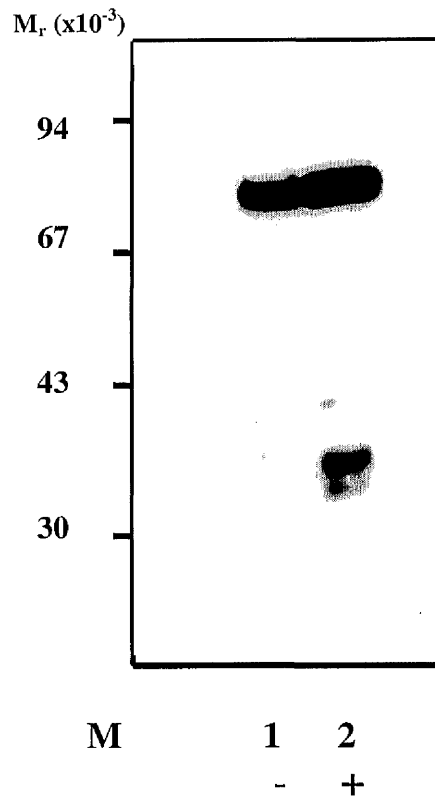


**Figure 4.1b Western blot analysis of E2**

Cultures grown in the absence (-) and presence (+) of exogenous lipoate were subjected to Western blotting using a monoclonal antibody (PD2) specific for lipoylated enzyme at 3h after induction.

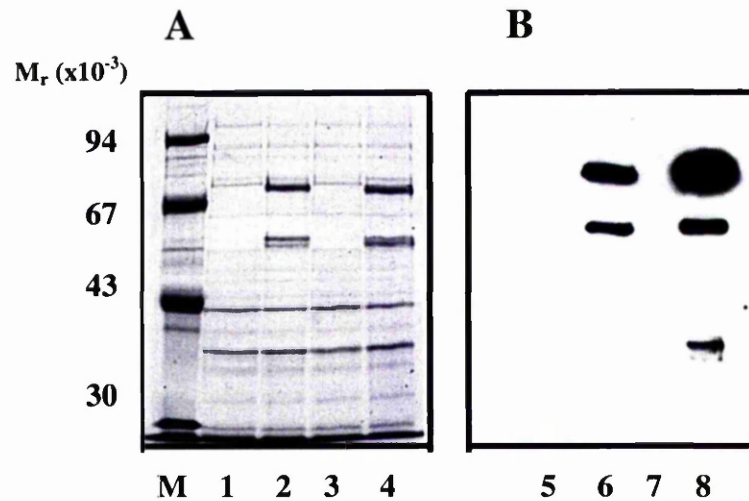


**Figure 4.1c Western blot analysis of cotransformed E2 and E3BP**

Western blot analysis was performed on cotransformed E2/E3BP grown in the absence (-) or presence (+) of exogenous lipoate using a monoclonal antibody (PD2) specific for lipoylated protein.

**Panel A:** SDS-PAGE analysis of the cotransformed cultures at  $T_0$  and  $T_3$  grown in the absence (lanes 1 and 2) and presence (lanes 3 and 4) of exogenous lipoate.

**Panel B:** Immunoblot of the cotransformed cultures. A strong enhancement in lipoylation is seen where the cultures were grown in the presence of exogenous lipoate (lane 8) as compared to the culture grown in the absence of lipoic acid (lane 6). This enhancement is much more pronounced for E2.

## **4.4 Purification of recombinant proteins**

All proteins cloned and expressed so far have been produced with a Histidine-tag attached at their N-termini. This tag can be utilised to achieve their rapid purification. In order to do this a metal chelate column attached to a BioCAD Sprint Perfusion Chromatography System was used for the initial purification step in most cases. The exception to this is the E1 component, which is discussed later in the chapter.

Recombinant proteins were routinely purified as described below.

### **4.4.1 Lysate preparation**

Large-scale protein induction was carried out as described previously and the cells pelleted by centrifugation. The pellets were resuspended in 20ml starting buffer and disrupted under high pressure using a French Press cell. Protease inhibitors were added to the cell extract and the supernatant clarified by centrifugation in preparation for loading on the metal chelate column (see Materials and Methods section 2.4.7 for details).

### **4.4.2 Purification of crude extracts**

The metal chelate column was routinely prepared for purification as described in Materials and Methods. Zinc ions were chosen as the most appropriate metal ion with which to saturate the chelating groups on the column since initial purifications were carried out using  $\text{Ni}^{2+}$  and it was found that this particular ion resulted in very strong binding of the His-tagged protein. Elution of the protein, therefore, occurred over an extended range with the majority of the bound protein eluting at very high imidazole concentrations. Zinc ions have a lower binding affinity for His than  $\text{Ni}^{2+}$  so allowing the target protein to be eluted earlier in the elution gradient.

After clarification of the supernatant and preparation of the column, the supernatant was loaded on to the column in 5ml aliquots. After each injection the column and loop were washed with starting buffer to ensure that all the lysate was washed onto the column. After the final injection the column was washed further with starting buffer to completely remove any unbound protein. The target protein was then eluted in an increasing linear gradient of imidazole (20-500mM) and 2ml fractions collected. After elution of the protein the column was washed in high imidazole buffer (buffer B) to ensure that all protein had eluted before washing the column in stripping solution to remove the metal ions and any residual protein. Aliquots of the relevant fractions were TCA precipitated and subjected to analysis by SDS-PAGE.

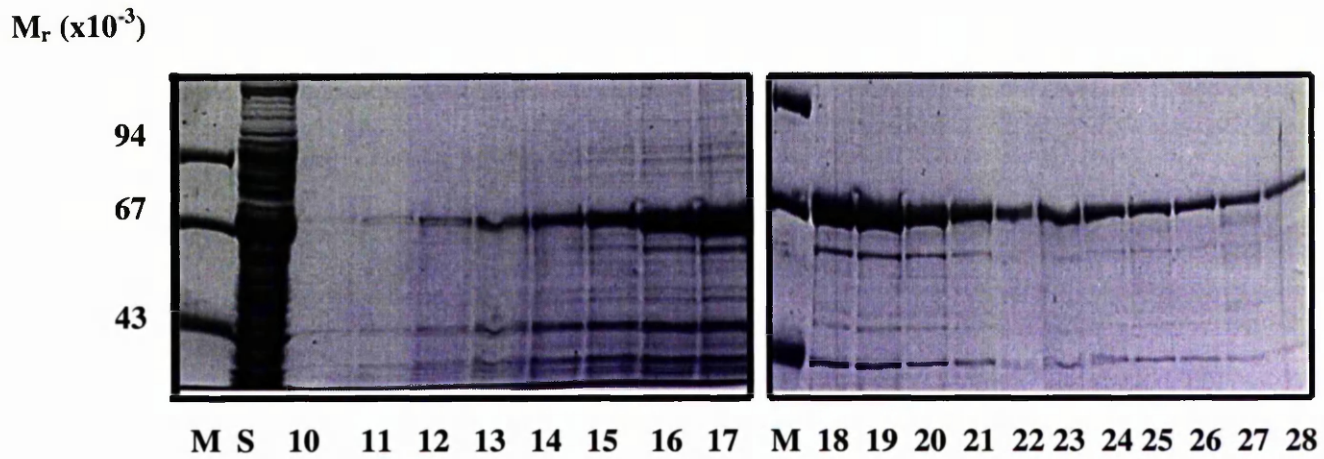
#### **4.5 Purification of E2**

Figure 4.2 shows a typical trace representing the purification of E2 obtained from half a litre of culture. It is common to see a smaller peak appearing before the major peak during purification of E2. Analysing the appropriate fractions on 10% SDS-PAGE usually indicates that the first peak consists mainly of loosely-bound contaminants with little or no target protein present in this peak. The second larger peak contains the protein of interest as well as small amounts of other contaminating bands. Figure 4.3 demonstrates the level of purity that can be achieved using this type of affinity chromatography. As this SDS-PAGE gel indicates, although E2 has been purified from the vast majority of bacterial proteins there are also a few contaminating bands present.

##### **4.5.1 Optimisation of purification using ion-exchange chromatography**

For some applications, further purification of the target protein was required using ion exchange chromatography. First, it was necessary to optimise the conditions under which ion-exchange chromatography would be successful for each enzyme.





**Figure 4.3 SDS-PAGE analysis of purified E2 from a metal chelate column**

Peak fractions from the purification of E2 were subjected to 10% SDS-PAGE analysis.

Protein bands were viewed by staining the gel with Coomassie Blue for 1h before destaining overnight.

M, low molecular mass markers; S, load fraction; 10-28, peak fractions from the column.

Again, these steps were performed using the BioCAD Sprint Perfusion Chromatography System. For optimising conditions several different matrices were tested over a pH range of 6-9. From these studies it was found that optimal conditions for purification occurred using the strong anion-exchange media, HQ with a Tris-HCl buffer at pH 7. The starting buffer consisted of 20mM NaCl, 50mM Tris-HCl, pH 7 while the protein was eluted in a linear salt gradient from 20mM to 1M NaCl. This was found to be the optimal conditions for further purification of all target proteins so far cloned (data not shown).

#### 4.5.2 Specific activity of E2

E2 can be assayed for activity as described in Materials and Methods. As already mentioned, the activity of E2 cannot be expressed in units since the precise molar extinction coefficient of the immediate product of the assay, 8-acetyl-dihydrolipoamide, cannot be determined; therefore E2 activity is recorded as the change in absorbance/min. A purification table can be constructed for E2 using  $\Delta A_{232}/\text{min}$  as the units for E2 activity as seen in Table 4.1.

	Vol (ml)	Protein (mg/ml)	Total protein (mg)	E2 activity ( $\Delta A_{232}/\text{min}/\text{ml}$ )	Total activity ( $\Delta A_{232}/\text{min}$ )	% E2 recovery	Activity ( $\Delta A_{232}/\text{min}/\text{mg}$ )	Purification factor
Load fraction (MC column)	20	19.2	384	15.4	308	100	0.8	1.0
Pool (after MC column)	30	1.6	48	14.5	435	141	9.1	11.3
Pool (after HQ column)	21	0.9	18.9	13.2	276.6	89	14.6	18.2

**Table 4.1 Purification table for E2**

According to Table 4.1, in this particular example the percentage recovery of protein was very high with little or no loss of recovery after purification on the metal chelate column. This may be due to the difficulties in assaying E2 for activity. Anion-exchange chromatography resulted in a percentage recovery of about 89%. The specific activity calculated here is  $14.6\Delta A_{232}/\text{min}/\text{mg}$ . This is in close agreement with that found in the literature. Purified recombinant E2 has been described as having a specific activity of  $19.4\Delta A_{232}/\text{min}/\text{mg}$  (Yang *et al*, 1997).

#### **4.6 Purification of E3BP**

The purification of E3BP follows a very similar protocol to the one described for E2. Figure 4.4 shows a typical profile for the purification of E3BP obtained from half a litre of culture. Again, as with E2, it is common to see a smaller peak eluting first which usually contains contaminating proteins while the larger peak, which elutes slightly later in the gradient contains the target protein. SDS-PAGE analysis of appropriate fractions from the purification of E3BP is seen in Figure 4.5. This gives an indication of the level of purity that can be achieved in a single step. Again, anion-exchange chromatography can be employed to remove minor contaminants and concentrate the protein.

#### **4.7 Purification of E3**

The purification of E3 was performed as above for the E2 and E3BP enzymes with the following modifications. E3 is, in itself, a very stable enzyme and it can be assayed for activity very efficiently. This enzyme can be heated at  $65^{\circ}\text{C}$  for up to 1h with no concomitant loss in activity as assessed by assaying E3 activity at time points throughout the heat treatment. This heat treatment acts as an additional purification step as many proteins,

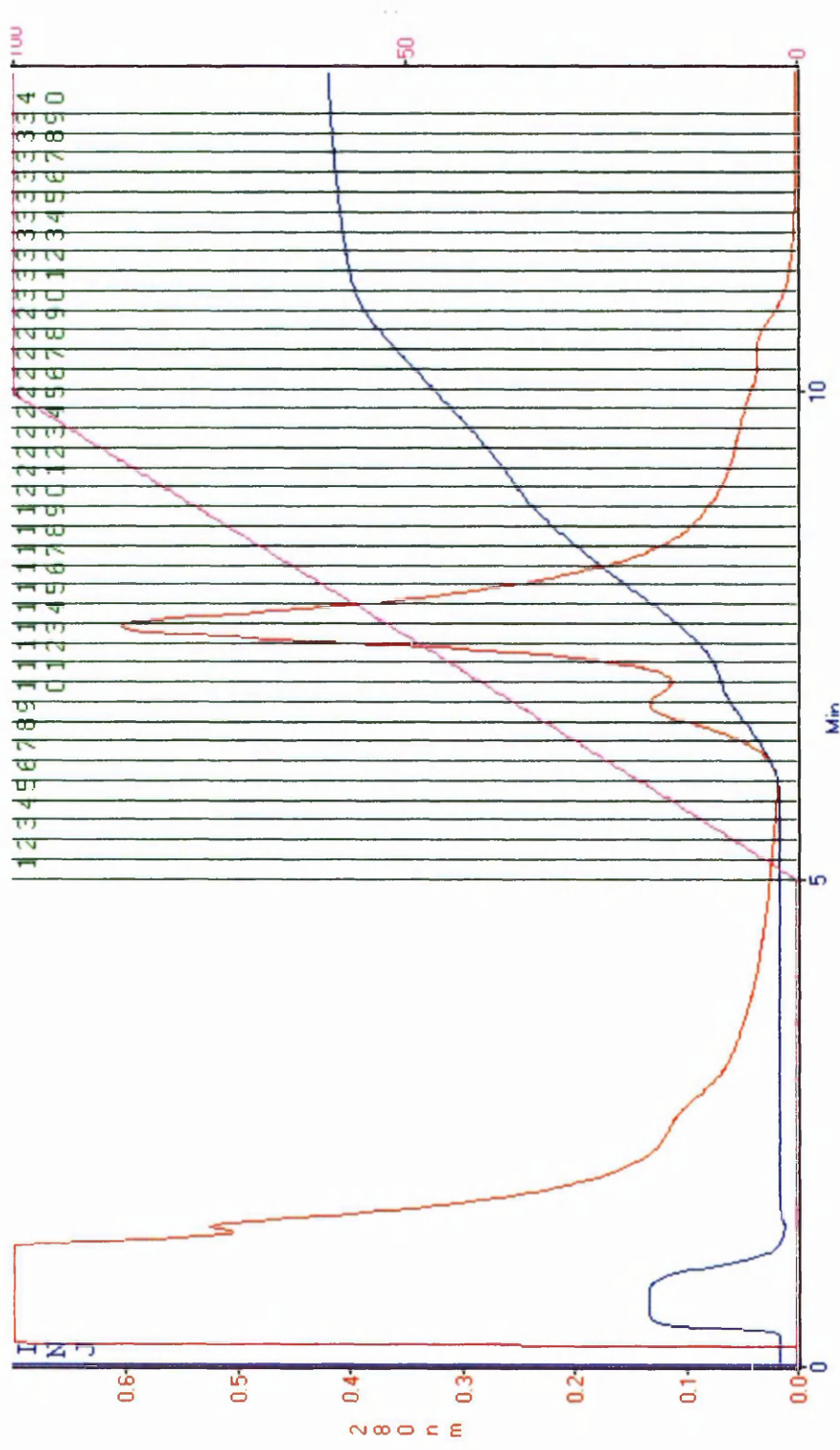


**Figure 4.4 Purification profile for E3BP**

An example of a purification trace from E3BP obtained from half a litre of culture. As with the previous example the red line shows the absorbance at 280nm, the blue line is the conductivity and the pink line represents the linear imidazole gradient. The numbers in green indicate the fraction numbers.

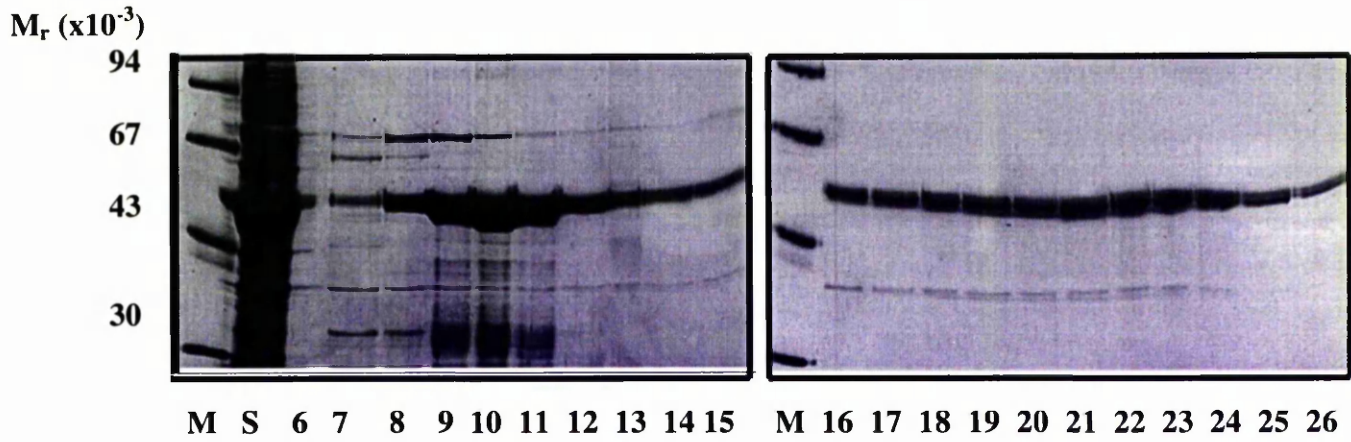


**Figure 4.5 SDS-PAGE analysis of the purification of E3BP**

Aliquots of the appropriate fractions were subjected to TCA precipitation and analysed by 10% SDS-PAGE. Protein bands were visualised after staining for 1h with Coomassie Blue before destaining overnight.

M, low molecular mass markers; S, load fraction; 6-26, represents the peak fractions analysed.

which are not heat-stable, are denatured and, when the supernatant is then clarified by centrifugation these proteins are pelleted while E3 remains in the soluble fraction. This supernatant is then loaded on to the metal chelate column in 5ml aliquots and eluted in an increasing gradient of imidazole over 8 column vol. Figure 4.6 shows a typical trace obtained from the purification of E3 from half a litre of culture. A symmetrical peak is usually obtained and upon analysis of the appropriate fractions on 10% SDS-PAGE it can be seen that E3 is purified to near-homogeneity. An example of this can be seen in Figure 4.7.

As well as giving an indication of the level of purity that is achieved through this 2 step purification of E3, the SDS-PAGE gel also shows that there is very little difference in the levels of E3 in the supernatant before (lane 1) and after (lane 2) heat treatment. Analysing the pellet (lane 3) after heat treatment indicated that there is very little E3 lost during heating. This can also be monitored by assaying the appropriate fractions for E3 activity. A purification table for E3 is shown in Table 4.2.

	Vol (ml)	Protein (mg/ml)	Total protein (mg)	E3 activity (U/ml)	Total activity (U)	% E3 recovery	Specific activity (U/mg)	Purification factor
Preheat	5	15.6	77.8	132.5	662.5	100	8.52	
Load	4.5	3.3	14.9	151.6	682.1	103	45.8	5.4
Pool	12	0.2	2.1	26.4	316.8	48	150.9	17.7

**Table 4.2 Purification table for E3**

The results shown in this purification table provides support for the conclusions drawn from analysing the SDS-PAGE gel. This confirms that no E3 activity is lost during the heat

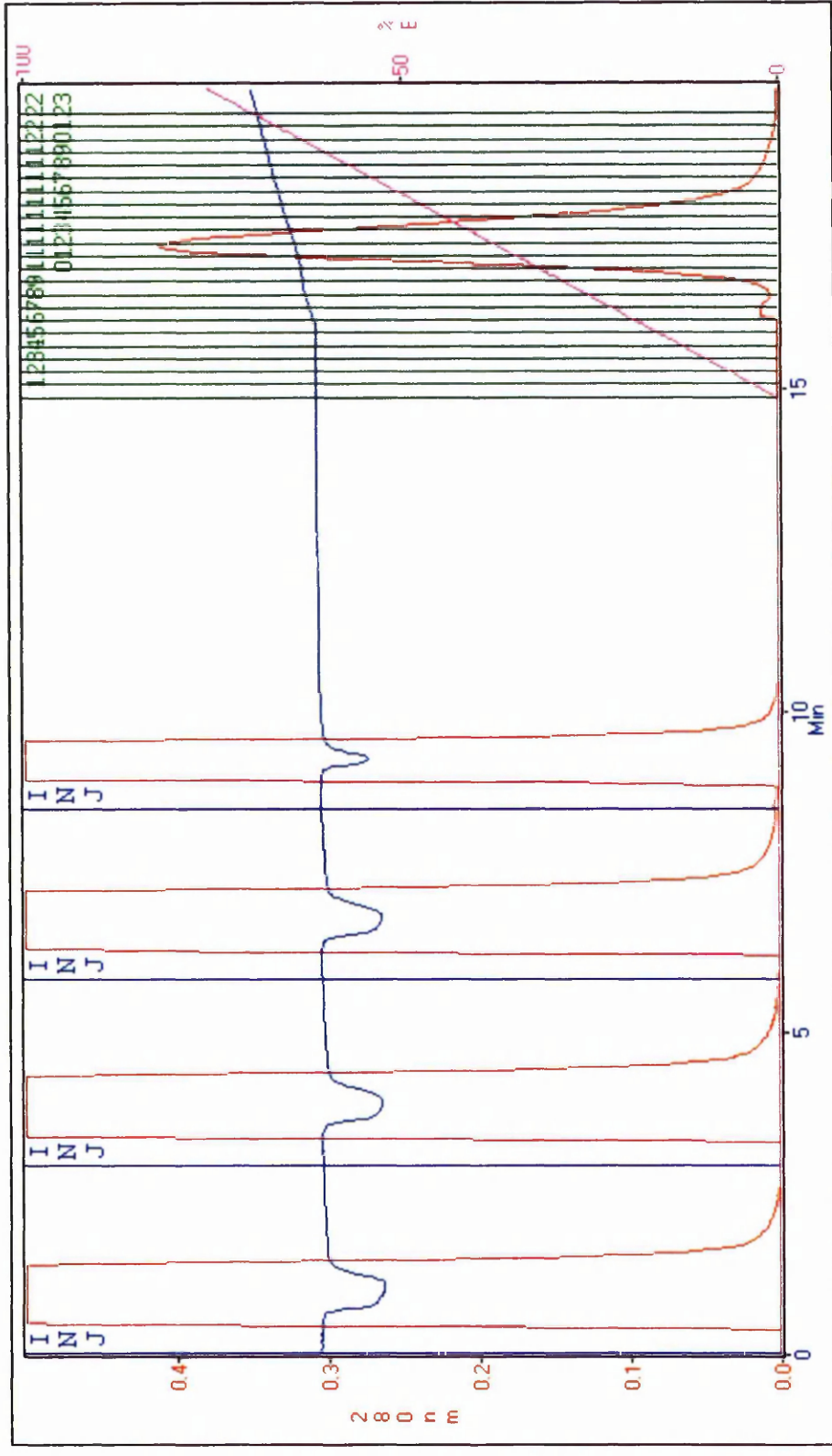


**Figure 4.6 Purification profile for E3**

E3 was purified on the metal affinity column after heating the enzyme to 65°C for 1 hour. The extract was applied to the metal chelate column in a series of injections. As before, the red line shows the absorbance at 280nm, the blue line is the conductivity and the pink line represents the elution gradient. The numbers in green represent the fraction numbers.

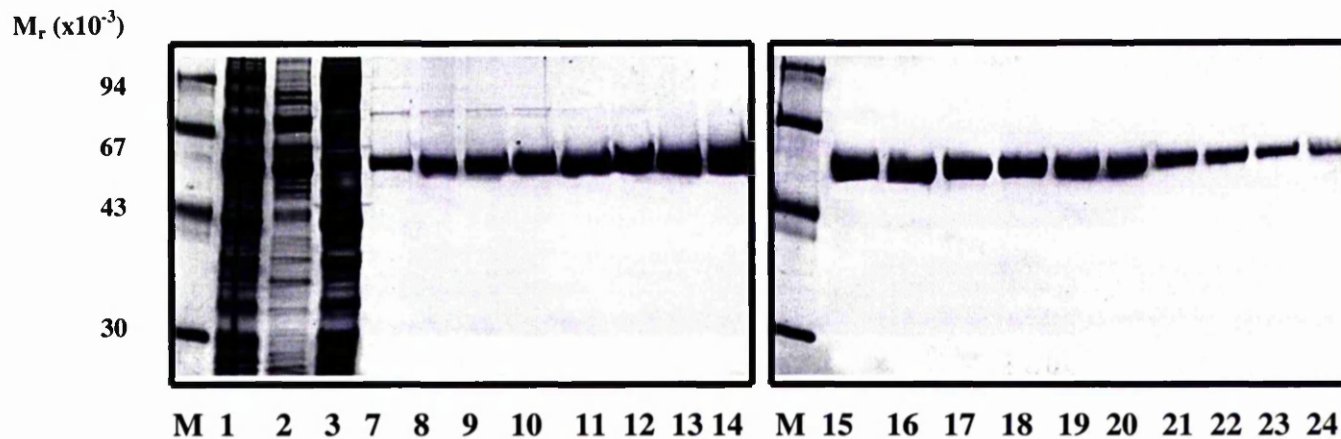


**Figure 4.7 SDS-PAGE analysis of the purification of E3**

E3 can be purified in 2 stages, by heating the crude extract to 65°C for 1h and then loading the clarified supernatant on to the metal chelate column. After extensive washing of the column, E3 is eluted in a linear increasing gradient of imidazole.

M, low molecular mass markers; 1, supernatant before heat treatment; 2, supernatant after heat treatment; 3, pellet after heat treatment; 7-24, represent the peak fractions analysed after elution.

treatment since the total activity of the sample taken before heating (Preheat) and then after heating (load fraction) is very similar. However, in this particular example approximately half the E3 activity is lost during purification on the metal chelate column. In this case, the specific activity of the load fraction is 45.8U/mg while the pool fraction was found to have a specific activity of 150.9U/mg. These specific activities are very close to the quoted values for native E3 that has been purified from bovine heart (refer to section 4.11)

#### 4.8 Purification of coexpressed E2/E3BP

Purification of coexpressed E2/E3BP is performed in a similar manner to the purification of the individual E2 and E3BP components. Figure 4.8 shows a typical example of a purification profile for E2/E3BP obtained from half a litre of culture. The red line on the trace follows the elution of the protein at 280nm.

Analysis of the appropriate fractions from the purification of E2/E3BP on 10% SDS-PAGE reveals that, although only E3BP has been cloned with a His-tag, the 2 proteins have coeluted in each fraction. This suggests that E2 and E3BP have bound to each other since E2 would not have bound to the column. Even under the high salt conditions (1M NaCl) of the purification protocol the E2/E3BP complex does not dissociate indicating that this complex is very stable, a situation similar to the native complex. Figure 4.9 illustrates this point showing that each eluted fraction contains both E2 and E3BP. In this case, the first larger peak contains most of the E2/E3BP, particularly in the first 4 fractions. This E2/E3BP subcomplex can be purified further and concentrated by performing anion-exchange chromatography as for the individual E2 and E3BP subunits (data not shown).

Ratio of E2/E3BP  
 Doubled in E3BP?  
 low MW material?

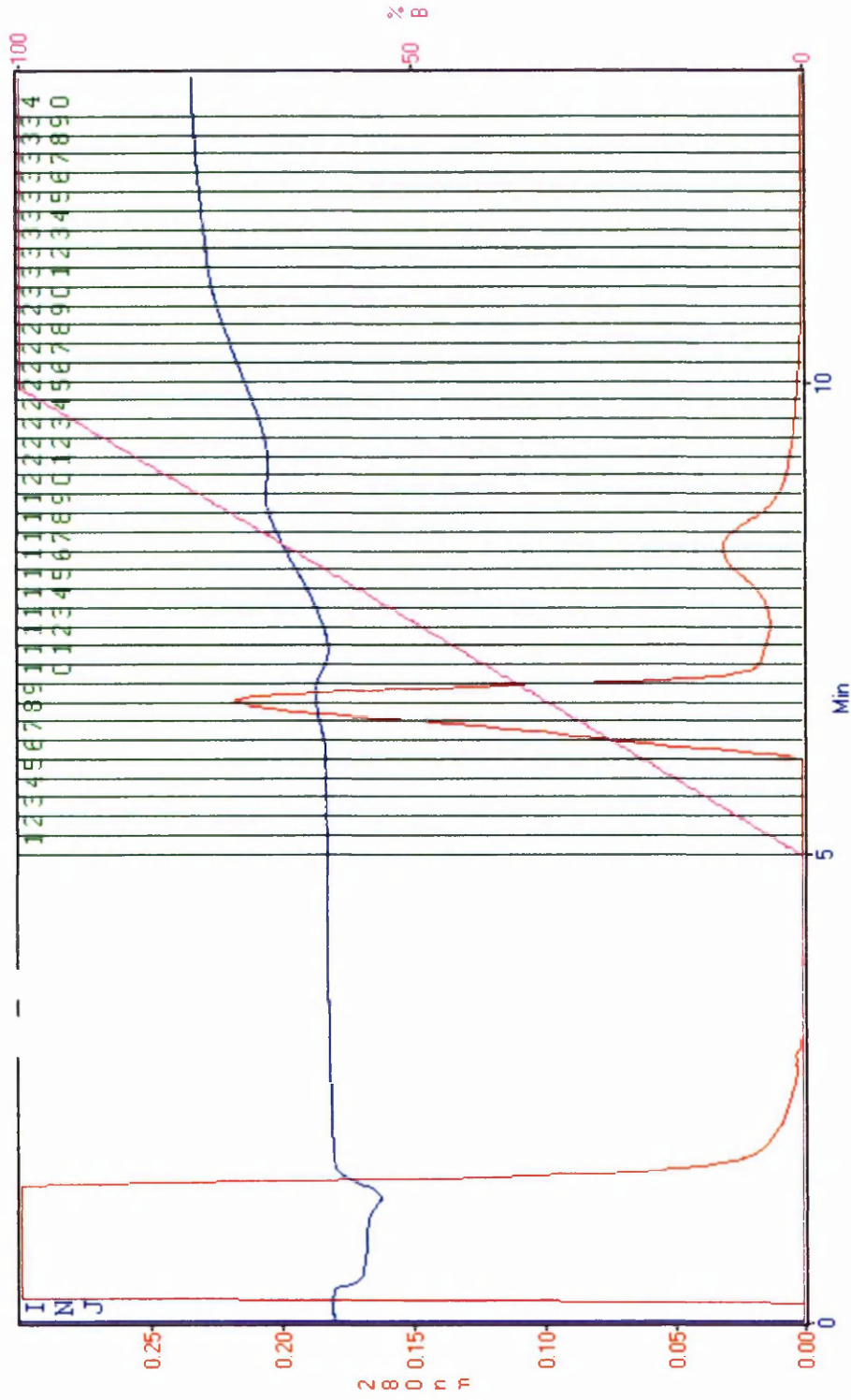


**Figure 4.8 Elution profile for coexpressed E2/E3BP**

Coexpressed E2/E3BP was purified as described previously. Aliquots of the relevant fractions were TCA precipitated as before and subjected to analysis on 10% SDS-PAGE. The fraction numbers are seen in green at the top.

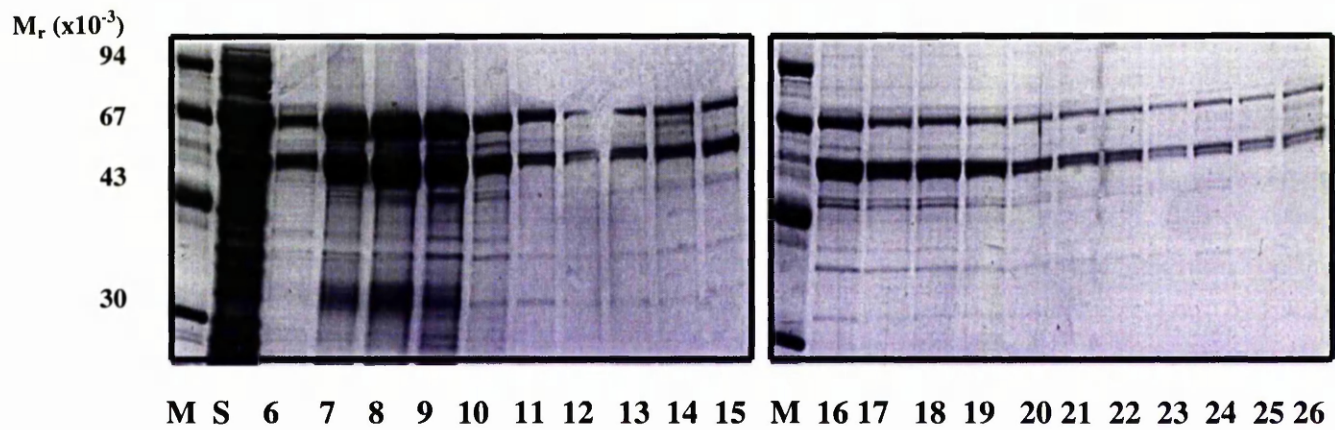


**Figure 4.9 SDS-PAGE analysis of the purification of E2/E3BP**

Fractions obtained from the elution of E2/E3BP were subjected to 10% SDS-PAGE analysis. Protein bands were visualised after staining in Coomassie Blue for 1h before destaining the gels overnight.

M, low molecular mass markers; S, load fraction; 6-26, represent peak fractions 6-26.

After purification the relevant fractions are pooled, dialysed into the appropriate buffer and concentrated for further study. Figure 4.10 shows a SDS-PAGE gel of all purified proteins after pooling and concentrating the relevant fractions. This provides an indication of the level of purity routinely achieved by following the protocol above.

#### 4.9 Purification of E1

As mentioned in a previous chapter, E1 was cloned by expressing the  $\alpha$  and  $\beta$  subunits on separate plasmids before coexpressing them in *E. coli* to produce an  $\alpha_2\beta_2$  E1 component. While this technique posed no problems for the coexpression of E2 and E3BP, E1 has proved problematic. It was always possible that difficulties would arise when cloning PDC-E1. Other investigators who have cloned this component both from PDC and BCOADC have reported difficulty in producing a soluble protein. In some cases, simply reducing the induction temperature to 25°C and increasing the time of induction from 3 to 16h (Korotchkina *et al*, 1995) seemed sufficient to produce appreciable levels of soluble E1. In other cases, it was found that the coexpression of the molecular chaperones GroEL and GroES were also required (Wynn *et al*, 1992) in order to produce soluble, active enzyme. This seems to be especially true in the case of the mammalian BCOADC-E1.

In our hands, when E1 $\alpha$  and E1 $\beta$  were expressed individually and assessed for solubility it was found that both subunits were essentially completely insoluble (data not shown). These recombinant plasmids were then cotransformed into *E. coli* and

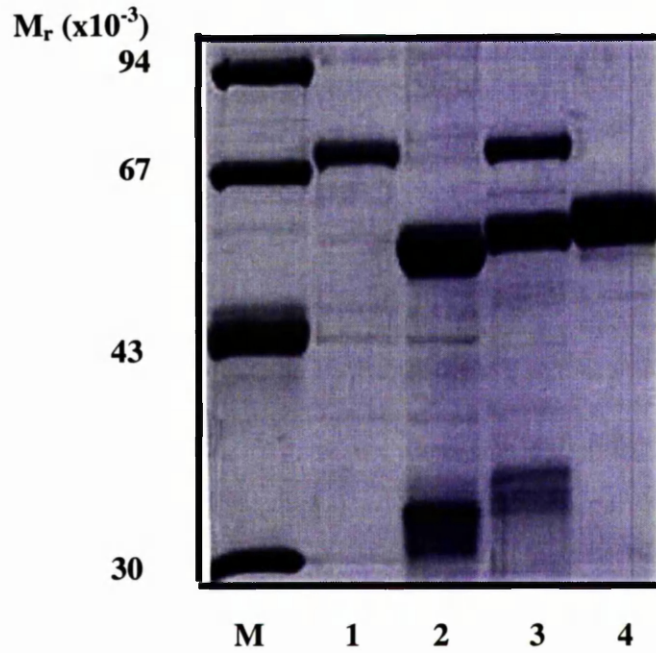


**Figure 4.10 SDS-PAGE analysis of the purification of the individual recombinant enzymes of human PDC**

Relevant fractions for each purification were pooled and concentrated before analysis by 10% SDS-PAGE.

M, low molecular mass markers; 1, E2; 2, E3BP; 3, coexpressed E2/E3BP; 4, E3;

induced as described for E2/E3BP. Examination of the cotransformed cultures, as shown in Figure 4.11, demonstrates that at all the temperatures studied, 25°C, 30°C and 37°C, both subunits again were insoluble. It is possible that there is a small amount of soluble material present in the supernatant, which may be more pronounced for the E1 $\beta$  subunit, but when the supernatants were assayed for enzymatic activity no significant E1 activity was detected. There is no clear difference in the levels of solubility at the lower temperatures when compared to the solubility levels at 37°C. These studies were initially performed using *E. coli* BL21 (DE3) pLysS cells. Induction of the cotransformed subunits was also performed in other *E. coli* strains, mainly BL21 (DE3), BL21 (DE3) CodonPlus, HMS174, AD494 and M15 cells. These studies were again conducted at 3 temperatures, 25°C for 16h and 30°C and 37°C for 3h. As was found previously, at all temperatures and with all strains used both subunits were found in the pellet with none present in the supernatant. This finding has obvious implications for obtaining sufficient amounts of active, purified E1 protein.

In order to produce soluble recombinant E1 it may be necessary to coexpress the subunits with molecular chaperones, in particular GroEL and GroES as described for the mammalian branched-chain 2-oxoacid dehydrogenase E1 component (Wynn & Davies, 1992; Chuang *et al*, 1999). However this in itself poses some difficulties as the molecular chaperones in question are contained on a separate plasmid. A number of plasmids containing the genes for GroEL and GroES are at our disposal thanks to a generous gift from Dr Peter Lund, University of Birmingham (plasmids pSUBH and pBADcmESL) and Dr Anthony Gattenby, Dupont (pGroESL). With E1 $\alpha$  and E1 $\beta$  also present on individual plasmids, the successful cotransformation of three separate

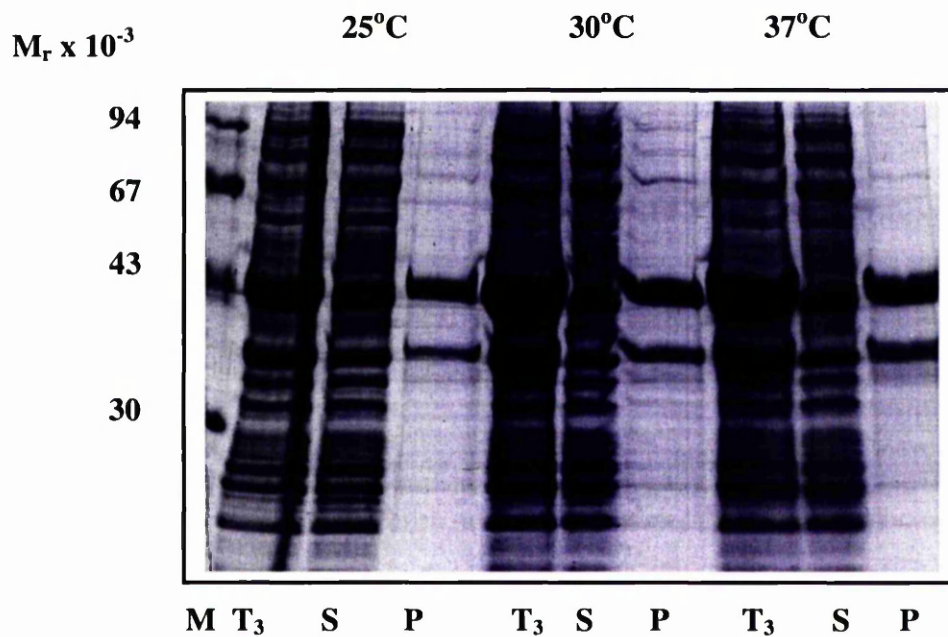


**Figure 4.11 Solubility studies on the coexpressed E1 $\alpha$  and E1 $\beta$  subunits**

The solubility of coexpressed E1 $\alpha$  and E1 $\beta$  was assessed at 3 different temperatures, 25°C, 30°C and 37°C. Samples of the supernatant and pellet fractions were TCA precipitated before electrophoretic separation by 15% SDS-PAGE.

M, low molecular mass markers; T<sub>3</sub>, sample taken 3h after IPTG induction; S, supernatant; P, pellet.

plasmids into *E. coli* is difficult to achieve due to the three different antibiotic resistance markers required. One way of overcoming this difficulty is to construct a plasmid that contains the genes for both E1 $\alpha$  and E1 $\beta$ . Each subunit would have its own promoter, there would be a His-tag to allow for purification on a metal affinity column and the plasmid would contain the gene for ampicillin resistance. Since all the plasmids containing the molecular chaperones are chloramphenicol-resistant this would allow cotransformation and selection of colonies containing both plasmids to take place on double-antibiotic resistance plates. In this way, it would be hoped that sufficient levels of soluble and active E1 could then be produced. This coexpression plasmid was constructed by modifying pET-14b into which E1 $\alpha$  had been cloned with a digested fragment of pET-11b into which E1 $\beta$  had been cloned. Figure 4.12 shows a map of the coexpression plasmid.

This coexpression plasmid was originally transformed into BL21 (DE3) pLysS cells for overexpression of protein and examined for solubility as described previously. As found for the individually expressed subunits, the coexpressed proteins proved to be insoluble at all temperatures studied, 25°C for 16h, 30°C and 37°C (data not shown). Overexpression in other *E. coli* strains, such as AD494, HMS174, BL21 (DE3) and BL21 (DE3) CodonPlus had no effect on the solubility of the E1 component.

However, this construct can now be used in conjunction with molecular chaperones in the hope that this strategy will produce soluble, active E1. Unfortunately preliminary studies using this coexpression plasmid with the molecular chaperones GroEL/GroES have not been encouraging. When transformed individually into *E. coli*, GroEL/GroES and E1 $\alpha$ /E1 $\beta$  express well but when cotransformed into the same cells

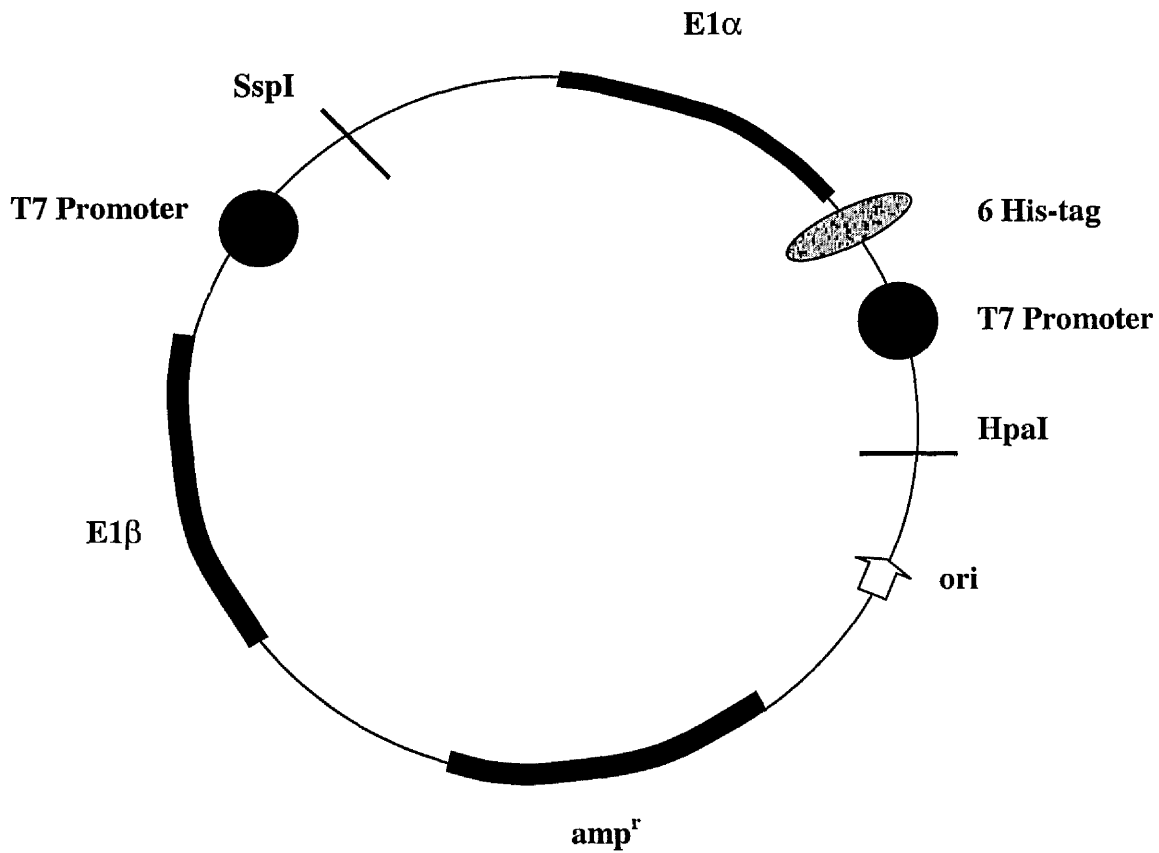


**Fig 4.12 Map of the coexpression plasmid, E1.**

The E1 coexpression plasmid was constructed by digesting a ScaI-SspI fragment from the pET-14b plasmid previously cloned with the E1 $\alpha$  subunit. This was ligated with the E1 $\beta$  subunit, which was digested from a pET-11b vector. The gene for ampicillin resistance also came from the pET-11b plasmid.

one or other of the plasmids will express but not both. It is unclear at present why this is the case. This approach requires further investigation.

#### **4.9.1 Solubilisation and purification of E1 from inclusion bodies**

While work on constructing a coexpression plasmid was ongoing, attempts were made to solubilise the cotransformed  $\alpha$  and  $\beta$  subunits of E1. The technique adopted was based on the methodology of the protein folding kit from Novagen. This protocol requires extensive washing of the pellet obtained from an overexpressed culture, thus resulting in an almost homogeneous inclusion body preparation. The washed pellet can then be subjected to treatment with detergents to solubilise the protein of interest.

##### **4.9.1.1 Solubilisation of E1 using N-lauroylsarcosine**

Insoluble protein can be solubilised by the use of detergents such as N-lauroylsarcosine. In this case, after extensively washing the pelleted extract, as described in Materials and Methods section 2.4.11, the pellet was resuspended in an appropriate buffer, usually 50mM potassium phosphate, pH 7.2, supplemented with 0.5% N-lauroylsarcosine. After incubating this mixture for 30 min, with agitation, the protein was centrifuged at 10,000 rpm for 15 min to pellet any insoluble material before dialysis. Dialysis typically took place at 4°C with multiple changes of dialysis buffer. After concentrating the protein, samples were analysed by 15% SDS-PAGE and by assaying for E1 activity.

E1 was assayed for activity by monitoring the decrease in absorbance at 600nm as the dye DCPIP becomes reduced in the presence of the substrate pyruvate. Some examples of the specific activity of solubilised E1 are noted in table 4.3. Both

examples are taken from different preparations of solubilised E1 and indicate that the method used is reproducible since the specific activity of each preparation is similar.

Sample	Vol (ml)	Protein (mg/ml)	Total protein (mg)	E1 activity (U/ml)	Total activity (U)	Specific activity (U/mg)
1	10	4.8	48	2.52	25.2	0.53
2	10	0.32	3.2	0.419	1.34	0.42

**Table 4.3 Specific activity of E1 solubilised from inclusion bodies**

According to the examples given in table 4.3 above the specific activities obtained for E1 from different preparations seem fairly consistent although the protein concentrations from each sample differ markedly. These activities correlate well with those quoted for recombinant E1 in the literature (refer to section 4.11).

*What about native?*

#### 4.10 Discussion

In this chapter, a protocol has been developed which has allowed the reproducible purification of the individual components of human PDC. These enzymes have been purified in active form by means of affinity chromatography. Table 4.4 indicates the typical yields obtained for each recombinant protein.

Recombinant protein	Vector	Yield (mg/litre)
E1 $\alpha$ /E1 $\beta$ (coexpression)	pET-28b/pET-11b	2-5mg/l
E1 (coexpression)	modified pET-14b	2-5mg/l
E2	pET-14b	10-20mg/l
E3BP	pET-14b	10-20mg/l
E2/E3BP (coexpression)	pET-11b/pET-28b	10-20mg/l
E3	pET-14b	20-30mg/l

**Table 4.4 Summary of the yields of individual enzymes cloned and expressed in *E. coli***

Measurement of the activity of the E2 and E3 enzyme components have indicated that these enzymes have been purified in active form and, in general, the specific activities described here correlate well with those quoted in the literature for the recombinant protein. For E3, the specific activity of 150.9U/mg compares well with that quoted for native bovine E3, cited at 174.33U/mg (R.G. McCartney, PhD thesis). For recombinant, purified E3 the specific activity has been found previously to be 776U/mg (Liu *et al*, 1995c) and 540U/mg (Liu *et al*, 1999) for two different preparations. These values are much higher than that obtained here but it should be noted that these investigators performed enzyme assays at 37°C, as opposed to 30°C. This higher temperature can result in a 2-3 fold increase in specific activity. For E2, the recombinant protein has previously been found to have a specific activity of 19.4 $\Delta A_{232}$ /min/mg (Yang *et al*, 1997) which is slightly higher than that described here (14.6 $\Delta A_{232}$ /min/mg) but these values do correlate well. Any differences in the assay

conditions used such as performing the assay at a slightly higher temperature or changing the pH can affect the measured activity of the enzyme.

Purification of the E1 component has proved to be more problematic. While sufficient overexpression of both subunits that comprise the human heterotetrameric E1 component has been consistently obtained, this may be part of the problem regarding the insolubility of these proteins. The production of recombinant protein often results in accumulation of these proteins in inclusion bodies, regardless of the host system used. Often, it is simply the case that the high level of expression of the recombinant protein exceeds the solubility limit of the host cell resulting in aggregation and subsequent sequestration in inclusion bodies. There are a number of factors which, when altered, may improve the solubility of the recombinant protein. Lowering the induction temperature or reducing the concentration of inducer (in this case IPTG) can often be effective in increasing the solubility of the target protein by limiting the induction of gene expression (Schein, 1989). In this case these steps proved ineffective in improving the solubility of E1.

There are also concerns over the use of detergents in obtaining soluble preparations of E1. While E1 solubilised in the presence of N-lauroylsarcosine appears to be active, this detergent seemed to have an adverse effect on the activity of purified native PDC from bovine heart (data not shown). This has obvious implications in performing any studies with E1 solubilised in this manner. N-lauroylsarcosine is a mild anionic detergent and is believed to be effective in refolding proteins by coating hydrophobic surfaces that may be exposed in an incorrectly folded protein thus minimising aggregation (Burgess, 1996). E1 purified in this manner has been found to be active as

shown in Table 4.3. However, when the specific activities quoted here are compared with that for purified native E1 from bovine heart which was determined to be 5.68 U/mg (R.G. McCartney, PhD thesis) it is obvious that there is a significant difference in the values obtained.

In this context, one unit of enzyme activity has been defined as 1 $\mu$ mol of substrate used or product formed per min at 30°C. According to Korotchkina and coworkers (1995) who cloned both subunits of human E1 using a coexpression plasmid, the specific activity of their recombinant, purified E1 has been quoted as 130.1 mU/mg where 1mU is defined as 1nmol of substrate used or product formed per min at 37°C. Converting this specific activity to U/mg results in an activity of 0.13 U/mg, which is a good correlation with the specific activities shown in Table 4.3 (0.53 and 0.42U/mg). It should be noted that E1 activity in this paper was measured by the formation of <sup>14</sup>CO<sub>2</sub> in the presence of potassium ferricyanide and not by the DCPIP assay. Likewise, Fang and coworkers (1998) have determined the specific activity of recombinant human E1 to be 31.7mU/mg and this was measured using the DCPIP assay. More recently, Korotchkina and coworkers (1999) have measured E1 activity by both the DCPIP assay and by measuring the formation of CO<sub>2</sub> and have published values of 149 and 64.3 mU/mg respectively. Recombinant *E. coli* E1 has been quoted as having a specific activity of 0.0106 U/mg (Yi *et al*, 1996). Taking these activities into account it would appear that the specific activities determined for the E1 clone described here are adequate. However, there are obvious discrepancies between these values and the value quoted for native bovine E1. It is worth noting at this point that the values for the native PDC quoted above are for the bovine complex. Other investigators who have examined the activity of both the native bovine and human

complexes found that the activity of human PDC was consistently measured at rates at least 3-5 fold lower than that of bovine PDC (Dr J.M. Palmer, personal communication). Since E1 is believed to catalyse the rate-limiting step in the catalytic mechanism it is entirely possible that this lower rate of enzyme activity is a consequence of the E1 component.

Other problems associated with this solubilisation method have arisen as a result of difficulties in removing detergent from the protein preparation. Substantial residual detergent has still been present after extensive dialysis of the sample. This has been a problem for other investigators using this approach (Burgess, 1996). Additionally, extensive dialysis has also frequently been found to result in precipitation of the protein.

Although E1 has been found to be active it is clear that an improved method of producing soluble E1 is required before studies using this component can progress. Coexpression of E1 with the molecular chaperones GroEL/GroES has not proved to be as straightforward as initially anticipated and this approach requires further investigation.

## **Chapter 5**

**Studies on the independent recombinant E3BP component  
and the structure and assembly of the recombinant E2/E3BP  
core**

## 5.1 Assembly of the structural core of human PDC

The 2-oxoacid dehydrogenase complexes are amongst the largest and most complex multienzyme structures known. Central to these complexes is the structural core formed by noncovalent interactions between multiple subunits of E2. In mammals, Gram positive bacteria, yeast and fungi 60 copies of the E2 polypeptide are organised into a pentagonal dodecahedral core structure with icosahedral symmetry. In PDCs from Gram negative bacteria and all known OGDCs and BCOADCs a cubic core with octahedral symmetry is formed from 24 copies of E2. This ability of E2 to form either a dodecahedron or a cube, depending on the species, makes the 2-oxoacid dehydrogenase complexes unique among macromolecular assemblies.

The atomic structure of the truncated C-terminal cubic core of *A. vinelandii* has been solved by x-ray crystallography (Mattevi *et al*, 1992; Mattevi *et al*, 1993). Crystal structures for the equivalent truncated dodecahedral cores of the *B. stearotherophilus* and *E. faecalis* complexes have also been reported (Izard *et al*, 1999) while the structure of the 60meric core from *S. cerevisiae* has been determined to low resolution by negative stain and cryoelectron microscopy (Stoops *et al*, 1992). A 3D reconstruction of bovine kidney PDC has recently been attempted using cryoelectron microscopy (Zhou *et al*, 2001). These studies have indicated that the basic building block for the structural core of both the cube and dodecahedron is a trimer of E2 subunits. Each E2 monomer is tightly associated with 2 identical subunits through extensive intermolecular connections to form a cone-shaped trimer. These trimers are then arranged along the 8 or 20 vertices of the cubic or dodecahedral structures, respectively. Trimers are thought to be interconnected by 'ball-and-socket' connections between a C-terminal anchor residue of one trimer and a hydrophobic

pocket formed by 2 adjacent monomers in a second trimeric unit. Two such connections on the 2-fold axis of symmetry appear sufficient to maintain the stable interactions between adjacent trimers (Mattevi *et al*, 1993). These trimers form a hollow cage-like structure with a maximum diameter for the dodecahedral structure of 237Å. The hollow cavity has a diameter of about 188Å while the faces of the core are approximately 52Å across. In the bacterial complexes these faces appear to allow the passage of substrate and product between the inner cavity and the outside of the complex. Evidence for this theory comes from the observation that in *A. vinelandii* PDC, access to the substrate-binding site is only possible from inside the cubic core (Mattevi *et al*, 1993b). However, in yeast and mammals, these faces have a role in binding an additional subunit, E3-binding protein (E3BP).

## 5.2 E3-binding protein (E3BP)

E3BP has been identified as an additional subunit in the pyruvate dehydrogenase complexes of mammals, yeast and in the parasitic nematode *Ascaris suum*, although in the latter example E3BP lacks an N-terminal lipoyl domain (Klingbeil *et al*, 1996). As yet, an equivalent to the E3BP has not been identified in PDC of any other organisms, nor has it been found in any OGDC or BCOADC complexes. It appears to have been derived from E2 by gene duplication and subsequently evolved to take on a specialised role in anchoring the E3 component to the core of the complex. Although the domain organisation of E3BP and E2 is very similar, both containing at least one lipoyl domain, a subunit-binding domain and a longer C-terminal domain, a catalytic function for E3BP has not yet been identified.

Densitometric scanning analysis of purified bovine E2/E3BP core and measurement of the acetyl groups incorporated from [2-<sup>14</sup>C] pyruvate revealed that there are 12 molecules of E3BP present in each mammalian PDC complex (Sanderson *et al*, 1996b) binding to the 12 faces of the dodecahedron. This suggests that the stoichiometry and organisation of E3BP is determined by the geometric constraints of the E2 scaffold and not by the number of potential binding sites. Maeng *et al* (1996) suggested that it was in fact E3BP itself which prevented full stoichiometric binding of E3BP to E2. This was proposed on the basis of their findings that E2 could bind approx. 20 copies of full length E3BP, 24 copies of E3BP lacking the lipoyl domain and approx. 31 copies of E3BP containing only the C-terminal domain. These studies were believed to show that segments of E3BP were causing steric hindrance and thus preventing full stoichiometric binding to the E2 core.

The interactions between E2 and E3BP are very tight making their separation in the native state very difficult to achieve. Indeed, it has been noted that while E1 and E3 can dissociate from the native PDC complex in relatively low levels of GdmCl of 0-0.2M (West *et al*, 1995) or in 1-2M NaCl, separation of E2 and E3BP can only occur under highly denaturing conditions such as 6M GdmCl. As a result of this tight association between these 2 components, independent studies on the isolated E3BP component have proved impossible. The production of an independent, soluble recombinant E3BP, first described by Palmer and coworkers (1999) and described here in chapter 3, can now allow this protein to be studied as an individual entity.

### 5.3 Aims of this chapter

- Determination of the oligomeric nature of E3BP using gel filtration chromatography and crosslinking studies.
- Determination of the folding and stability of the independent E3BP by means of circular dichroism and fluorescence spectroscopy.
- Studies on the recombinant E2/E3BP core using gel filtration and densitometric scanning analysis.

### 5.4 Results

#### 5.4.1 Determining the oligomeric nature of E3BP by gel filtration

In order to determine the oligomeric nature of the independent E3BP component, gel filtration chromatography using a size-exclusion column was utilised. A Superose 6 column was equilibrated in 50mM potassium phosphate, 150mM NaCl, 1mM DTT, pH 7.2. It was then calibrated with a series of proteins of known  $M_r$  value to construct a calibration curve of relative molecular mass against  $V_e/V_o$ , where  $V_e$  represents the elution volume of the protein under investigation and  $V_o$  is the void volume of the column.

Purified, concentrated E3BP was loaded on to the column and the elution profile of the protein monitored at 280nm. These experiments, using E3BP, have been repeated with different protein preparations in an attempt to generate reproducible results.

Despite optimising the conditions used, the elution profile for E3BP proved difficult to reproduce. A small peak often eluted at the void volume of the column while a second, generally larger peak, eluted later. The volume of elution of this second peak

varied, sometimes being representative of a monomeric species for E3BP, while at other times it eluted earlier in the column resulting in an estimated molecular mass of about 100 000 which is indicative of a dimer of E3BP. Elution at the void volume suggests that aggregation of protein was occurring on occasion. The interaction between E2 and E3BP is likely to be hydrophobic in nature and it may be that hydrophobic patches on E3BP, normally involved in the association with E2 are now exposed and cause E3BP to self-aggregate. This tendency of E3BP to aggregate is also discussed in section 6.4.

Given the variability in gel filtration profiles it was concluded that the native molecular mass of E3BP was unable to be accurately determined by this method. Thus crosslinking studies of E3BP, at specific protein concentrations, were undertaken in order to solve this problem.

#### **5.4.2 Crosslinking studies on E3BP**

Crosslinking experiments are a fast and relatively simple method for determining the oligomeric state of a protein and can be conducted at low protein concentrations. In this particular crosslinking experiment, glutaraldehyde was used as the crosslinker. Glutaraldehyde is a non-specific reagent that targets the amino side chains of lysine residues.

The crosslinking reaction was performed on purified E3BP that had been dialysed into 50mM potassium phosphate pH 7.2. A number of samples were subjected to crosslinking over a range of protein concentrations, from 0 to 1mg/ml. As a control,

purified E3 was also subjected to crosslinking as this enzyme is known to run as a dimer on SDS-PAGE after it has been subjected to the crosslinking reaction.

Figure 5.1 indicates that over this range of protein concentrations (0-1mg/ml) E3BP exists as a monomer. There is no indication of dimers forming at the low concentrations used in this study. The crosslinked proteins have a higher mobility compared to the control lanes since intra-subunit crosslinking results in a more compact protein after SDS treatment. This is illustrated very clearly by E3, where the crosslinked dimer (lane 2) runs at a molecular mass very much lower (approx. 80kDa) than the expected 110kDa of the native protein.

## **5.5 Circular dichroism**

Circular dichroism (CD) is a very useful technique for studying various aspects of protein structure. Used in conjunction with other techniques such as chemical crosslinking and gel permeation analysis it can provide useful information about the relationship between secondary, tertiary and the quaternary structures of a protein.

At present, CD is commonly employed to probe changes in the conformation of a macromolecule and to examine its interaction with small molecules. It is also used to determine empirically the secondary structure content of a protein. The stability of a protein can also be conveniently assessed by CD on addition of chemical denaturants such as GdmCl or urea, and to assess the effect of other parameters, mainly temperature or pH, on the native state of the protein.

The far-UV CD spectra (typically 240nm to 180 or 190nm) can be used to assess the overall secondary structure content of a protein. In this range, the principal absorbing

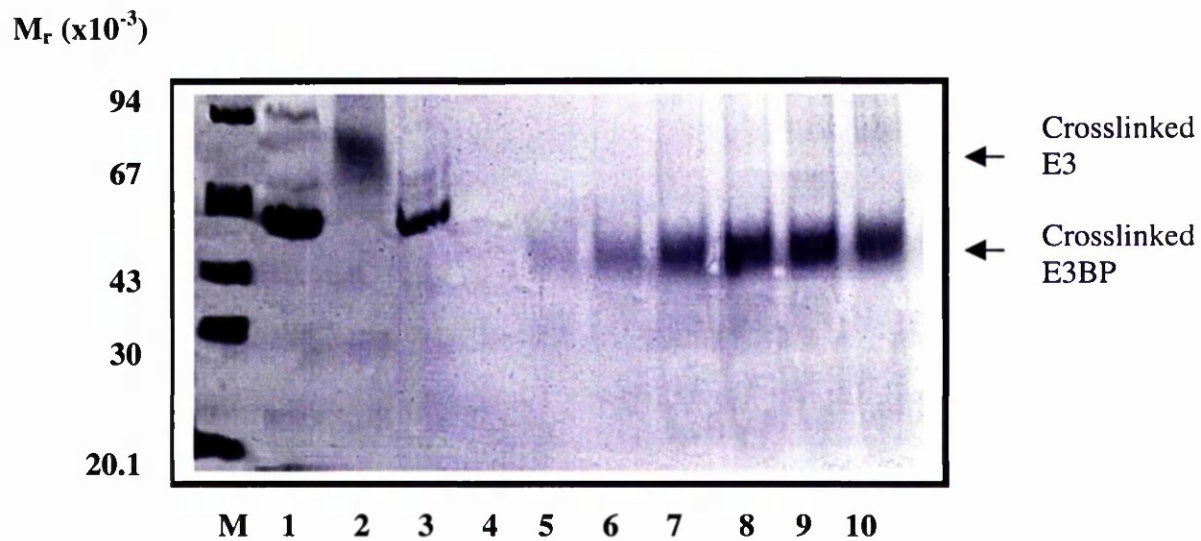


**Fig 5.1 Crosslinking studies on purified recombinant E3BP**

E3BP, at concentrations ranging from 0-1mg/ml, was subjected to crosslinking using glutaraldehyde. The crosslinked reactions were electrophoretically separated on 6% sodium phosphate SDS-PAGE gels before visualising by staining with Coomassie blue. E3 was treated in the same manner as a positive control.

M: low molecular mass markers, 1: uncrosslinked E3, 2: crosslinked E3 (positive control), 3: uncrosslinked E3BP, 4-10: crosslinked E3BP at concentrations of 0, 0.1, 0.2, 0.3, 0.5, 0.75 and 1mg/ml respectively.

group is the peptide bond. Given that the different types of regular secondary structure found in peptides and proteins exhibit distinct spectra in this range, it is possible to assess quantitatively the overall secondary structure content of the protein.

In the near-UV CD spectra (250 to 340nm), signals are obtained from the environments of the aromatic amino acid side chains, tryptophan, tyrosine, phenylalanine and to a lesser extent, cysteine. In a folded protein, the side chains of these amino acids are likely to be placed in a chiral environment thus giving rise to CD spectra that can provide information on the tertiary structure of the protein (for reviews see Kelly & Price, 2000; Rodger & Ismail, 2000; Kelly & Price, 1997).

### 5.5.1 Circular dichroism studies on the independent recombinant E3BP

Circular dichroism was used to monitor the stability of the recombinant full-length and didomain E3BP proteins. Figure 5.2 shows the far-UV CD spectra obtained when 0.5mg/ml full-length E3BP was incubated in varying concentrations of GdmCl for 15 min before measuring the CD signal. This data shows that, even in 6M GdmCl, this protein has not fully unfolded (for a fully unfolded protein ellipticity at 222nm would be expected to be close to zero).

Figure 5.3 shows the % total change in folded protein as a function of GdmCl concentration. The CD spectra of both the full-length E3BP and the didomain, which consists of the lipoyl domain and subunit-binding domain cloned as a His-tagged protein, have been plotted on the same graph for ease of comparison. They have been plotted as % total change of native protein since, in both cases, neither protein has fully unfolded under these experimental conditions.

Erron?  
How d)kl?

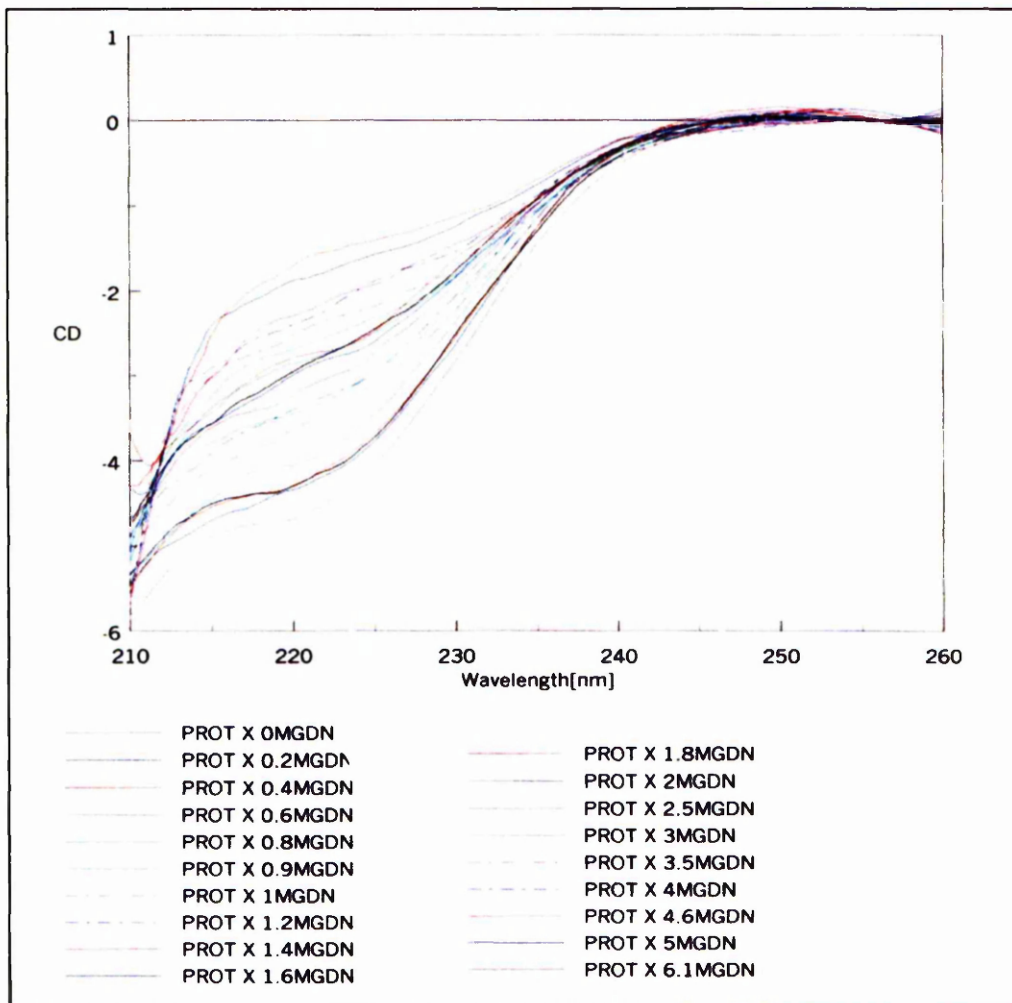


**Figure 5.2 Far-UV CD spectra of mature E3BP**

CD spectra for full-length E3BP were obtained after incubating 0.5mg/ml E3BP in increasing concentrations of GdmCl (0-6.1M) as noted in the legend above. The CD signal was measured as ellipticity (Y axis) as a function of wavelength (X axis).

(Prot X, E3BP; GDN, guanidinium chloride)

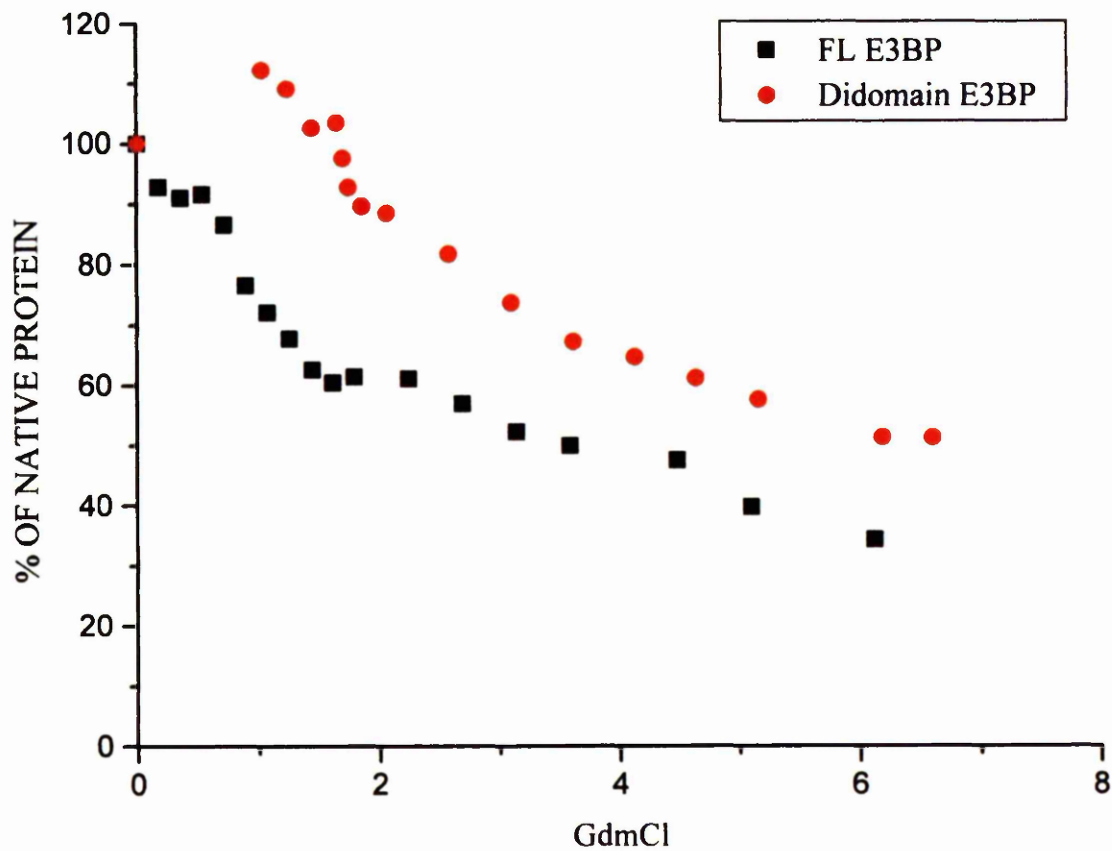


**Figure 5.3** Graph showing the % total change in folded protein as a function of GdmCl concentration.

Samples were incubated for 15 min in increasing concentrations of GdmCl before measuring their CD spectra. The % total change in folded protein was then plotted with respect to GdmCl concentration.

FL, full-length E3BP

Looking at the graph for the full-length protein it can be seen that there appears to be a biphasic, and possibly a triphasic, unfolding event occurring. An initial unfolding event takes place in concentrations of about 0.8M to 1.8M GdmCl, a second event occurs at concentrations of 2-4M GdmCl while a third possibly occurs at the higher concentration of 4.5-6M. However, this last unfolding event does not reach an endpoint, this protein being approx. 70% unfolded. Given that E3BP consists of 3 domains that are known to be capable of independent folding, it is highly likely that they also unfold independently of each other. This may be the most probable explanation for what can be observed in the CD spectra. The least stable domain will unfold first in the lower GdmCl concentrations while the other 2 domains only start to unfold in concentrations over 2M.

Comparison of the CD spectra of the full-length protein with that of the didomain provides information as to which domain is the least stable. The CD spectra indicates that the didomain is more stable than the mature protein with approx. 50% of the didomain unfolding in 6M GdmCl. An interesting point to note is that, on addition of GdmCl to the didomain there is an initial increase in the stability of the didomain which was not observed in the full-length protein. It is unclear why this should occur but it is possible that GdmCl has a salt stabilisation effect. The didomain appears to start to unfold in concentrations over 1.6M GdmCl to approx. 2.5M after which the CD signal begins to level off in a manner similar to that of the full-length E3BP.

### **5.5.2 Secondary structure determination of recombinant E3BP**

The far-UV CD spectrum allows the secondary structure content of a protein to be estimated. Several programs have been developed to facilitate this analysis. In this

case, the analysis, by Dr Sharon M. Kelly, was performed using the CONTIN procedure (Sreerama & Woody, 1993). The results of this analysis are shown in Table 5.1 below. These results indicate that the majority of the recombinant full-length E3BP (74%) consists of  $\beta$ -sheet while only 8% of the total protein is composed of  $\alpha$ -helix leaving the remainder of the protein (18%) as random coil.

Secondary structure element	% of total protein
$\alpha$ -helix	8
$\beta$ -sheet	43
$\beta$ -turn	31
Random coil	18

**Table 5.1 Secondary structure content of the full length recombinant E3BP**

The secondary structure content of recombinant E3BP was determined from the far-UV CD spectra. Analysis was performed using the CONTIN procedure.

However, the question is, how well does this correlate with what is known about the native protein? The 3D structure of the lipoyl domain from bacterial sources has shown it to have a predominantly  $\beta$ -sheet content (Dardel *et al*, 1993) while the peripheral subunit-binding domain is known to be formed from 2 short parallel  $\alpha$ -helices (Kalia *et al*, 1993). Taking this information into account, the data presented above indicates that the small amount of  $\alpha$ -helix noted here is likely to be found in the subunit-binding domain while the C-terminal domain would possess mainly  $\beta$ -sheet structure and random coil. The linker regions separating each domain are also likely to consist of random coil.

## 5.6 Protein fluorescence

Used in conjunction with circular dichroism, protein fluorescence can be used as a means to investigate conformational changes in proteins. The fluorogenic chromophores in proteins are the aromatic amino acids, tryptophan (trp), tyrosine (tyr) and phenylalanine (phe). Each of these amino acids has a distinct fluorescence spectra but in proteins which contain all 3 amino acids, the fluorescence signal is dominated by tryptophan.

Fluorescence emission occurs when an excited electron returns from the first excited state back to the ground state. Non-fluorogenic chromophores lose this energy as heat but for the aromatic amino acids some of this energy is emitted as light. Due to the loss of some energy as heat fluorescence emission is shifted to longer wavelengths compared with the absorption of the chromophore.

The fluorescent signal depends on the environment of the fluorophore and so it provides information on the tertiary structure of the protein. By investigating the fluorescence signal as the protein is unfolded in the presence of denaturing agents, this allows the conformational stability of the protein to be investigated.

### 5.6.1 Fluorescence studies on the independent recombinant E3BP

Fluorescence spectroscopy was performed on the full-length E3BP component as well as the didomain. Tryptophan fluorescence was selectively investigated by exciting the sample at 295nm. The emission spectrum was then recorded from 310-400nm. Figure 5.4 shows the complete fluorescence spectrum obtained for full-length E3BP after incubating the purified protein in varying concentrations of GdmCl (0-6M) for 15

min. The fluorescence spectrum for the didomain followed a similar pattern and, therefore, has not been shown. As is often the case in fluorescence experiments, there is an increase in the fluorescent signal when the concentration of denaturant is increased. This is often observed when the fluorogenic chromophore becomes more exposed to the solvent on denaturation of the protein. There is also a wavelength shift from 340nm in the native state to approx. 355nm in the fully unfolded protein. This is also indicative of the tryptophan residues becoming exposed to the solvent. The overall trend in the fluorescent signal at 350nm has been plotted in Figure 5.5. As with the CD data this has been plotted as % change in native protein since the protein has not fully unfolded in 6M GdmCl. The didomain has been plotted on the same graph, again for ease of comparison.

Full length E3BP contains three tryptophan residues, two of which are found in the lipoyl domain region. One of these is present on the boundary between the edge of the domain and the hinge region while the third tryptophan residue is found in the C-terminal domain. Therefore, this study demonstrates the unfolding of these two domains. There is a steady increase in denaturation of protein between 0-2M GdmCl after which the fluorescent signal levels off. However, even in 6M GdmCl this protein is only approx. 70% unfolded.

Since the didomain was constructed lacking the C-terminal domain, analysis of the fluorescent signal for the didomain gives an indication of the unfolding of the lipoyl domain alone. There is an initial unfolding event taking place between 1-2M GdmCl and this may reflect exposure of the tryptophan residue located at the boundary of the

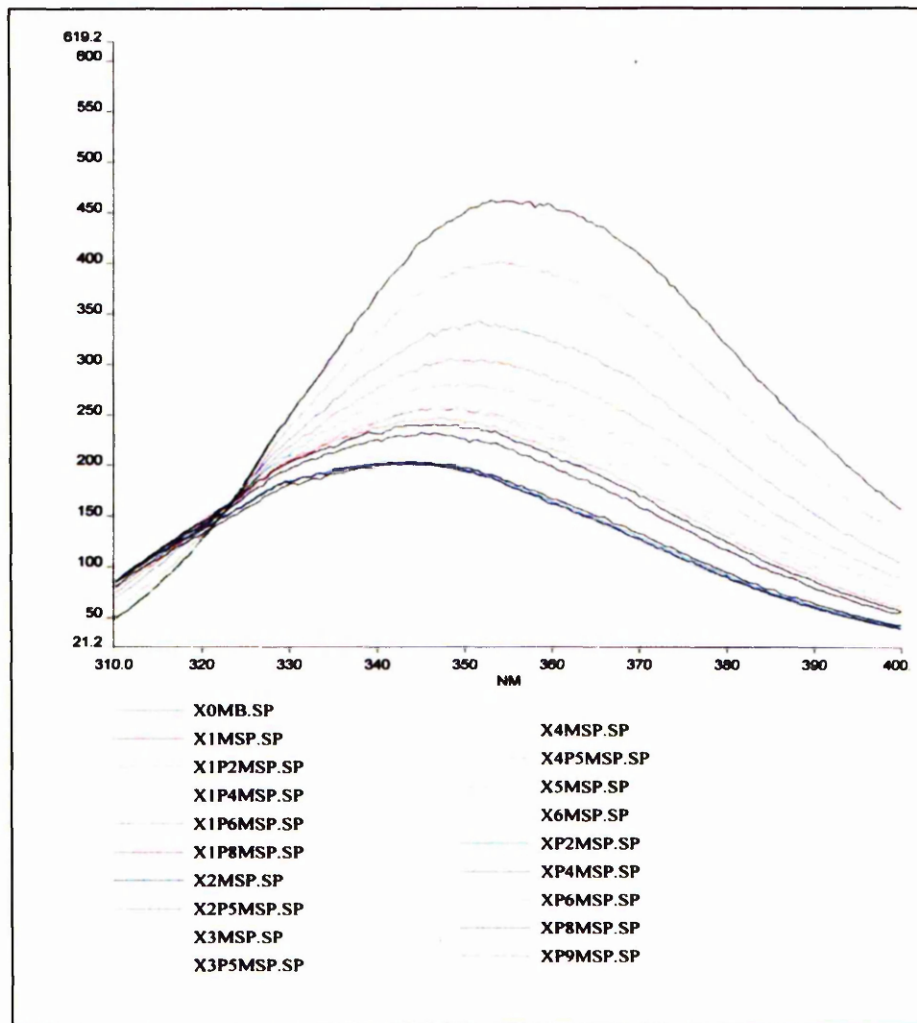


**Fig 5.4 Fluorescence spectroscopy of the full-length E3BP**

Fluorescence data for E3BP was collated by incubating the protein in varying concentrations of GdmCl (as noted above) for 15 min. The samples were then analysed for fluorescence. Excitation occurred at 295nm and fluorescence was recorded over the range 310-400nm. Relative fluorescence is shown on the Y axis while wavelength is plotted on the X axis.

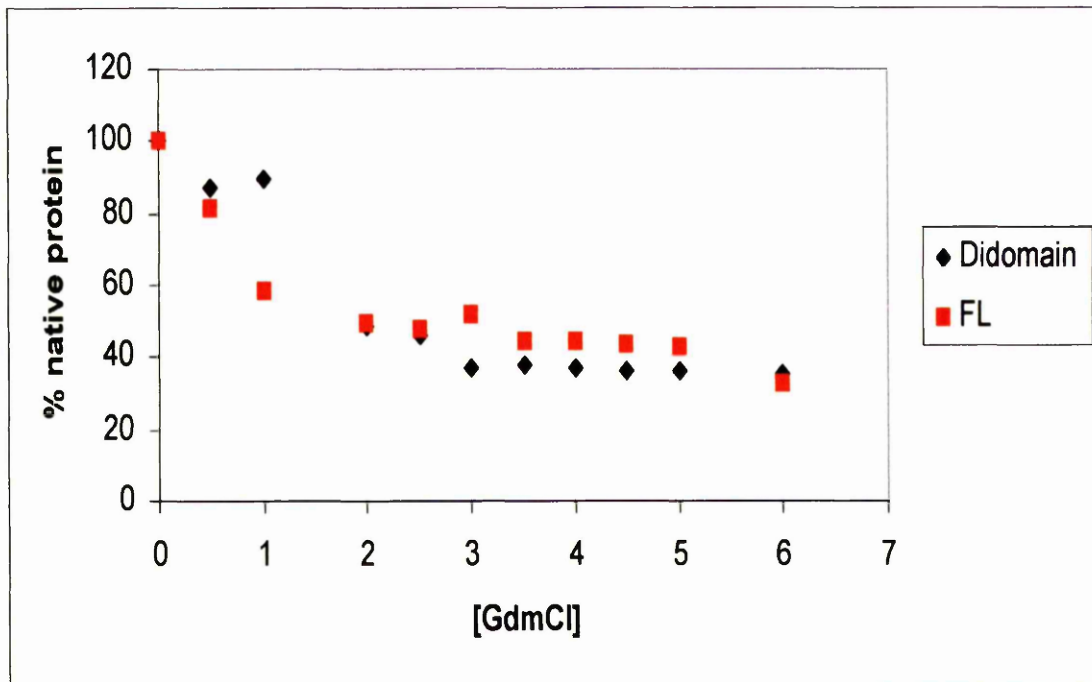


**Fig 5.5 Unfolding of E3BP (full-length and didomain) as monitored by the change in fluorescence at 350nm**

Relative fluorescence at 350nm, expressed as the % change in native protein, was plotted against GdmCl concentration to assess the overall trend in fluorescent signal.

lipoyl domain and linker region to solvent. The signal then levels off in a manner similar to that of the full-length protein.

On the basis of these results it seems highly probable that the lipoyl domain is the most stable of the three domain found in E3BP. This domain is probably responsible for the fact that neither the full-length E3BP nor its didomain have fully unfolded in 6M GdmCl. Given the increased stability of the didomain compared with the full-length protein, it would also appear that the C-terminal domain is the least stable of the three domains and therefore unfolds in the lower concentration of denaturant. This could provide a means of studying the association between E2 and E3BP *in vitro* (refer to Discussion section 5.9).

### **5.7 Studies on the E2 and E3BP components of human PDC**

Production of independent E2 and E3BP components as well as the coexpression of an E2/E3BP core provides a unique opportunity to examine the assembly of the structural core of human PDC. A major aspect to be studied is the nature of the association between these two proteins. Can E2 and E3BP form a stable association in a post-translational manner or is co-translation of the two proteins a prerequisite for the formation of the E2/E3BP core complex?

Gel filtration chromatography provides a convenient means of determining the  $M_r$  value of a native protein as described for E3BP. However, it is also a technique well-suited for analysing protein-protein interactions. Proteins that form a tightly bound complex can be investigated using simple gel filtration as in the case here.

### **5.7.1 Gel filtration analysis of the E2 and E3BP components of human PDC**

Several samples were analysed using this technique. Independently expressed E2, coexpressed E2/E3BP and a sample of independently expressed E2 and E3BP which had been mixed in equal amounts were loaded on to the Superose 6 gel filtration column and their elution profile monitored at 280nm.

### **5.7.2 Gel filtration analysis of independently expressed E2**

Purified E2, dialysed into elution buffer, was analysed on a Superose 6 gel filtration column. Elution of protein was monitored at 280nm and peak fractions collected for analysis by 10% SDS-PAGE. For each sample of E2 that was loaded on the column, a similar elution profile was observed. A peak was obtained at the void volume of the column with another, much smaller, peak eluting later in the column volume. The volume of elution of this second peak was determined to be representative of a molecular weight of between 50 and 100kDa. This is a very good approximation of the molecular weight of a monomer of E2 (molecular weight of recombinant E2 is 70kDa). The first peak, obtained at the void volume is likely to represent an oligomeric E2. The most likely explanation of this result is that E2 is forming the oligomeric core complex and this is what is detected at the void volume while unassociated monomers of E2 are eluted later. There was no evidence of trimer formation although the apparent monomeric nature of this species was not demonstrated conclusively.

### **5.7.3 Gel filtration analysis of the E2/E3BP recombinant core**

In order to determine if coexpressed E2/E3BP had formed a stable subcomplex, gel filtration analysis of these samples was performed.

Purified coexpressed E2/E3BP was loaded on to a gel filtration column and its elution profile at 280nm monitored as before. Two elution peaks were observed (Fig 5.6) and these peak fractions were collected for analysis by 10% SDS-PAGE. The first peak eluted at the void volume of the column while the second peak eluted at a volume consistent with the  $M_r$  value for monomeric E3BP. In this case, if E2 and E3BP had formed a stable complex it would be expected that both proteins would be present in the fractions corresponding to the first peak. The second peak might contain excess E3BP with respect to E2. SDS-PAGE analysis of the appropriate fractions confirmed these predictions (Figure 5.7).

From Fig 5.7 it can be seen that fractions 8 and 9, representing the peak obtained at the void volume of the column, contains both E2 and E3BP proteins. Analysis of the fractions from the second peak (fractions 16-20) shows that this peak contains E3BP alone. This result suggests that coexpressed E2/E3BP does indeed form a stable core assembly. Under these conditions, E3BP is overexpressed with respect to E2 and so excess E3BP remains unbound and is eluted later in the column volume.

#### **5.7.4 Gel filtration analysis of individually expressed E2 and E3BP, mixed in equal amounts**

While the result described above appears to confirm that E2 and E3BP, when coexpressed in the same bacterial cells, form a stable core complex it was still unclear whether, when expressed individually and then mixed in equal amounts, these 2 proteins could interact with each other in a stable manner. In order to answer this question individually expressed E2 and E3BP were purified and dialysed separately into the column elution buffer. After determining the concentrations of each purified

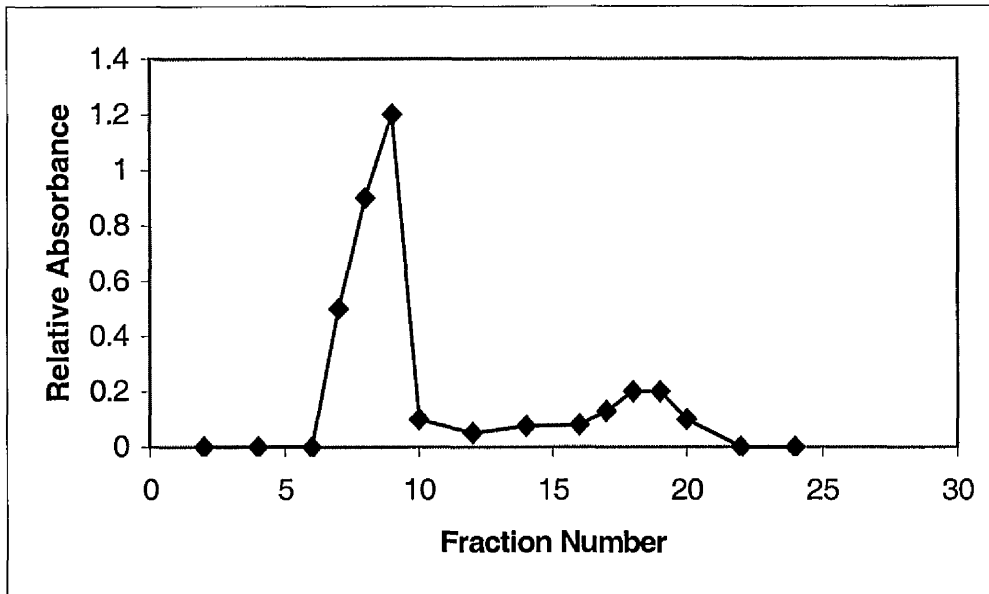


**Figure 5.6 Gel filtration analysis of recombinant coexpressed E2/E3BP core**

E2-PDC and E3BP were co-expressed in *E. coli* and analysed on a Pharmacia (10/30) Superose 6 gel filtration column equilibrated in 150mM NaCl, 1mM DTT, 50mM potassium phosphate, pH 7.2. Elution of protein was monitored at 280nm and the appropriate fractions kept for analysis by SDS-PAGE.

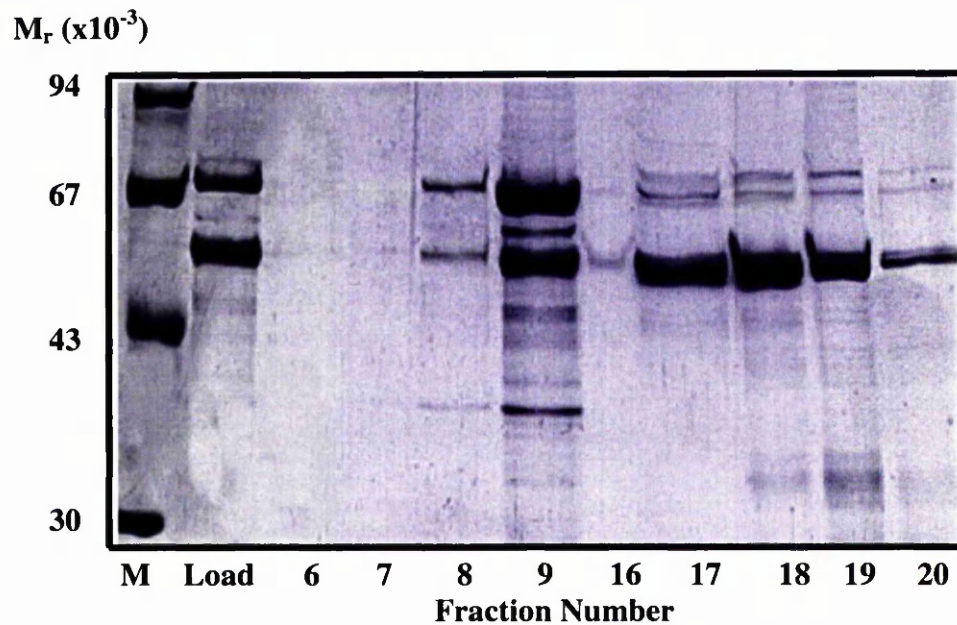


**Figure 5.7 SDS-PAGE analysis of co-expressed E2-PDC and E3BP after Superose 6 gel filtration**

Eluted fractions from the gel filtration analysis of coexpressed E2/E3BP were TCA precipitated and analysed on SDS-PAGE before staining with Coomassie blue.

M: low  $M_r$  markers, Load: sample of loaded fraction, 6-20: represent peak fraction numbers

component, the 2 proteins were mixed in equal amounts so that there was a vast excess of E3BP present and incubated at 4°C before loading a sample on the gel filtration column. Again, the elution profile at 280nm was monitored and peak fractions collected.

As seen before, 2 peaks were observed on the chromatogram (Fig 5.8). The first peak eluted at the void volume while the second appeared further down the column. These fractions were subjected to TCA precipitation and then analysed by 10% SDS-PAGE (Figure 5.9).

From Fig 5.9 it can be seen that fractions 8 and 9, representing the void volume of the column contain only E2 while the fractions collected for the second peak (15-20) contain E3BP. It can also be clearly seen that there are other bands present which appear to run at the size expected of E2. Given that E2 alone produces 2 peaks representing oligomeric E2 and excess monomers it is possible that the same situation is occurring here and that excess E2 elutes at about the same column volume as E3BP.

When comparing the results of these 2 experiments it is clear that the coexpressed E2/E3BP proteins have formed a stable complex and coelute at the void volume. This experiment also shows that E3BP is overexpressed with respect to E2 and excess monomers elute later in the column volume. However when E2 and E3BP are expressed individually and then mixed together, they do not stably associate with one another as is the case with the coexpressed proteins. There is no clear evidence to suggest that the individual proteins have formed a stable complex. This result

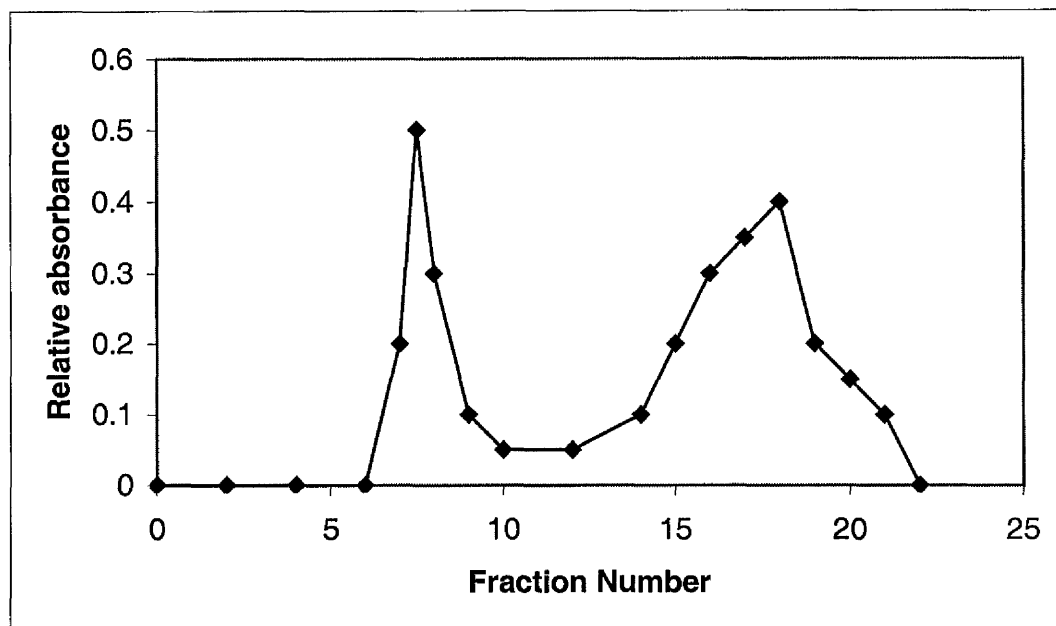


**Figure 5.8 Gel filtration analysis of individually expressed E2 and E3BP mixed in equal amounts**

E2-PDC and E3BP were expressed individually in *E. coli* and mixed in equal amounts before being analysed on a Pharmacia Superose 6 gel filtration column equilibrated in 150mM NaCl, 1mM DTT, 50mM potassium phosphate, pH 7.2. Elution of protein was monitored at 280nm.

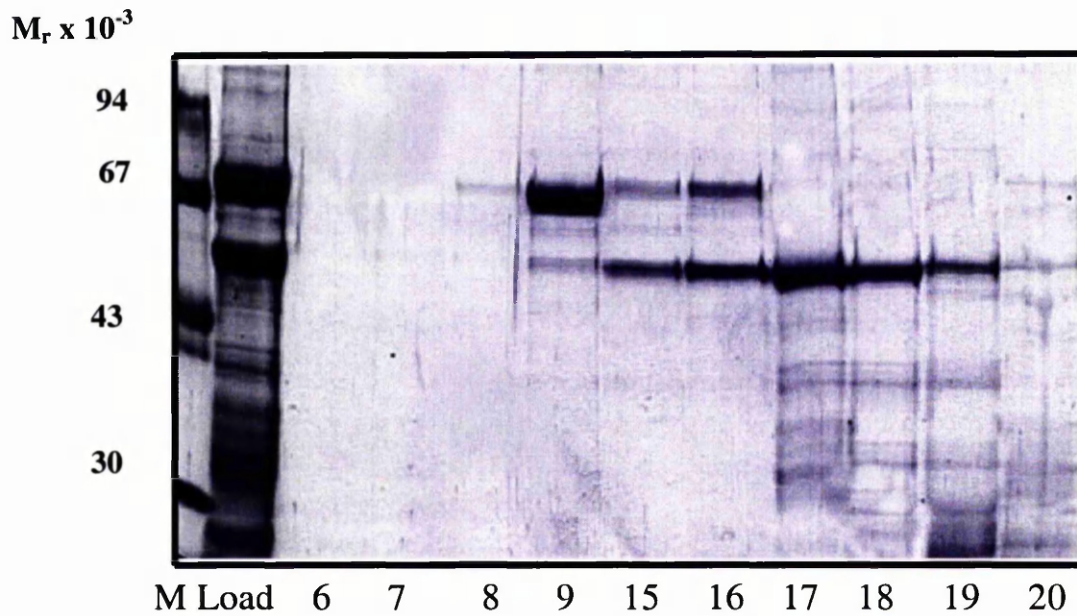


**Fig 5.9 SDS-PAGE analysis of equal amounts of E2 and E3BP after Superose 6 gel filtration.**

Eluted fractions from the gel filtration analysis of individually expressed E2 and E3BP were TCA precipitated and analysed by SDS-PAGE before staining with Coomassie blue.

M: molecular weight markers, Load: sample of loaded fraction, 6-20: represent peak fractions 6-20.

indicates that the formation of the E2/E3BP core complex occurs in a co-translational manner and may involve association via folding intermediates.

### **5.8 Densitometric scanning analysis of the recombinant E2/E3BP core**

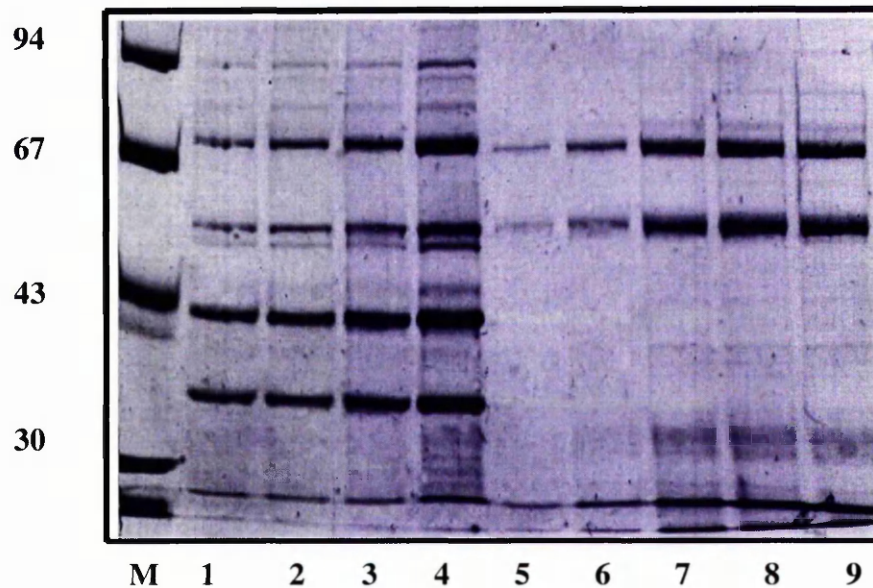
Having shown that coexpression of recombinant E2 and E3BP in *E. coli* is required in order for the E2/E3BP core to assemble, it is of great interest to determine whether these two proteins assemble with the correct stoichiometry. To this end densitometric scanning analysis was employed in order to address this question.

Purified recombinant E2/E3BP core was subjected to gel filtration in order to separate any excess E3BP from the core complex. The relevant fractions were pooled and resolved by electrophoresis on 10% SDS-PAGE. Purified native (bovine) PDC was also resolved by electrophoresis. Different concentrations of both the recombinant and native proteins (from 2.5-20 $\mu$ g) were loaded (Fig 5.10). After staining with Coomassie blue the gels were subjected to densitometric scanning (in duplicate) and the relative intensities of the protein bands corresponding to E2 and E3BP were measured. The ratio of E3BP:E2 was then calculated for each lane and the ratios obtained for the recombinant and native proteins compared. The results are shown in Table 5.2.

Native ( $\mu\text{g}$ )	Ratio	Average	Samples ( $\mu\text{g}$ )	Ratio	Average
5	2.13	$2.31 \pm 0.21$	5	1.35	$1.4 \pm 0.143$
10	2.13		10	1.29	
20	2.48		15	1.61	
			20	1.35	

**Table 5.2 Densitometric scanning analysis of recombinant and native E2/E3BP core**

From the preliminary data presented in this table and Fig 5.10 it can be seen that there appears to be more E3BP present in the recombinant core than in the native complex. This could be due to a number of factors. The resolving power of the gel filtration column used may not have been sufficient to completely separate the two peaks obtained on the chromatogram. As observed in Fig 5.6 the two peaks are separated by only a couple of fractions and there was a constant absorbance at 280nm between peaks. Fractions taken at the end of the first peak may contain excess E3BP if the two peaks were not sufficiently resolved. There may also be aggregation of E3BP, which would not be detected in the presence of E2. This study should also be performed using a higher salt concentration, possibly 1M NaCl, in order to ensure that any loosely bound E3BP has been removed. At this salt concentration it is known that native E2 and E3BP do not dissociate from one another.

$M_r \times 10^{-3}$ 

**Figure 5.10 Resolved native bovine PDC and recombinant E2/E3BP core**

Native PDC purified from bovine heart and recombinant E2/E3BP core analysed by gel filtration were electrophoresed on 10% SDS-PAGE. After staining with Coomassie blue this was subjected to densitometric scanning analysis.

M: molecular weight markers, lanes 1-4: native PDC at 2.5, 5, 10 and 20 $\mu$ g respectively, 5-9: recombinant E2/E3BP core after gel filtration at 2.5, 5, 10, 15 and 20 $\mu$ g respectively.

## 5.9 Discussion

In this chapter studies on the recombinant E3BP have focussed on assessing its oligomeric state, the stability of the protein and in examining its interaction with E2. Extensive studies have not previously been performed on E3BP. Attempts have been made to elucidate the role it plays in the pathogenesis of the autoimmune disease primary biliary cirrhosis (Palmer *et al*, 1999), while studies conducted to determine whether E3BP has any catalytic activity showed that E3BP has a purely structural role in the functioning of the pyruvate dehydrogenase complex (Seyda & Robinson, 2000).

Studies on the recombinant E3BP described here have shown that this protein exists as a monomer, at least at low concentrations. It also appears to be prone to aggregation as evidenced by the initial gel filtration trials. This tendency of E3BP to aggregate is also described in chapter 6. Denaturation of E3BP and analysis by circular dichroism and fluorescence has indicated that the unfolding of this protein is of a biphasic, and possibly even triphasic, nature. This suggests that each independently folding domain of E3BP displays a particular sensitivity to GdmCl.

In order to confirm which domain is the least stable and therefore unfolds in the lower concentration of denaturant, the E3BP didomain was subjected to CD and fluorescence under the same experimental conditions as the full-length protein. This didomain does not contain the C-terminal domain of the protein. The lipoyl domain is known to be a stable entity while the subunit-binding domain is the smallest known protein or domain which can fold independently in the absence of any stabilising disulphide bridges or metal ions (Spector *et al*, 1998). Comparison of the data obtained for the full-length and didomain proteins does indeed indicate that the lipoyl domain is the

most stable of the three domains. This stability is reflected in the fact that neither of these proteins were fully unfolded in 6M GdmCl. The increased stability of the didomain compared with the full-length protein also indicates that the C-terminal domain is the least stable of the three domains and therefore unfolds first. The unfolding of the C-terminal domain of E3BP in low concentrations of denaturant could provide an elegant means of examining the assembly of the E2/E3BP core. By selectively denaturing the inner domain of E3BP, its integration into the E2 core complex could be studied more extensively *in vitro*.

It has previously been shown for the native complex that E2/E3BP has a high intrinsic capacity to self-assemble (McCartney *et al*, 1997). The studies described in this chapter have shown that coexpression of the recombinant E2 and E3BP is required in order for a stable E2/E3BP subcomplex to assemble. This is in good agreement with the findings of Harris *et al*, (1997) who showed that combining extracts containing coexpressed recombinant human E2/E3BP with E1 resulted in assembly of a macromolecular complex as seen by elution of the complex at the void volume of a gel filtration column. However, this study did not examine the possibility of a post-translational association between E2 and E3BP. Li *et al* (1992) showed that free E3BP, functional in binding E3, did not bind to resolved native E2 oligomer depleted in E3BP. In contrast, it has been suggested that yeast E2 and E3BP, when expressed independently and then mixed can form a stable subcomplex. This would indicate that yeast E3BP can associate with E2 in a post-translational manner (Maeng *et al*, 1996).

There are a number of differences between yeast and mammalian PDC that may account for this apparent disparity in the assembly of human and yeast E2/E3BP core.

Human E3BP has a longer linker region between the C-terminal domain and the subunit-binding domain than does the yeast E3BP (Harris *et al*, 1997). This is in keeping with the observation that, from cryoelectron micrographs the yeast E3BP appears to reside inside the E2 core with E3 extending into the central cavity. From these low resolution studies it has been suggested that the binding site for E3BP may be formed by the inner tip of the E2 trimer (Stoops *et al*, 1997). This may mean that the yeast E2 core must first be assembled in order for the binding sites for E3BP to become available. In comparison, in mammalian PDC, E3 (and E1) appears to be tethered to the complex, with a clear gap between E3 and the core domain (Wagenknecht *et al*, 1991; Roche *et al*, 1993). Thus, in the mammalian complex it would seem that E3 (and E3BP) and E1 extend outwards from the core complex.

Analysing the stoichiometry of the association of the coexpressed E2/E3BP would provide further support for the proposal that the assembly of the E2/E3BP core occurs through a defined series of folding intermediates. This question was addressed using densitometric scanning analysis. This technique, although perhaps not ideal, suggests that there is excess E3BP present in the recombinant core than in the native complex. This can also be observed on the SDS-PAGE gel. It may simply be the case that separation of E2/E3BP core from loosely associated E3BP or any aggregates of E3BP was not sufficient. The use of a larger gel filtration column to provide higher resolving power and performing this study in a higher salt (1M NaCl) concentration to remove any non-specifically bound protein should be able to provide more definitive answers to the question of the stoichiometry of the recombinant E2/E3BP core complex.

Another technique which can be used to address this question is radiolabelling of these proteins with the sulphhydryl reagent [2,3-<sup>14</sup>C] N-ethylmaleimide (NEM) as has been described previously (Hodgson *et al*, 1986; Sanderson *et al*, 1996b). In the presence of NADH, NEM would label the reduced sulphhydryls on the lipoyl domains. After resolving the labelled proteins electrophoretically, the radioactivity incorporated into each protein could be counted and this would allow the stoichiometry of these two proteins to be analysed. This technique is likely to prove a more accurate method for determining the stoichiometry of binding of the recombinant E2/E3BP core than densitometry.

## **Chapter 6**

### **Stoichiometry and affinity of E3-E3BP and E3-E2**

**interactions as measured by isothermal titration calorimetry**

## 6.1 Constituents of human PDC

The pyruvate dehydrogenase complex has been extensively studied from a wide variety of prokaryotic and eukaryotic organisms and is known to consist of multiple copies of three individual enzymes bound in a non-covalent manner, as described previously.

The structure of E3 has been solved from a number of sources mainly of bacterial origin. To date only one eukaryotic E3 structure has been solved, from yeast at 2.7Å resolution (Toyoda *et al*, 1998). However, the crystallisation and preliminary X-ray analysis of pig heart E3 has recently been reported (Toyoda *et al*, 1998b). Comparison of these known structures shows that the same basic tertiary structure is present in both eukaryotic and prokaryotic complexes.

In the human and yeast PDC complexes, E3BP was identified as an additional subunit that has been shown to play a pivotal role in binding E3 to the E2 core. However, there is some debate as to the stoichiometry of binding of E3 to E3BP and thus to the number of E3 dimers present per complex. In the *B. stearrowthermophilus* complex it was demonstrated that 1 E3 dimer binds to 1 peripheral subunit-binding domain of E2 (Hipps *et al*, 1994). This apparent inability of E3 to interact with two subunit-binding domains, despite its dimeric structure, was attributed to steric hindrance or a conformational change in E3 on binding of the subunit-binding domain. More recently, the crystal structure of the *B. stearrowthermophilus* E3 component complexed with the peripheral subunit-binding domain has been solved to 2.6Å resolution (Figure 6.1). This structure confirmed the 1:1 binding ratio and showed that the

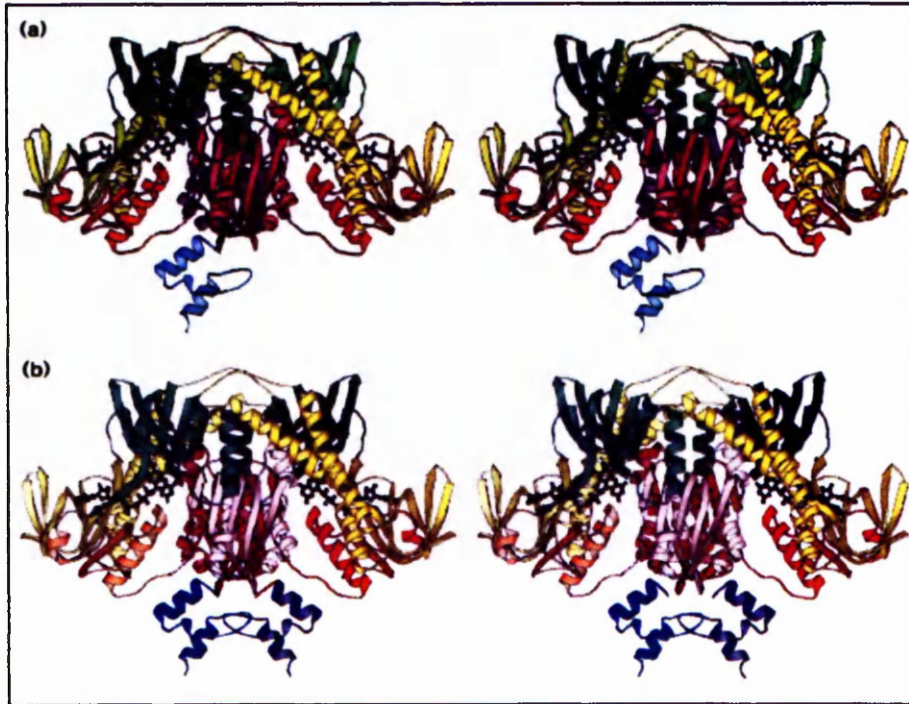


**Figure 6.1** Crystal structure of E3 complexed with E2-SBD from *B.*

*stearothermophilus*

The four domains of each subunit of E3 are shown in different colours: yellow, FAD-binding domain; green, NAD-binding domain; red, central domain; magenta, interface domain. The E2-SBD (blue) is shown bound to one E3 dimer (panel A). The FAD cofactor bound to each E3 subunit is represented as a ball-and-stick.

Panel B shows a hypothetical model of two E2-binding domains bound to the E3 dimer.

binding site for the E2-binding domain is situated close to the twofold axis of symmetry on E3 (Mande *et al.*, 1996). These authors also discovered that comparison of the complexed E3 with the uncomplexed enzyme showed that there was no significant conformational change in E3 on binding to the subunit-binding domain. This favours the argument that steric hindrance prevents simultaneous binding of two SBDs to the E3 dimer. In the hypothetical model shown in panel B of Fig 6.1, where a second SBD was modelled, there is a steric clash between the loops of the symmetry-related binding domains and this accounts for the binding of a single E2-SBD per E3 dimer. This means that in the *B. stearothersophilus* PDC, 6 E3 dimers are present in each complex.

In the mammalian complex, the stoichiometry of binding of E3 has been examined using equilibrium binding experiments (Wu & Reed, 1984). These studies indicated that E2 from bovine kidney and heart contained 6 identical, noninteracting sites which each bind 1 E3 dimer and suggested that the optimum binding ratio for the mammalian complex was 60 E2 subunits, 12 E1 components and 6 E3 dimers. However, the validity of these results was cast into doubt on the discovery of the E3BP component in the mammalian complex. It is now generally accepted that at maximal occupancy, 30 E1 heterotetramers bind to 60 E2 subunits and that 12 E3BP molecules are bound to the E2 core (Sanderson *et al.*, 1996a). However the stoichiometry of binding of E3BP to E3 remains in doubt. Does 1 E3 dimer bind to 1 E3BP monomer implying that there are 12 E3 subunits present per complex or can 1 E3 bind to 2 E3BP molecules resulting in 6 E3 dimers being present in a functional complex?

## 6.2 Isothermal titration calorimetry

A number of techniques have been developed in recent years that allow the stoichiometry and affinity of binding of two proteins to be determined with great accuracy. One such technique is isothermal titration calorimetry (ITC). This technique utilises the fact that formation of a protein-protein complex is either an exothermic or endothermic event, and that the heat exchange is proportional to the fraction of protein bound. By measuring this heat of binding, the stoichiometry of the protein-protein interaction can be determined, as can the binding constant and the enthalpy of binding for the particular interaction under investigation.

Figure 6.2 shows a schematic representation of an ITC instrument. It consists of two lollipop-shaped cells, one of which is the reference cell containing water or buffer and the other containing the protein solution. On injection of ligand into the protein solution heat is either absorbed or evolved depending on the nature of the interaction between the two proteins. Thermopile and thermocouple detectors present on the cells detect any change in temperature between the two cells and activate the feedback heater in order to maintain equal temperature between the reference and sample cells. The power supplied to the sample cell is the observable signal in an ITC experiment and is a direct measure of the heat change on binding of a ligand to a macromolecule.

## 6.3 Aims of this chapter

- To determine the stoichiometry and affinity of binding of E3BP to E3 using both full-length and truncated constructs of E3BP.

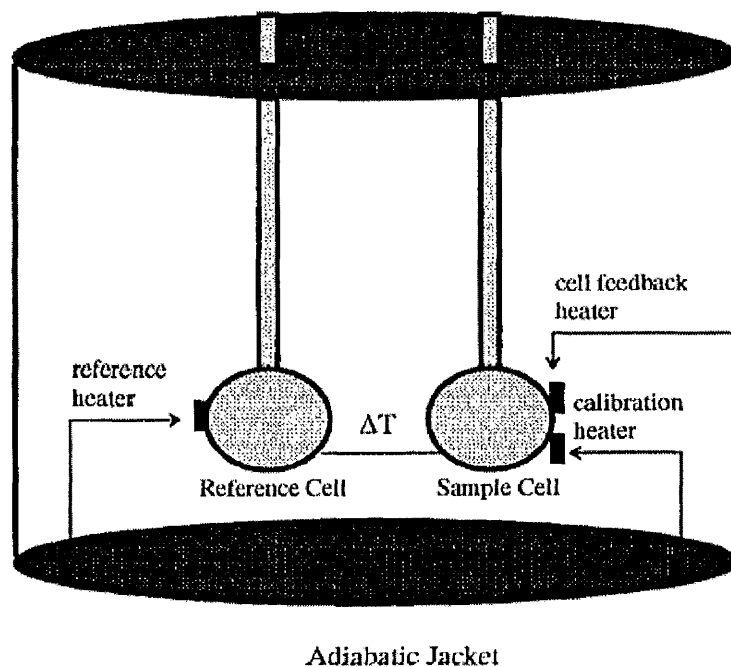


**Figure 6.2 Schematic diagram of an ITC instrument**

(Taken from Pierce *et al*, 1999)

This diagram shows the inside of an ITC instrument containing two lollipop-shaped cells within an adiabatic jacket. The reference heater sustains a small continuous power to the reference cell. Depending on the nature of the interaction between ligand and macromolecule, the feedback heater will either increase or decrease power to the sample cell in order to maintain equal temperature with the reference cell.

## 6.4 Results

### 6.4.1 Binding studies using full length mature E3BP

Before performing an isothermal titration calorimetry experiment, the heats of dilution of the ligand must be determined. A complete automated titration of 26 cycles is therefore performed in which ligand is injected into buffer. In all figures in this chapter, the data presented have been corrected for the heats of dilution.

Initially, ITC was performed using the full-length mature E3BP subunit. Figure 6.3 shows the results of E3BP (154 $\mu$ M) titrated into E3 (7.4 $\mu$ M). The upper panel demonstrates that each 10 $\mu$ l injection of E3BP into E3 results in an exothermic heat pulse. At the start of the titration each injection results in a large response as all or most of the protein injected binds E3. The response gradually decreases in size as more protein is bound to E3 before saturation is reached after about 15 injections. The response then levels off as no more protein can bind. However, when the integrated heat data (lower panel) are analysed, an unusual and unexpected effect is observed. There appears to be two distinct binding events occurring suggesting that a standard single-site binding model is not appropriate in this case. The best fit for this set of data was seen with a two-site binding model. One possible explanation for this effect is that, at the high concentrations of protein required for these experiments E3BP has aggregated and is forming oligomers. On dilution, these aggregates may dissociate and so binding sites, which were previously masked by aggregation, are now available to bind E3. In chapter 5 crosslinking studies showed that at lower protein concentrations (up to 1mg/ml) E3BP exists as a monomer. However, the gel filtration experiments described in chapter 5 indicated that E3BP may be forming aggregates

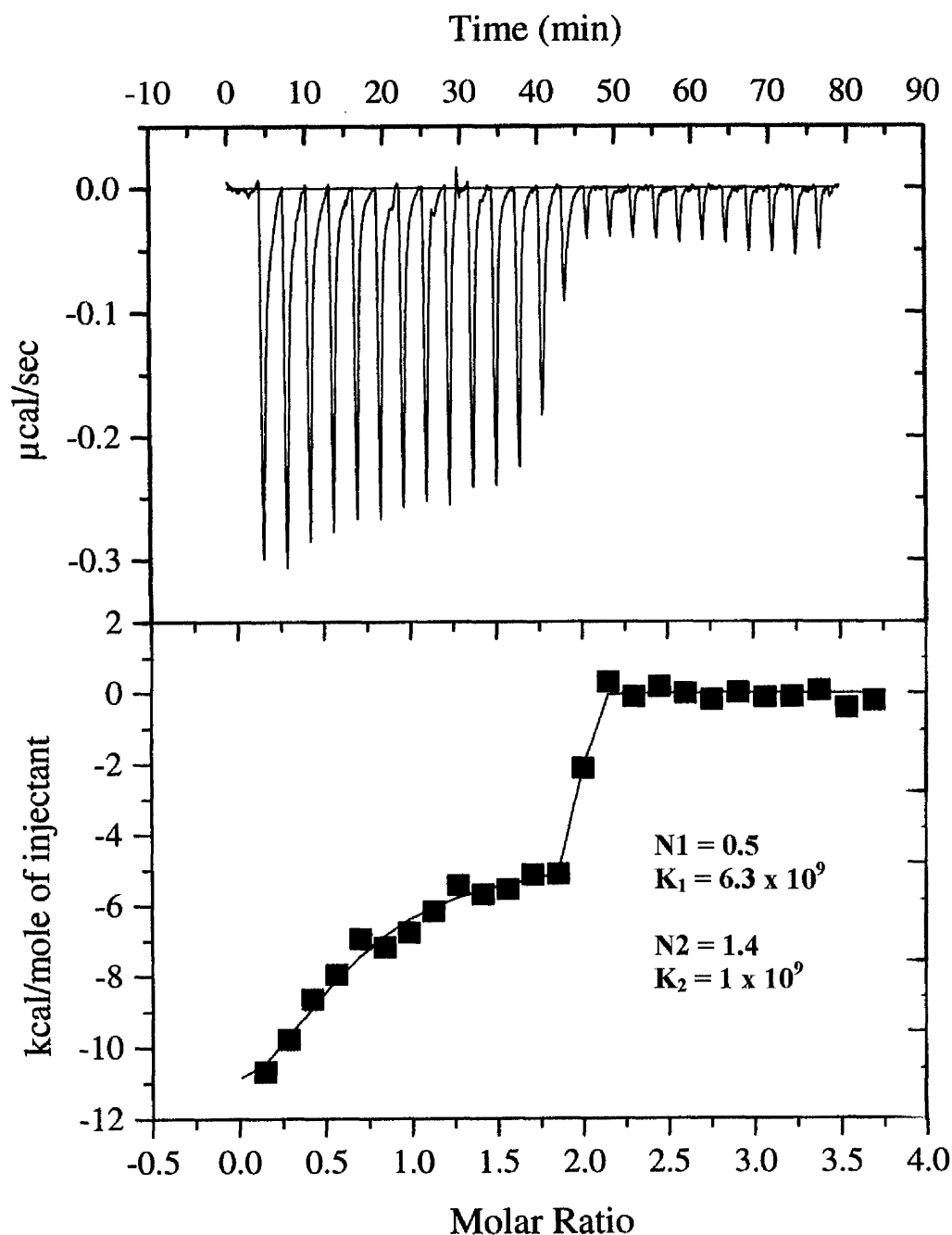


**Figure 6.3 Titration of E3BP into E3.**

E3BP ( $154\mu\text{M}$ ) was titrated into E3 ( $7.4\mu\text{M}$ ). Analysis of the data indicated that there is more than one binding event taking place. Using a two-site binding model the combined stoichiometry ( $N_1 + N_2$ ) is 1.9:1. The association constants ( $K_1$  and  $K_2$ ) are very tight, being in the nanomolar range.

and that this was concentration-dependent. It is possible that the higher concentrations required for this study (10mg/ml or greater) may promote aggregation of E3BP. An unusual event was also observed when the heats of dilution of E3BP were determined (data not shown). The first 10 injections of protein into buffer resulted in an exothermic heat pulse after which the response became endothermic. This phenomenon is not normally seen on determining the heats of dilution and is further evidence to suggest that aggregation of E3BP is occurring.

Also of interest in this study is the association constant ( $K$ ) which is in the nanomolar range. This indicates that the affinity of binding of these two proteins is very tight. Analysis of  $N$ , defined as the average number of binding sites per mole of protein in solution, reveals an unexpected stoichiometry of binding. These data suggest that 2 moles of E3BP bind to 1 mole of E3, that is, 2 E3BP monomers bind to 1 dimer of E3. This would indicate that homodimeric human E3 contains 2 binding sites for E3BP. This is inconsistent with what has been found for E3 from other organisms, most notably from *B. stearothermophilus*. According to Mande and coworkers (1996), who crystallised E3 complexed with the peripheral subunit-binding domain (P-SBD) of E2, one E2 molecule can bind to E3. Steric hindrance precludes the possibility of a second P-SBD being bound in this case.

Due to the biphasic binding event observed in the first titration, the study was repeated by reversing the titration in that E3 (56.5 $\mu$ M) was injected into E3BP (5.8 $\mu$ M). Fig 6.4 shows the result of this study. In this case, the endpoint of the reaction was reached very quickly, after 4 injections. This is probably as a result of

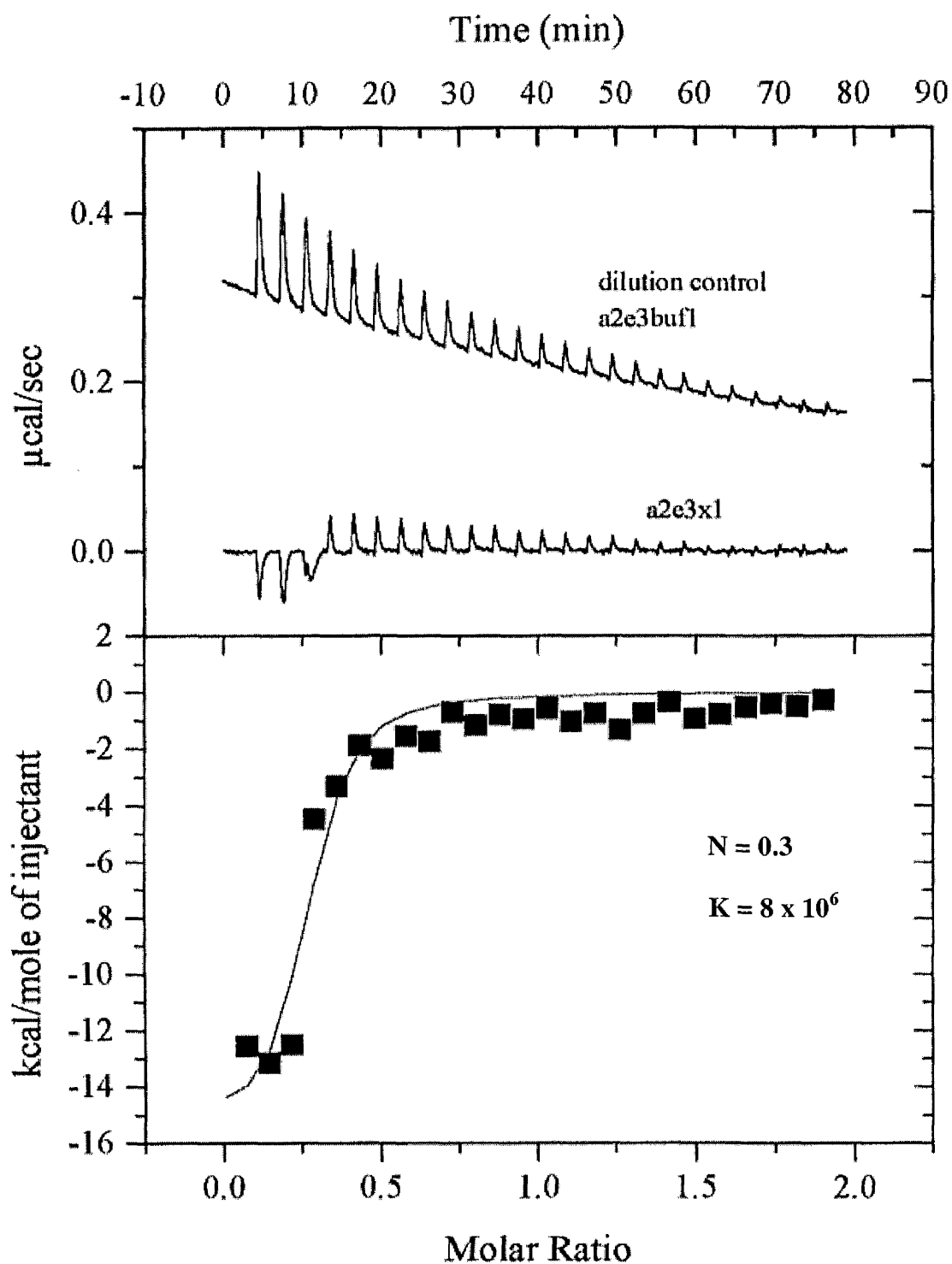


**Figure 6.4 Titration of E3 into E3BP**

E3 ( $56.5\mu\text{M}$ ) was titrated into E3BP ( $5.4\mu\text{M}$ ). The heats of dilution (dilution control) are large possibly obscuring the binding heats. In this study  $N$  has been determined at 0.3 while the association constant,  $K$ , is in the micromolar range.

the low concentrations of protein used in this experiment. As such, a proper saturation curve has not been obtained therefore it is highly likely that the data obtained in this study is inaccurate. The upper panel also presents the dilution control for this study, which shows that the heats of dilution of E3 are quite large. Binding of E3 to E3BP is an exothermic event but once saturation is reached the endothermic effects of the heats of dilution of E3 is observed. The stoichiometry of binding,  $N$ , has been measured at 0.3 while the association constant,  $K$ , is in the micromolar range. This smaller association constant is unexpected for the interaction between E3 and E3BP and it is likely that the large heats of dilution observed in this study have partially obscured the heats of binding. This would also account for the lower than expected stoichiometry observed in this particular titration. However, there is no indication of a biphasic response in this titration, providing further support for the aggregation of E3BP in the initial study. It should be emphasised that this study is likely to be inaccurate thus it is important that this titration is repeated. Due to time constraints, this was not possible at this time.

#### **6.4.2 Binding studies using truncated constructs of E3BP**

In order to clarify the data obtained with the full-length E3BP ITC was performed using truncated constructs of E3BP, specifically the peripheral subunit-binding domain (SBD) itself, which was cloned as a GST fusion protein. It had also been hoped to conduct these experiments with the didomain of E3BP, containing the lipoyl domain and the subunit-binding domain. However, at the time that these experiments were performed this clone was unavailable. The E3BP didomain has since been cloned as a His-tagged protein and at time of writing ITC studies using this protein are underway.

Before performing the study using the SBD the heats of dilution were determined as before. Figure 6.5 shows the titration of E3 (0.2mM) into the subunit-binding domain of E3BP (10.4 $\mu$ M). This titration resulted in a very tight binding curve. The upper panel of Figure 6.5 shows that the first 7 or 8 injections of E3 into the protein solution results in an endothermic heat pulse. However this signal was smaller than that obtained for the dilution of E3 into buffer which was also endothermic (data not shown). This suggests that the binding of E3 to the SBD is exothermic since the endothermic effect of the dilution of E3 has to be overcome before the heat of binding can be observed. As the titration progresses, the heat pulses become exothermic as more protein is bound until saturation point is reached after 15 injections. At this point the endothermic effects of the heats of dilution of E3 are once again observed.

The integrated heat data (lower panel) show that the binding of E3 to E3BP-SBD is extremely tight and under these particular conditions, the association constant,  $K$ , cannot be accurately determined. In this instance  $K$  was fixed in order to give a better ~~of~~ fit of the data. At first glance, the stoichiometry of binding of these 2 proteins seems unusual based on the results obtained previously. The stoichiometry of binding,  $N$ , has been measured at 2, that is, 2 moles of E3 bind to 1 mole of E3BP-SBD. This is apparently in direct contrast to the stoichiometry measured using the full-length E3BP protein. However it must be remembered that the subunit-binding domain has been cloned as a GST fusion protein, which exists as a dimer. It might, therefore, be expected that there are 2 subunit-binding domains present in the GST fusion protein.

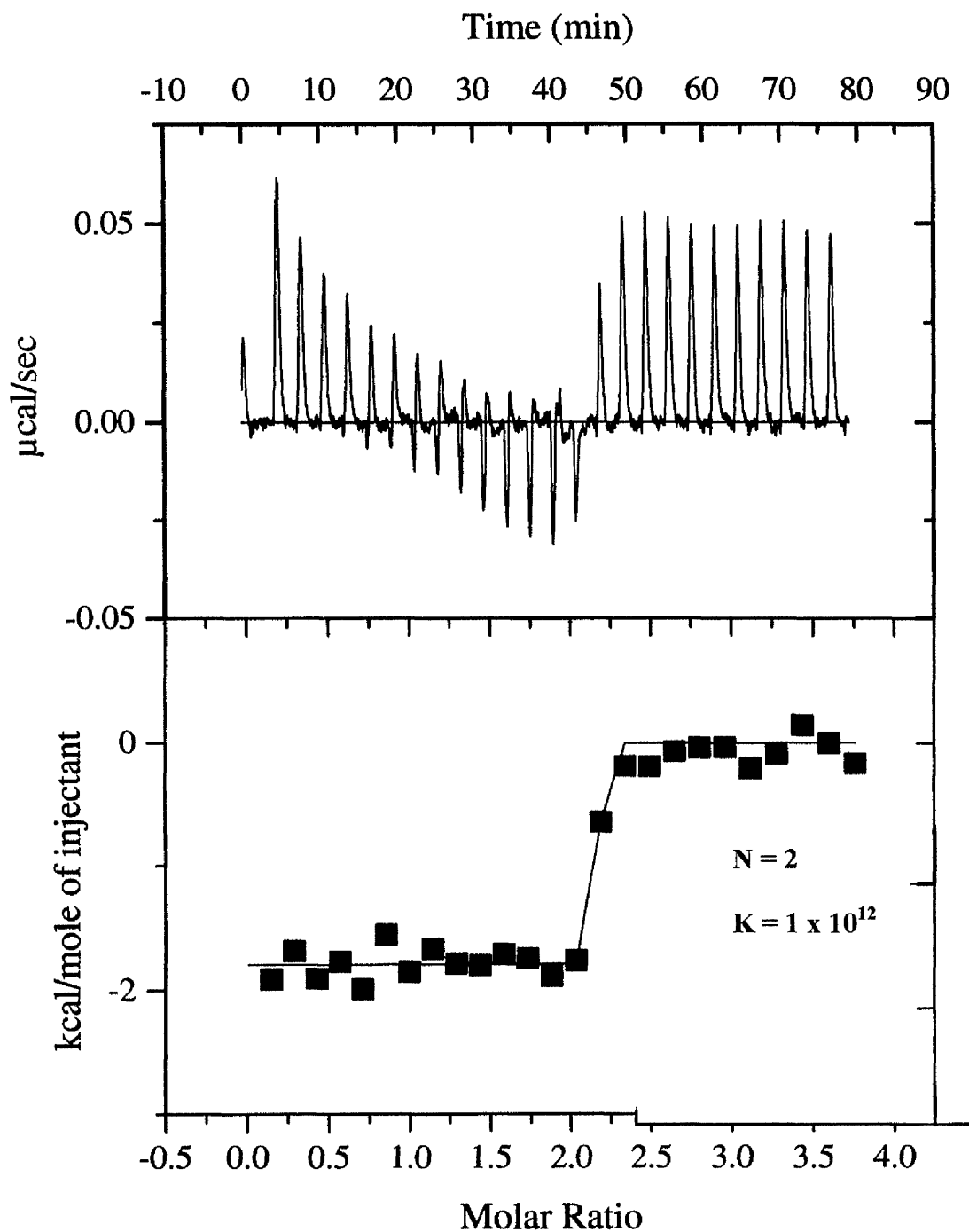
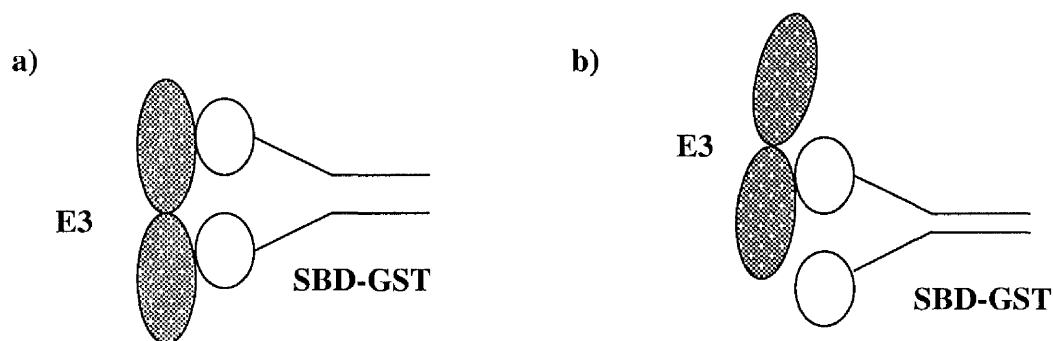


**Figure 6.5 Titration of E3 into the subunit-binding domain of E3BP**

This data shows that the association constant,  $K$ , is very high and is, in fact, too tight to measure accurately. The stoichiometry of binding,  $N$ , has been measured to be 2.

The molar concentration of the GST protein has been expressed in its monomeric form while the concentration of E3 has been expressed as a dimer. Adjusting the concentration of the GST-SBD fusion to take into account its dimeric form results in an actual stoichiometry of 1:1 for this interaction. There are a number of possible explanations for this result. If there are two binding sites on E3 as the data using full-length E3BP suggests it may be that one E3 dimer may bind to both subunit-binding domains of the GST fusion protein. Alternatively, it is possible that the GST fusion protein is folded in such a way that only one subunit-binding domain is accessible to E3 while access to the binding site on the second domain is prevented. Thus one P-SBD would bind only one E3 dimer. A simple model demonstrating these two possibilities is shown below. Panel A shows one E3 binding to both subunit binding domains of the GST fusion, while in panel B, E3 binds only one subunit binding domain, steric hindrance preventing the second domain from being occupied. Occupancy of both binding sites on E3 is dependent on the spatial organisation of the subunit binding domains on the GST.



## 6.5 Analysis of binding of E3 to E2

Evidence from a variety of sources has indicated that while E3 principally binds to E3BP in PDC, it is also capable of binding rather more weakly to the subunit-binding domain of E2. This has been found to be the case *in vivo* where patients who lack any immunologically detectable E3BP can still maintain PDC activity at 10-20% of the levels of normal individuals (Marsac *et al*, 1993; Geoffroy *et al*, 1996). It is believed that this basal level of activity is due to the presence of low affinity binding sites specific for E3 on the E2 polypeptide. Reconstituted bovine PDC, lacking the E3BP component, can sustain overall complex activity in the presence of a large molar excess of E3 (McCartney *et al*, 1997). This is in contrast to the situation in yeast PDC where the E2 component, devoid of E3BP, was found to be unable to support any PDC activity in the presence of high levels of E3 (Yang *et al*, 1997).

Preliminary biochemical studies to examine this phenomenon were performed by a previous researcher in the laboratory. By utilising a truncated construct of E2 consisting of the inner lipoyl domain and the subunit-binding domain, termed the didomain, surface plasmon resonance (SPR) experiments were carried out to measure the binding affinity of E3 to the E2 didomain. It was found that these 2 proteins had an association constant in the  $\mu\text{M}$  range. This was in direct comparison with the measurement of E3BP complexed with E3, which resulted in an association constant in the nanomolar range (S.D. Richards, PhD thesis) thus providing definitive evidence that E3 can bind specifically to E2 but that the binding is very much weaker than to E3BP. This last result with E3BP is also in good agreement with the results obtained using ITC (Figure 6.3).

In order to confirm this weak interaction between E3 and the E2 didomain, the binding of these constructs was examined by ITC. The association of E3 to the subunit-binding domain alone was also studied. Figure 6.6 demonstrates the titration of E3 (200 $\mu$ M) into the didomain of E2 (0.995 $\mu$ M). This study supports the data collected using surface plasmon resonance in that the interaction between these 2 proteins is very weak,  $K$  being in the low  $\mu$ M range ( $2 \times 10^5$ ). This binding is more than a thousand-fold weaker than that measured for E3 and E3BP which was  $6.3 \times 10^9$ . This provides good evidence that E3 and E2 can associate with each other in the absence of E3BP but that the interaction is very much weaker.

As a confirmation of these results the same experiment was conducted using the subunit-binding domain of E2 alone. Like the subunit-binding domain of E3BP, this was cloned as a GST fusion. The results of this experiment can be seen in Figure 6.7.

Again, very weak binding is observed with  $K$  being measured at  $2 \times 10^5$ . This is in good agreement with that measured for the didomain. However, at this level of binding the stoichiometry cannot be determined with any accuracy and so, in this particular case,  $N$  was fixed at 0.5 in order to give a better fit of the data. Nevertheless this study supports the previous experiment using the didomain and the results obtained with surface plasmon resonance, confirming that E3 can indeed bind to E2 with low affinity.

## 6.6 Discussion

Isothermal titration calorimetry (ITC) is one of a number of techniques that can directly measure the affinity of binding between two proteins. One other technique that has already been mentioned in this chapter is surface plasmon resonance (SPR).

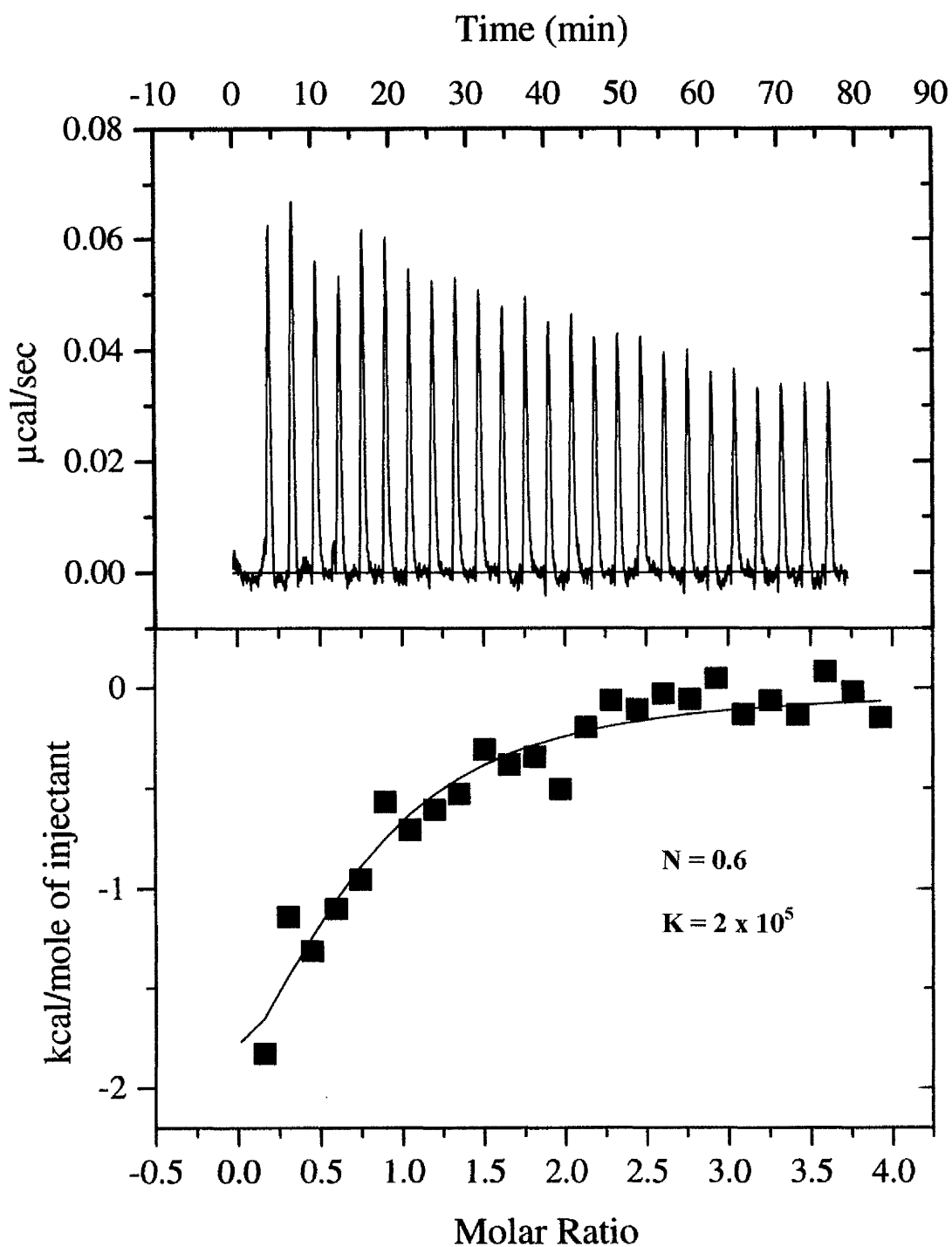


**Figure 6.6** Titration of E3 into the E2 didomain

The binding of E3 to E2 is very weak as indicated by an association constant,  $K$ , of  $2 \times 10^5$ . At this level of binding the stoichiometry cannot be determined with any accuracy but is indicated at approximately 0.6.

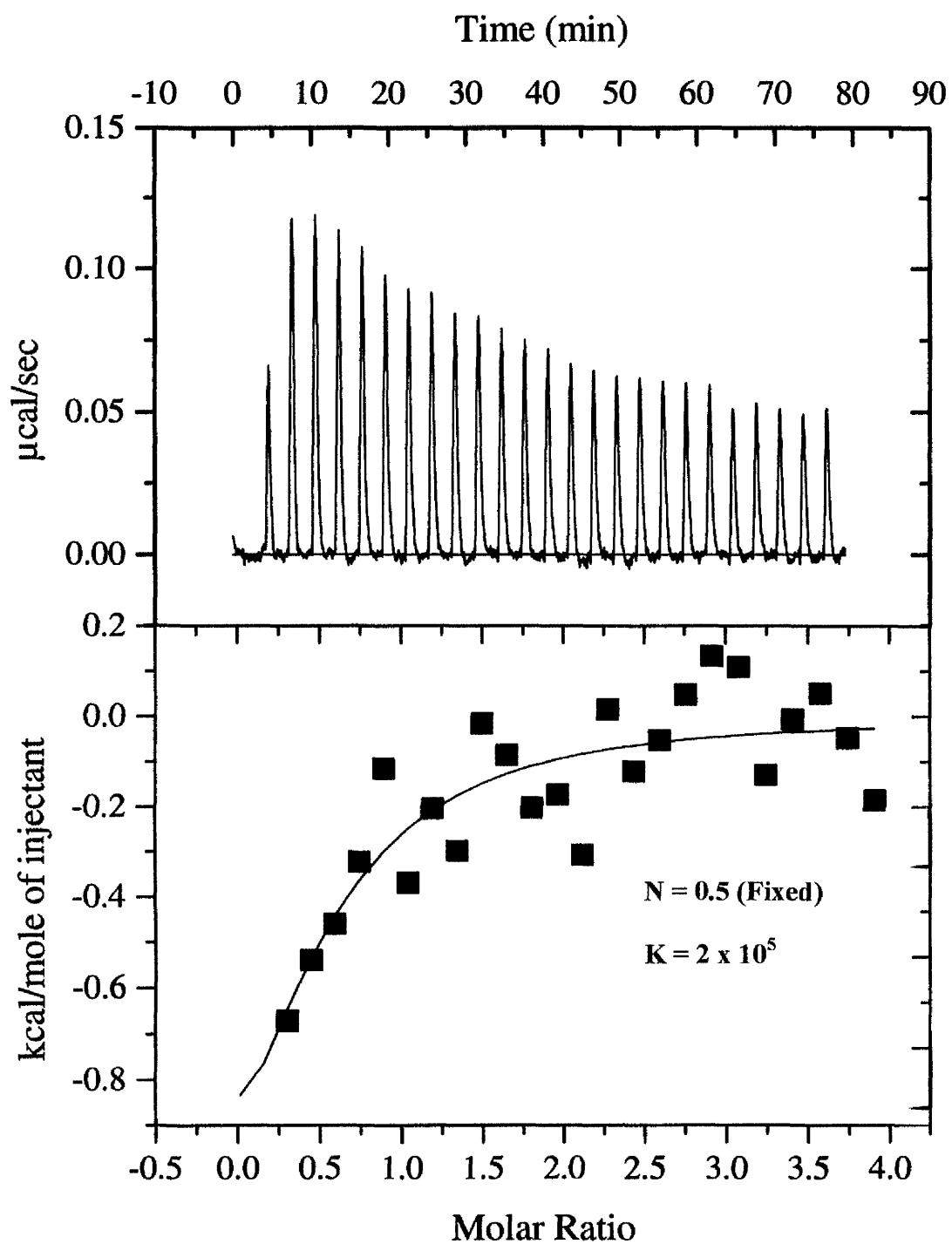


**Figure 6.7 Titration of E3 into the subunit-binding domain of E2**

The association constant,  $K$ , has been measured at  $2 \times 10^5$  while the stoichiometry,  $N$ , was fixed at 0.5 to allow for a better fit of the data.

These methods both have advantages and disadvantages. A major disadvantage of SPR is that it assumes a 1:1 binding model, which can limit the interpretation of the data. ITC makes no such assumption and has the additional benefit of being able to measure the stoichiometry of binding between the proteins of interest with great accuracy. The high concentrations of protein required for these studies can prove problematic however. In this instance the consistently high levels of overexpression obtained for each recombinant protein, as demonstrated in an earlier chapter, has meant that studies using ITC were feasible. The main limitation of these studies is that the perceived results may not necessarily reflect the situation in the native complex. The fully assembled native complex will be subject to structural limitations such as the spatial geometry and steric constraints, which cannot be accounted for in these studies.

The first part of this chapter was concerned with investigating the stoichiometry and association constant for the interaction between E3 and E3BP. These studies have produced an interesting result, which could have important implications for the structural organisation of this complex. The titration of E3BP into E3 suggested that one E3 dimer contains 2 binding sites for E3BP and that both sites are accessible to the binding domain while the titration of E3 into the E3BP-SBD showed an actual stoichiometry of 1:1. This could be as a result of both binding domains of the GST fusion protein binding to one E3 dimer but this is by no means clearcut. An alternative explanation is that one subunit-binding domain binds to E3 while the second is prevented from binding due to steric hindrance. However, this would theoretically leave the second binding site on E3 available and it might be expected that a second GST-tagged subunit-binding domain would bind to E3 resulting in a 2:1

stoichiometry. Given the 1:1 stoichiometry observed this may favour the first scenario as the appropriate explanation. In both these studies association constants were obtained in the nanomolar range or higher ( $6.3 \times 10^9$  and  $1 \times 10^9$  for the titration of full-length E3BP into E3, and  $1 \times 10^{12}$  for the subunit-binding domain although this was fixed as the binding was very tight). This is in agreement with the association constants obtained using surface plasmon resonance (SPR). The full-length E3BP was found to bind to E3 with an association constant of  $1.1 \times 10^8$ , while the didomain (cloned without a His-tag) had an affinity constant of  $1.9 \times 10^8$  (S.D. Richards, PhD thesis).

The data obtained in these studies opens up an exciting theory relating to the level of structural organisation in the human pyruvate dehydrogenase complex, which has not previously been recognised.

Given that this data suggests that one E3 dimer binds two E3BP monomers this would mean that six E3 dimers are present in each complex. Spatially, this suggests the possibility that each E3 dimer extends across two of the 12 faces of the E2 pentagonal dodecahedron. This spatial arrangement has been proposed previously (Wu & Reed, 1984) when the stoichiometry of these complexes was first discussed. However, if it is indeed the case that there are 6 E3 dimers present per complex, it is known that there are 12 E3BP molecules and 60 E2 subunits also present. Given that there are believed to be 30 E1  $\alpha_2\beta_2$  heterotetramers it is an attractive proposition to speculate that while 2 E3BP monomers bind to one E3 subunit, one E1 heterotetramer may bind to two E2 subunits. Therefore, the E1 subunits may extend along the edges of the E2 core structure while E3 extends across the faces. This in effect would provide a series

of crossbridges around the human pyruvate dehydrogenase complex. A schematic model of the proposed mode of binding between E3 and E3BP, and E1 and E2, is shown in Figure 6.8.

The presence of crossbridges in the complex may be beneficial for a number of reasons. The discovery of the E3BP component in mammalian PDC and its function in attaching E3 to the core of the complex suggests that the human complex is much more structured than, for example, the bacterial complexes where E3 and E1 have been shown to compete for the same binding site on E2 (Lessard *et al*, 1996). An important part of the catalytic efficiency of human PDC may be based on a precise subunit stoichiometry. E3BP may have evolved in order to allow this to happen as it contains a binding site specific for E3. The presence of crossbridges may provide yet another level of structure for this complex. These crossbridges would effectively bring E1 in close proximity to E2 and likewise, E3BP in close proximity to E3. In this way E1 may interact preferentially with E2, acetyl groups or electrons may then be passed directly from E2 to E3BP with E3 interacting preferentially with E3BP. This may suggest that there is a defined route of acetyl and electron migration around the human pyruvate dehydrogenase complex. These crossbridges may also allow the lipoyl domains to be more directed in targeting the active sites, which may, in turn, increase the efficiency of the catalytic mechanism.

As well as allowing the lipoyl domains to be directed to the active sites, the presence of crossbridges may aid the regulation of this complex. It is known that the PDC-associated kinase is present on the complex in very small amounts. The best estimates

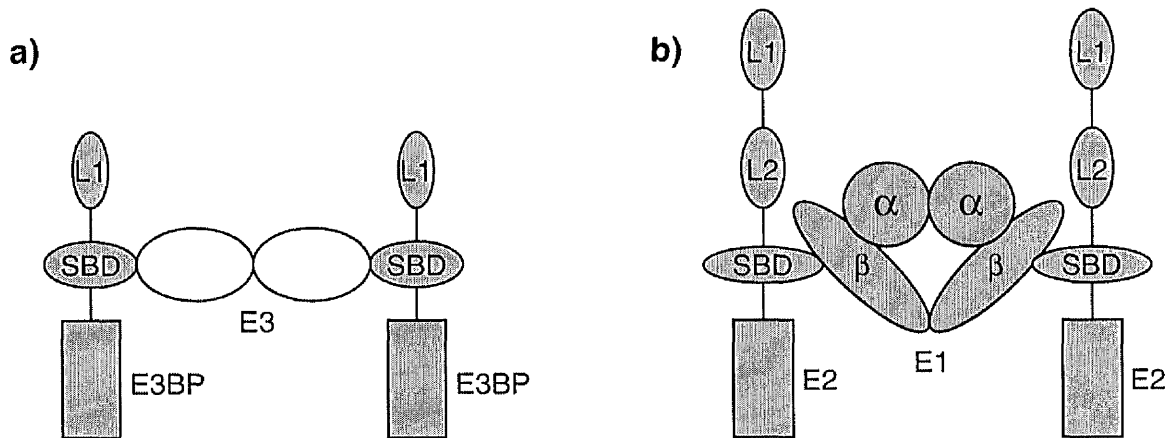


**Figure 6.8 Hypothetical model of the proposed binding arrangement between E3 and E3BP, and E1 and E2.**

**Panel A:** Proposed model of binding between E3 and E3BP showing one E3 dimer, with a binding site on each monomer, binding to two E3BP subunits.

**Panel B:** Proposed model of binding between E1 and E2 suggesting that human PDC-E1 contains two binding sites for E2. Binding is known to be mediated via the  $\beta$  subunits.

L1, inner lipoyl domain; L2, outer lipoyl domain; SBD, subunit-binding domain

suggest that there is a maximum of three kinase molecules present per complex (Brandt & Roche, 1983). Given the physical size of these complexes it is difficult to envisage how the kinase can function effectively in the regulation of PDC. It has been proposed previously that the kinase moves around the complex by a “hand over hand” mechanism, by a process of partial dissociation followed by interchange to another lipoyl domain (Liu *et al*, 1995b). The presence of crossbridges may facilitate the movement of the kinase around the complex thus allowing it to function more effectively in phosphorylating the relevant serine residues on the E1 $\alpha$  subunit.

This chapter also examined the binding between E3 and E2. Using truncated constructs of E2, specifically the didomain and the subunit-binding domain, the association constants were measured in the micromolar range ( $2 \times 10^5$  for the didomain and  $2 \times 10^5$  for the subunit-binding domain). These results are in agreement with that obtained using SPR. The E2 didomain had an association constant of  $2.52 \times 10^6$  while the full-length E2 bound to E3 with an association constant of  $8.38 \times 10^6$  (S.D. Richards, PhD thesis). The stoichiometry of binding measured in these studies should be viewed with caution since, at this level of weak binding, measurement of the stoichiometry of binding becomes less accurate. Tentatively however, the stoichiometry of binding between E3 and the E2 didomain has been measured to be 0.6, indicating that 0.5 mole of E3 binds to one E2 didomain. This could confirm the presence of two binding sites on the E3 dimer. The data obtained for the subunit-binding domain, which was cloned as a GST-tagged protein is more difficult to interpret. As with the subunit-binding domain of E3BP, it would be expected that there would be two binding domains present in the expressed protein, thus resulting in a 1:1 stoichiometry. However, this was fixed at 0.5 in order to find the best fit for this

set of data. There is a greater variation in the data obtained for the subunit-binding domain than for the didomain, which resulted in difficulties in performing the analysis. The stoichiometry of binding was also fixed at 1.0 (data not shown) and the best fit for the data assessed. On comparing the two models it was observed that a fixed stoichiometry of 0.5 resulted in a better fit for the data and so this is the analysis shown in Figure 6.7.

Perhaps most importantly the results obtained here again confirm that there is an interaction, albeit a weak one, between E3 and E2. The affinity of binding between these two proteins is significantly less than that between E3 and E3BP, as expected. In order to clarify the results described above, further studies are required. As mentioned earlier ITC studies using a His-tagged E3BP didomain are underway at time of writing. This didomain is a monomer and should make clear the stoichiometry of the interaction between E3 and E3BP. The study using the full-length E3BP, where E3 is titrated into E3BP should also be repeated. The lower association constant obtained in this study ( $8 \times 10^6$ ) compared to that obtained for the other studies using E3BP constructs and the results obtained using SPR is a good indication that this study is not representative of the actual binding between these two proteins. This is likely to be due to the low concentrations of protein used in this particular study and also because of the large heats of dilution observed, which can mask the heats of binding. This could also account for the lower than expected stoichiometry seen in this case.

In order to validate the theory postulated above it is necessary to conduct ITC studies to examine the stoichiometry of binding between E1 and E2. To date, this has not

been possible due to the great difficulty in obtaining soluble recombinant E1. The solubility problem of E1 has proved to be the major stumbling block in achieving the original aim of this thesis. Efforts to improve the solubility of E1 are ongoing in our laboratory and once sufficient quantities of active protein have been obtained ITC studies will be performed using E1 with the E2 didomain and the subunit-binding domain. Ideally the interaction between full length E2 and E1 would also be studied but since recombinant E2 assembles into a 60meric structure this would make any meaningful analysis of the data difficult to achieve and limit the interpretation.

Therefore it is preferable to use the truncated E2 clones.

Importantly, the data presented in this chapter has hinted at a new and novel level of structural organisation within the human pyruvate dehydrogenase complex, which has not previously been recognised. Further studies, such as those described above, are required in order to validate the hypothesis stated here and these studies are a top priority in our laboratory. However, it is also important to consider that the observations found under these experimental conditions may not necessarily be representative of the situation in the native complex and this must also be taken into account.

## **General discussion**

The 2-oxoacid dehydrogenase multienzyme complexes are a source of great interest in terms of studying protein-protein interactions, cooperativity in multistep enzymatic processes and in the importance of post-translational modification. Our knowledge of these complexes has increased greatly in recent years but it has also become apparent that there is still much to be learned from the study of these vast macromolecular assemblies.

There is a great deal to be gained from extending our understanding and knowledge of the human pyruvate dehydrogenase complex. Mutations in this complex are associated with potentially severe inborn errors of metabolism. Over 200 mutations have so far been identified with most being found in the E1 $\alpha$  subunit of this complex. However, knowledge of the effects that these mutations have on complex activity and assembly remains limited. A model complex, whereby natural mutations could be introduced *in vitro* could be extremely advantageous in increasing our understanding of the consequences of these mutations on the complex as a whole. The reconstitution of a recombinant complex *in vitro* will also allow the assembly of the complex to be studied more fully in terms of the dynamics of binding and interactions between enzymes, which may only be observed on assembly of an intact complex. Another interesting aspect of producing a recombinant model is that it will eventually allow the association of PDC-associated kinase and phosphatase to be examined. Both of these regulatory enzymes are believed to bind to the inner lipoyl domain of E2.

Reconstitution of *B. stearothermophilus* PDC, using the recombinant enzymes, has been described previously (Domingo *et al*, 1999). In this complex, it has been found that E1 and E3 can compete for binding and are capable of displacing one another

from the subunit-binding domain of E2 (Lessard *et al*, 1996). It was also shown that in the presence of either E1 or E3, E2 had the capacity to bind a maximum of 60 subunits. However, in the assembled complex, when both E1 and E3 are present only approx. 60% of the potential binding sites become occupied (Domingo *et al*, 1999). These investigators suggested that this may be because E1 and E3 have different preferred binding sites on the surface of the E2 core and that this only becomes clear when both subunits are present and competing for binding. Thus it would appear that, at least for the *B. stearothermophilus* complex, assembly is not only dependent on spatial and geometric constraints but also by previously unrecognised interactions by all subunits involved.

The main aim of this thesis was in producing a recombinant model of the human pyruvate dehydrogenase complex. To this end, the cloning strategy has been described which has been used in order to overexpress the individual components of human PDC. His-tags have been incorporated into the N-termini of these recombinant proteins in order to facilitate their rapid purification using affinity chromatography. It has been shown here, and elsewhere, that the addition of an N-terminal His-tag has no significant effect on either the folding of these proteins or on their catalytic activity. In all cases, with the exception of the E1 component, induction of heterologous protein at 30°C was sufficient to produce soluble protein. Importantly, these proteins are also active, as evidenced by enzymatic assay and comparing their specific activities with those quoted in the literature. Immunoblotting with a specific monoclonal antibody showed that the N-terminal lipoyl domains of E2 and E3BP were folded correctly.

## Solubility of E1

As mentioned above, this has not been the case for E1. Although the recombinant protein appears to be active, it has not been produced in soluble form. The method of solubilisation described in this thesis, the use of N-lauroylsarcosine, has not proved to be a satisfactory means of producing E1 in a form that can be used in subsequent studies. N-lauroylsarcosine appears to have a detrimental effect on PDC activity as a whole (data not shown) and, while substantial amounts of detergent can be removed by dialysis, residual levels remaining in the protein preparation can affect any subsequent studies. Clearly an improved method of producing soluble E1 is required before further studies can be undertaken and this is a top priority in our laboratory. Other investigators have also reported difficulties in producing a soluble recombinant E1 component. Mammalian E1 from the branched chain 2-oxoacid dehydrogenase complex was shown to require the presence of additional molecular chaperones GroEL and GroES in order for an active  $\alpha_2\beta_2$  heterotetramer to assemble (Wynn *et al*, 1992). While human E1-PDC does not appear to require the presence of additional molecular chaperones, factors which do seem important in producing soluble, active recombinant E1 include using a low concentration of inducer (0.1mM IPTG in some cases), a lower induction temperature (often 22°C) and coexpression of the two E1 subunits in *E. coli* (Korotchkina *et al*, 1995). These conditions have been repeated in our laboratory and, unfortunately have not proved successful in producing soluble E1.

The lack of a soluble E1 component has proved to be the main rate-limiting factor in preventing the reconstitution of a recombinant human PDC *in vitro*. However, while work to produce a soluble E1 component was ongoing a number of interesting findings were obtained for the other components of PDC.

### **Unfolding studies on recombinant E3BP**

Unfolding studies on the independently expressed E3BP component has revealed that each of the three domains unfolds in discrete concentrations of GdmCl. This is consistent with the view that each domain can fold independently of one another and hence, also unfold independently of each other. It also indicates that some domains are more stable than others. The lipoyl domain in particular is very stable and it is this domain which is likely to be the last to unfold. It is this stability which probably results in neither the full-length E3BP nor the didomain being fully denatured in 6M GdmCl. Performing the same study using the didomain of E3BP has shown that the didomain is more stable than the full-length protein. The didomain consists of the lipoyl domain and subunit-binding domain of E3BP cloned as a His-tagged protein. This would suggest that the C-terminal domain is the least stable of the three domains of E3BP. This information can now be utilised to provide an elegant means of examining the assembly and integration of E3BP into the E2 core *in vitro*. By selectively denaturing the C-terminal domain of E3BP in the appropriate concentration of GdmCl, it could then be observed if the denatured C-terminal domain could stably interact with a fully assembled E2 core. Reversible dissociation of E2 to trimers using intermediate levels (1.8-2.8M) of GdmCl (McCartney *et al*, 1997) together with selective denaturation of the C-terminal domain of E3BP could also be employed to examine the nature of the association between these two proteins.

### **Assembly of the E2/E3BP structural core**

Studies using coexpressed E2/E3BP and individually expressed E2 and E3BP has revealed that coexpression of these two subunits is necessary in order for the two components to assemble into the core structure. Mixing the individually expressed

subunits in equal amounts so that there was a vast excess of E3BP did not produce a stable integrated E2/E3BP core. Preliminary analysis of the stoichiometry in the coexpressed E2/E3BP core has suggested that there is an excess of E3BP present in the recombinant core when compared with the native complex. However, it should be emphasised that this is preliminary data and this study will be repeated in the presence of 1-2M NaCl in order to remove any E3BP, which may be non-specifically bound to the core and also any aggregates. While these original experiments to examine the stoichiometry of binding were performed using densitometric scanning analysis, it is hoped that radiolabelling of these subunits with [2,3-<sup>14</sup>C] NEM will provide another, more accurate means, of determining the stoichiometry of the recombinant core. If the stoichiometry proves to be as expected this provides further evidence that the assembly of the E2/E3BP core is likely to follow a defined pathway of folding intermediates.

### **Stoichiometry of binding of E3-E2 and E3-E3BP**

Isothermal titration calorimetry (ITC) has been employed in this thesis to measure the stoichiometry and affinity of binding between E3 and E2, and E3 and E3BP. The interaction between E3 and E2 has been studied previously using surface plasmon resonance. The studies described here, where E3 was shown to interact with E2 with a weak affinity, has confirmed the interaction described previously (S.D. Richards, PhD thesis). Here, the affinity of binding between E3 and the truncated constructs of E2 used in these studies has been shown to lie in the micromolar range. This is very much weaker than that described for the interaction between E3 and E3BP and provides support for the observation that E2 preferentially binds to E1 but has also retained a residual binding affinity for E3. It also shows that this binding between E2

and E3 is specific in nature, and not just the result of random collision. This provides a molecular basis as to why E3BP-deficient patients retain residual PDC activity. Binding studies, again using isothermal titration calorimetry, of recombinant E3 and E3BP proteins have revealed an unexpected stoichiometry of binding. It has been shown that two E3BP monomers can bind to one E3 dimer. This would indicate that there are six E3 dimers present per complex and these would be likely to extend across the twelve faces of the E2 core. These studies have been performed using both the full-length E3BP and subunit-binding domain (SBD) of E3BP, cloned as a GST-fusion protein. In order to fully clarify the results obtained, repeating the experiment using the E3BP didomain will be required. However, the presence of six E3 dimers per complex could indicate that E3 forms a network of crossbridges around the complex, linking pairs of E3BP monomers. It will be of great interest to determine the stoichiometry of binding between E1 and E2. Given that there are 60 E2 subunits present in each complex and that, at maximal occupancy there are believed to be 30 E1 heterotetramers it is feasible that two E1 subunits may bind to one E2. If this is indeed the case it is possible that E1 may also form a network of crossbridges. Cryoelectron microscopy of PDC from bovine kidney has recently suggested that the flexibility of E1 and its linker is largely constrained (Zhou *et al*, 2001b). This lack of flexibility may be a direct consequence of the arrangement of E1 about the complex as a series of crossbridges.

There are a number of possible reasons and benefits as to why this may be the case. The presence of crossbridges linking pairs of E2 subunits and pairs of E3BP monomers would suggest that while E3BP preferentially interacts with E3, E1 may interact preferentially with E2. This indicates that there is a defined route of electron

transport and transfer of acetyl groups and reducing equivalents around the human pyruvate dehydrogenase complex. This may result in the lipoyl domains being more directed to the active sites of the enzymes, which may in turn increase the efficiency of the catalytic mechanism.

The presence of crossbridges may also have a role in the regulation of the complex. There are estimated to be a maximum of three kinase molecules present in the intact PDC complex and these kinases are believed to bind to the inner lipoyl domain of E2. It has been proposed that the kinase moves around the complex in a “hand-over-hand” mechanism involving a steady process of partial dissociation of one kinase subunit followed by interchange to another lipoyl domain on the E2 core (Liu *et al*, 1995b). The presence of crossbridges on this complex may help facilitate the movement of the kinase around the complex enabling it to phosphorylate 20-30 E1 $\alpha$  subunits in a rapid and efficient manner.

It is important to remember that these studies have not been performed on an intact complex. In the native state these subunits are subjected to spatial and geometric constraints which cannot be accounted for under these experimental conditions. As was noted when the *B. stearothermophilus* PDC was reconstituted *in vitro*, there may be interactions between subunits which only manifest themselves during the assembly process (Domingo *et al*, 1999).

The data presented in this thesis has hinted at a new level of structural organisation within the PDC complex. Previously, it was thought that E2 and E3BP provided the structural framework of the complex while E1 and E3 were purely mechanistic in

purpose. The evidence presented here suggests that E1 and E3 also have a structural function. They may modulate the movement of the lipoyl domain and are potentially involved in supporting the function of the kinase and phosphatase.

Future work will be aimed at improving the solubility of the E1 component. This will allow binding studies to be performed using isothermal titration calorimetry in order to determine the stoichiometry and affinity of binding between E1 and E2. This will hopefully provide further evidence for the presence of crossbridges in human PDC. Reconstitution of a model complex will also be attempted which should provide further insight into the ordered folding events involved in the assembly of these vast macromolecular machines.

## References

- Ali, M. S., Roche, T. E. & Patel, M. S. (1993) Identification of the Essential Cysteine Residue in the Active Site of Bovine Pyruvate Dehydrogenase. *J. Biol. Chem.* **268**, 22353-22356.
- Ali, M. S., Shenoy, B. C., Eswaran, D., Andersson, L. A., Roche, T. E. & Patel, M. S. (1995) Identification of the Tryptophan Residue in the Thiamin Pyrophosphate Binding Site of Mammalian Pyruvate Dehydrogenase. *J. Biol. Chem.* **270**, 4570-4574.
- Aral, B., Benelli, C., Ait-Ghezala, G., Amessou, M., Fouque, F., Maunoury, C., Creau, N., Kamoun, P. & Marsac, C. (1997) Mutations in PDX1, the Human Lipoyl-Containing Component X of the Pyruvate Dehydrogenase-Complex Gene on Chromosome 11p1, in Congenital Lactic Acidosis. *Am. J. Hum. Genet.* **61**, 1318-1326.
- Arjunan, P., Nemeria, N., Brunskill, A., Chandrasekhar, K., Sax, M., Yan, Y., Jordan, F., Guest, J. R. & Furey, W. (2002) Structure of the Pyruvate Dehydrogenase Multienzyme Complex E1 Component From *Escherichia Coli* at 1.85Å Resolution. *Biochemistry* **41**, 5213-5221.
- Ævarsson, A., Seger, K., Turley, S., Sokatch, J. R., & Hol, W. G. (1999) Crystal Structure of 2-Oxoisovalerate and Dehydrogenase and the Architecture of 2-Oxo Acid Dehydrogenase Multienzyme Complexes. *Nat. Struct. Biol.* **6**, 785-792.
- Ævarsson, A., Chuang, J. L., Wynn, R. M., Turley, S., Chuang, D. T. & Hol, W. G. (2000) Crystal Structure of Human Branched-Chain Alpha-Ketoacid Dehydrogenase and the Molecular Basis of Multienzyme Complex Deficiency in Maple Syrup Urine Disease. *Structure. Fold. Des.* **8**, 277-291.

- Behal, R. H., Browning, K. S., Hall, T. B. & Reed, L. J. (1989) Cloning and Nucleotide Sequence of the Gene for Protein X From *Saccharomyces Cerevisiae*. *Proc. Natl. Acad. Sci. U. S. A.* **86**, 8732-8736.
- Behal, R. H., Buxton, D. B., Robertson, J. G. & Olson, M. S. (1993) Regulation of the Pyruvate Dehydrogenase Multienzyme Complex. *Annu. Rev. Nutr.* **13**, 497-520.
- Berg, A., Vervoort, J. & de Kok, A. (1997) Three-Dimensional Structure in Solution of the N-Terminal Lipoyl Domain of the Pyruvate Dehydrogenase Complex From *Azotobacter Vinelandii*. *Eur. J. Biochem.* **244**, 352-360.
- Bowker-Kinley, M. M., Davis, W. I., Wu, P., Harris, R. A. & Popov, K. M. (1998) Evidence for Existence of Tissue-Specific Regulation of the Mammalian Pyruvate Dehydrogenase Complex. *Biochem. J.* **329**, 191-196.
- Brandt, D. R. & Roche, T. E. (1983) Specificity of the Pyruvate Dehydrogenase Kinase for Pyruvate Dehydrogenase Component Bound to the Surface of the Kidney Pyruvate Dehydrogenase Complex and Evidence for Intracore Migration of Pyruvate Dehydrogenase Component. *Biochemistry* **22**, 2966-2971.
- Brown, R. M., Dahl, H. H. & Brown, G. K. (1989) X-Chromosome Location of the Functional Gene for the E1 $\alpha$  Subunit of the Human Pyruvate Dehydrogenase Complex. *Genomics* **4**, 174-181.
- Bukau, B. & Horwich, A. (1998) The Hsp70 and Hsp60 chaperone machines. *Cell* **92**, 351-366.

Burgess, R. R. (1996) Purification of Overproduced *Escherichia Coli* RNA Polymerase  $\sigma$  Factors by Solubilising Inclusion Bodies and Refolding From Sarkosyl. *Methods Enzymol.* **273**, 145-149.

Carothers, D. J., Pons, G. & Patel, M. S. (1989) Dihydrolipoamide Dehydrogenase: Functional Similarities and Divergent Evolution of the Pyridine Nucleotide-Disulfide Oxidoreductases. *Arch. Biochem. Biophys.* **268**, 409-425.

Chuang, D. T., Davie, J. R., Wynn, R. M., Chuang, J. L., Koyata, H. & Cox, R. P. (1995) Molecular Basis of Maple Syrup Urine Disease and Stable Correction by Retroviral Gene Transfer. *J. Nutr.* **125**, 1766S-1772S.

Chuang, J. L., Wynn, R. M., Song, J-L. & Chuang, D. T. (1999) GroEL/GroES-dependent reconstitution of  $\alpha_2\beta_2$  tetramers of human mitochondrial branched-chain  $\alpha$ -ketoacid decarboxylase. *J. Biol. Chem.* **274**, 10395-10404.

Chun, K., MacKay, N., Willard, H. F. & Robinson, B. H. (1990) Isolation, characterisation and chromosomal localisation of cDNA clones for the E1 $\beta$  subunit of the pyruvate dehydrogenase complex. *Eur. J. Biochem.* **194**, 587-592.

Chun, K., MacKay, N., Petrova-Benedict, R. & Robinson, B. H. (1993) Mutations in the X-Linked E1 Alpha Subunit of Pyruvate Dehydrogenase Leading to Deficiency of the Pyruvate Dehydrogenase Complex. *Hum. Mol. Genet.* **2**, 449-454.

- Ciszak, E., Korotchkina, L. G., Hong, Y. S., Joachimiak, A. & Patel, M. S. (2001) Crystallization and Initial X-Ray Diffraction Analysis of Human Pyruvate Dehydrogenase. *Acta Crystallogr. D.* **57**, 465-468.
- Conner, M., Krell, T. & Lindsay, J. G. (1996) Identification and Purification of a Distinct Dihydrolipoamide Dehydrogenase From Pea Chloroplasts. *Planta* **200**, 195-202.
- Cook, R. M., Munro, A. W. & Lindsay, J. G. (1996) Distinct Forms of the FAD Containing Enzyme Dihydrolipoamide Dehydrogenase (E3) Are Found in Tubers and Leaves of Potato (*Solanum Tuberosum*). *Flavins & Flavoproteins*, 659-661.
- Coppel, R. L., McNeilage, L. J., Surh, C. D., Van de, W. J., Spithill, T. W., Whittingham, S. & Gershwin, M. E. (1988) Primary structure of the human M2 mitochondrial autoantigen of primary biliary cirrhosis: Dihydrolipoamide acetyltransferase. *Proc.Natl.Acad.Sci.U.S.A* **85**, 7317-7321.
- Dahl, H. M., Hunt, S. M., Hutchison, W. M. & Brown, G. K. (1987) The Human Pyruvate Dehydrogenase Complex. *J. Biol. Chem.* **262**, 7398-7403.
- Dahl, H. M., Brown, R. M., Hutchison, W. M., Maragos, C. & Brown, G. K. (1990) A Testis-Specific Form of the Human Pyruvate Dehydrogenase E1 $\alpha$  Subunit Is Coded for by an Intronless Gene on Chromosome 4. *Genomics* **8**, 225-232.
- Dahl, H-H.M. (1995) Pyruvate dehydrogenase E1 $\alpha$  deficiency-Males and females differ yet again. *Am. J. Hum. Genet.* **56**, 553-557.

- Dardel, F., Davis, A. L., Laue, E. D. & Perham, R. N. (1993) Three-Dimensional Structure of the Lipoyl Domain From *Bacillus Stearotherophilus* Pyruvate Dehydrogenase Multienzyme Complex. *J. Mol. Biol.* **229**, 1037-1048.
- Davie, J. R., Wynn, R. M., Cox, R. P. & Chuang, D. T. (1992) Expression and assembly of a functional E1 component ( $\alpha_2\beta_2$ ) of mammalian Branched-chain  $\alpha$ -ketoacid dehydrogenase complex in *Escherichia coli*. *J. Biol. Chem.* **267**, 16601-16606.
- de Kok, A., Hengeveld, A. F., Martin, A. & Westphal, A. H. (1998) The Pyruvate Dehydrogenase Multi-Enzyme Complex From Gram-Negative Bacteria. *Biochim. Biophys. Acta.* **1385**, 353-366.
- De Marcucci, O. G., Gibb, G. M., Dick, J. & Lindsay, J. G. (1988) Biosynthesis, Import and Processing of Precursor Polypeptides of Mammalian Mitochondrial Pyruvate Dehydrogenase Complex. *Biochem. J.* **251**, 817-823.
- Denton, R. M. & McCormack, J. G. (1990) Ca<sup>2+</sup> As a Second Messenger Within Mitochondria of the Heart and Other Tissues. *Annu. Rev. Physiol.* **52**, 451-466.
- Domingo, G. J., Chauhan, H. J., Lessard, I. A., Fuller, C. & Perham, R. N. (1999) Self-Assembly and Catalytic Activity of the Pyruvate Dehydrogenase Multienzyme Complex From *Bacillus Stearotherophilus*. *Eur. J. Biochem.* **266**, 1136-1146.
- Endo, T., Mitsui, S., Nakai, M. & Roise, D. (1996) Binding of Mitochondrial Presequences to Yeast Cytosolic Heat Shock Protein 70 Depends on the Amphiphilicity of the Presequence. *J. Biol. Chem.* **271**, 4161-4167.

- Fang, R., Nixon, P. F. & Duggleby, R. G. (1998) Identification of the Catalytic Glutamate in the E1 Component of Human Pyruvate Dehydrogenase. *FEBS Lett.* **437**, 273-277.
- Fujiwara, K., Okamura-Ikeda, K. & Motokawa, Y. (1994) Purification and Characterisation of Lipoyl-AMP:N<sup>ε</sup>-Lysine Lipoyltransferase From Bovine Liver Mitochondria. *J. Biol. Chem.* **269**, 16605-16609.
- Fujiwara, K., Suzuki, M., Okumachi, Y., Okamura-Ikeda, K., Fujiwara, T., Takahashi, E. & Motokawa, Y. (1999) Molecular cloning, structural characterisation and chromosomal localisation of human lipoyltransferase gene. *Eur. J. Biochem.* **260**, 761-767.
- Fussey, S. P., Guest, J. R., James, O. F., Bassendine, M. F. & Yeaman, S. J. (1988) Identification and Analysis of the Major M2 Autoantigens in Primary Biliary Cirrhosis. *Proc. Natl. Acad. Sci. U. S. A* **85**, 8654-8658.
- Fussey, S. P., Bassendine, M. F., Fittes, D., Turner, I. B., James, O. F. W. & Yeaman, S. J. (1989) The E1 $\alpha$  and  $\beta$  subunits of the pyruvate dehydrogenase complex are M2'd' and M2'e' autoantigens in primary biliary cirrhosis. *Clin. Sci.* **77**, 365-368.
- Fussey, S. P. M., Ali, S. T., Guest, J. R., James, O. F. W., Bassendine, M. F. & Yeaman, S. J. (1990) Activity of Primary Biliary Cirrhosis Sera With *Escherichia Coli* Dihydrolipoamide Acetyltransferase (E2p): Characterisation of Main Immunogenic Region. *Proc. Natl. Acad. Sci. U. S. A* **87**, 3987-3991.
- Geoffroy, V., Fouque, F., Benelli, C., Poggi, F., Saudubray, J. M., Lissens, W., Meirleir, L. D., Marsac, C. & Sanderson, S. J. (1996) Defect in the X-Lipoyl-Containing

Component of the Pyruvate Dehydrogenase Complex in a Patient With a Neonatal Lactic Acidemia. *Pediatrics* **97**, 267-272.

Gershwin, M. E., Mackay, I. R., Sturgess, A. & Coppel, R. L. (1987) Identification and specificity of a cDNA encoding the 70kD mitochondrial antigen recognised in primary biliary cirrhosis. *J.Immunol.* **138**, 3525-3531.

Gibson, G. E., Zhang, H., Sheu, K. F., Bogdanovich, N., Lindsay, J. G., Lannfelt, L., Vestling, M. & Cowburn, R. F. (1998)  $\alpha$ -Ketoglutarate Dehydrogenase in Alzheimer Brains Bearing the APP670/671 Mutation. *Ann. Neurol.* **44**, 676-681.

Gibson, G. E., Park, L. C. H., Sheu, K. F., Blass, J. P. & Calingasan, N. Y. (2000) The  $\alpha$ -Ketoglutarate Dehydrogenase Complex in Neurodegeneration. *Neurochem. International* **36**, 97-112.

Green, D. E., Morris, T. W., Green, J., Cronan, J. E., Jr. & Guest, J. R. (1995) Purification and Properties of the Lipoate Protein Ligase of *Escherichia Coli*. *Biochem. J.* **309**, 853-862.

Green, J. D., Perham, R. N., Ullrich, S. J. & Appella, E. (1992) Conformational Studies of the Interdomain Linker Peptides in the Dihydrolipoyl Acetyltransferase Component of the Pyruvate Dehydrogenase Multienzyme Complex of *Escherichia Coli*. *J. Biol. Chem.* **267**, 23484-23488.

Green, J. D., Laue, E. D., Perham, R. N., Ali, S. T. & Guest, J. R. (1995b) Three-Dimensional Structure of a Lipoyl Domain From the Dihydrolipoyl Acetyltransferase

- Component of the Pyruvate Dehydrogenase Multienzyme Complex of *Escherichia Coli*.  
*J. Mol. Biol.* **248**, 328-343.
- Gudi, R., Bowker-Kinley, M. M., Kedishvili, N. Y., Zhao, Y. & Popov, K. M. (1995)  
Diversity of the Pyruvate Dehydrogenase Kinase Gene Family in Humans. *J. Biol. Chem.*  
**270**, 28989-28994.
- Guest, J. R. (1987) Functional Implications of Structural Homologies Between  
Chloramphenicol Acetyltransferase and Dihydrolipoamide Acetyltransferase. *FEMS*  
*Microbiol. Lett.* **44**, 417-422.
- Harris, R. A., Bowker-Kinley, M. M., Wu, P., Jeng, J. & Popov, K. M. (1997)  
Dihydrolipoamide Dehydrogenase-Binding Protein of the Human Pyruvate  
Dehydrogenase Complex. DNA-Derived Amino Acid Sequence, Expression, and  
Reconstitution of the Pyruvate Dehydrogenase Complex. *J. Biol. Chem.* **272**, 19746-  
19751.
- Hartl, F. U. (1996) Molecular chaperones in cellular protein folding. *Nature* **381**, 571-  
580.
- Hawkins, C. F., Borges, A. & Perham, R. N. (1989) A Common Structural Motif in  
Thiamin Pyrophosphate-Binding Enzymes. *FEBS Lett.* **255**, 77-82.
- Hipps, D. S., Packman, L. C., Allen, M. D., Fuller, C., Sakaguchi, K., Appella, E. &  
Perham, R. N. (1994) The Peripheral Subunit-Binding Domain of the Dihydrolipoyl  
Acetyltransferase Component of the Pyruvate Dehydrogenase Complex of *Bacillus*

*Stearothermophilus*: Preparation and Characterization of Its Binding to the Dihydrolipoyl Dehydrogenase Component. *Biochem. J.* **297**, 137-143.

Hodgson, J. A., De Marcucci, O. G. & Lindsay, J. G. (1986) Lipoic Acid Is the Site of Substrate-Dependent Acetylation of Component X in Ox Heart Pyruvate Dehydrogenase Multienzyme Complex. *Eur. J. Biochem.* **158**, 595-600.

Hong, Y. S., Kerr, D. S., Liu, T. C., Lusk, M., Powell, B. R. & Patel, M. S. (1997) Deficiency of Dihydrolipoamide Dehydrogenase Due to Two Mutant Alleles (E340K and G101del). Analysis of a Family and Prenatal Testing. *Biochim. Biophys. Acta*, **1362**, 160-168.

Howard, M. J., Fuller, C., Broadhurst, R. W., Perham, R. N., Tang, J-G., Quinn, J., Diamond, A. G. & Yeaman, S. J. (1998) Three-dimensional structure of the major autoantigen in primary biliary cirrhosis. *Gastroenterology* **115**, 139-146.

Huang, B., Gudi, R., Wu, P., Harris, R. A., Hamilton, J. & Popov, K. M. (1998) Isoenzymes of Pyruvate Dehydrogenase Phosphatase. DNA-Derived Amino Acid Sequences, Expression, and Regulation. *J. Biol. Chem.* **273**, 17680-17688.

Ito, M., Kobashi, H., Naito, E., Saijo, T., Takeda, E., Huq, A. H. & Kuroda, Y. (1992) Decrease of Pyruvate Dehydrogenase Phosphatase Activity in Patients With Congenital Lactic Acidemia. *Clin. Chim. Acta*, **209**, 1-7.

Izard, T., Ævarsson, A., Allen, M. D., Westphal, A. H., Perham, R. N., de Kok, A. & Hol, W. G. (1999) Principles of Quasi-Equivalence and Euclidean Geometry Govern the

- Assembly of Cubic and Dodecahedral Cores of Pyruvate Dehydrogenase Complexes. *Proc. Natl. Acad. Sci. U. S. A.*, **96**, 1240-1245.
- Jentoft, J. E., Shoham, M., Hurst, D. & Patel, M. S. (1992) A Structural Model for Human Dihydrolipoamide Dehydrogenase. *Proteins*, **14**, 88-101.
- Jilka, J. M., Rahmatullah, M., Kazemi, M. & Roche, T. E. (1986) Properties of a Newly Characterised Protein of the Bovine Kidney Pyruvate Dehydrogenase Complex. *J. Biol. Chem.* **261**, 1858-1867.
- Jones, S. M. A. & Yeaman, S. J. (1986) Oxidative Decarboxylation of 4-Methylthio-2-Oxobutyrate by Branched-Chain 2-Oxoacid Dehydrogenase Complex. *Biochem. J.* **237**, 621-623.
- Joplin, R. & Gershwin, M.E. (1997) Ductular expression of autoantigens in primary biliary cirrhosis. *Semin. Liver Dis.* **17**, 97-103.
- Joplin, R. E., Wallace, L. L., Lindsay, J. G., Palmer, J. M., Yeaman, S. J. & Neuberger, J. M. (1997) The human biliary epithelial cell plasma membrane antigen in primary biliary cirrhosis: Pyruvate dehydrogenase X? *Gastroenterology* **113**, 1727-1733.
- Jordan, S. W. & Cronan, J. E. Jr. (1997) A New Metabolic Link. The Acyl Carrier Protein of Lipid Synthesis Donates Lipoic Acid to the Pyruvate Dehydrogenase Complex in *Escherichia Coli* and Mitochondria. *J. Biol. Chem.* **272**, 17903-17906.
- Kalia, Y. N., Brocklehurst, S. M., Hipps, D. S., Appella, E., Sakaguchi, K. & Perham, R. N. (1993) The High-Resolution Structure of the Peripheral Subunit-Binding Domain of

- Dihydrolipoamide Acetyltransferase From the Pyruvate Dehydrogenase Multienzyme Complex of *Bacillus Stearotherophilus*. *J. Mol. Biol.* **230**, 323-341.
- Kelly, S. M. & Price, N. C. (1997) The application of circular dichroism to studies of protein folding and unfolding. *Biochim.Biophys.Acta* **1338**, 161-185.
- Kelly, S. M. & Price, N. C. (2000) The use of circular dichroism in the investigation of protein structure and function. *Current Protein and peptide Science* **1**, 349-384.
- Khailova, L. S. & Korotchkina, L. G. (1982) Determination of the Number of Active Centres in the Pyruvate Dehydrogenase Component of the Pyruvate Dehydrogenase Complex From Pigeon Breast Muscle. *Biochem. Int.* **5**, 525-532.
- Kim, H., Liu, T-C. & Patel, M. S. (1991) Expression of cDNA Sequences Encoding Mature and Precursor Forms of Human Dihydrolipoamide Dehydrogenase in *Escherichia Coli*. *J. Biol. Chem.* **266**, 9367-9373.
- Kim, H. & Patel, M. S. (1992) Characterisation of Two Site-Specifically Mutated Human Dihydrolipoamide Dehydrogenases (His-452->Gln and Glu-457->Gln). *J. Biol. Chem.* **267**, 5128-5132.
- Klingbeil, M.M., Walker, D.J., Arnette, R., Sidawy, E., Hayton, K., Komuniecki, P.R. & Komuniecki, R. (1996) Identification of a novel dihydrolipoyl dehydrogenase-binding protein in the pyruvate dehydrogenase complex of the anaerobic parasitic nematode, *Ascaris suum*. *J. Biol. Chem.* **271**, 5451-5457.

- Korotchkina, L. G. & Patel, M. S. (1995) Mutagenesis Studies of the Phosphorylation Sites of Recombinant Human Pyruvate Dehydrogenase. Site-Specific Regulation. *J. Biol. Chem.* **270**, 14297-14304.
- Korotchkina, L. G., Tucker, M. M., Thekkumkara, T. J., Madhusudhan, K. T., Pons, G., Kim, H. & Patel, M. S. (1995) Overexpression and Characterization of Human Tetrameric Pyruvate Dehydrogenase and Its Individual Subunits. *Protein Expr. Purif.* **6**, 79-90.
- Korotchkina, L. G., Showkat, A. M. & Patel, M. S. (1999) Involvement of Alpha-Cysteine-62 and Beta-Tryptophan-135 in Human Pyruvate Dehydrogenase Catalysis. *Arch. Biochem. Biophys.* **369**, 277-287.
- Korotchkina, L. G. & Patel, M. S. (2001) Site-Specificity of Four Pyruvate Dehydrogenase Kinase Isoenzymes Towards the Three Phosphorylation Sites of Human Pyruvate Dehydrogenase. *J. Biol. Chem.* **276**, 37223-37229.
- Lawson, J. E., Behal, R. H. & Reed, L. J. (1991) Disruption and Mutagenesis of the *Saccharomyces Cerevisiae* PDX1 Gene Encoding the Protein X Component of the Pyruvate Dehydrogenase Complex. *Biochemistry*, **30**, 2834-2839.
- Lee, J., Ryou, C. & Kwon, M. (2001) Molecular Cloning and Expression of Human Dihydrolipoamide Dehydrogenase-Binding Protein in Escherichia Coli. *J. Microbiol. Biotechnol.*, **11**, 592-597.
- Leslie, A. G. W. (1990) Refined Crystal Structure of Type III Chloramphenicol Acetyltransferase at 1.75Å Resolution. *J. Mol. Biol.* **213**, 167-186.

- Lessard, I. A. & Perham, R. N. (1994) Expression in *Escherichia Coli* of Genes Encoding the E1 $\alpha$  and E1 $\beta$  Subunits of the Pyruvate Dehydrogenase Complex of *Bacillus Stearothermophilus* and Assembly of a Functional E1 Component ( $\alpha_2\beta_2$ ) *in Vitro*. *J. Biol. Chem.* **269**, 10378-10383.
- Lessard, I. A. & Perham, R. N. (1995) Interaction of Component Enzymes With the Peripheral Subunit-Binding Domain of the Pyruvate Dehydrogenase Multienzyme Complex of *Bacillus Stearothermophilus*: Stoichiometry and Specificity in Self-Assembly. *Biochem. J.* **306**, 727-733.
- Lessard, I. A., Fuller, C. & Perham, R. N. (1996) Competitive Interaction of Component Enzymes With the Peripheral Subunit-Binding Domain of the Pyruvate Dehydrogenase Multienzyme Complex of *Bacillus Stearothermophilus*: Kinetic Analysis Using Surface Plasmon Resonance Detection. *Biochemistry* **35**, 16863-16870.
- Li, L., Radke, G. A. & Roche, T. E. (1992) Additional Binding Sites for the Pyruvate Dehydrogenase Kinase but Not for Protein X in the Assembled Core of the Mammalian Pyruvate Dehydrogenase Complex: Binding Region for the Kinase. *Arch. Biochem. Biophys.* **296**, 497-504.
- Lilie, H., Schwarz, E. & Rudolph, R. (1998) Advances in refolding of proteins produced in *E. coli*. *Curr.Opin.Biotechnol.* **9**, 497-501.
- Ling, M., McEachern, G., Seyda, A., MacKay, N., Scherer, S. W., Bratinova, S., Beatty, B., Giovannucci-Uzielli, M. L. & Robinson, B. H. (1998) Detection of a Homozygous

- Four Base Pair Deletion in the Protein X Gene in a Case of Pyruvate Dehydrogenase Complex Deficiency. *Hum. Mol. Genet.* **7**, 501-505.
- Linn, T. C., Pettit, F. H. & Reed, L. J. (1969) Regulation of the Activity of the Pyruvate Dehydrogenase Complex From Beef Kidney Mitochondria by Phosphorylation and Dephosphorylation. *Proc. Natl. Acad. Sci. U. S. A.*, **62**, 234-241.
- Lissens, W., De Meirleir, L., Seneca, S., Liebaers, I., Brown, G. K., Brown, R. M., Ito, M., Naito, E., Kuroda, Y., Kerr, D. S., Wexler, I. D., Patel, M. S., Robinson, B. H. & Seyda, A. (2000) Mutations in the X-Linked Pyruvate Dehydrogenase (E1) Alpha Subunit Gene (PDHA1) in Patients With a Pyruvate Dehydrogenase Complex Deficiency. *Hum. Mutat.* **15**, 209-219.
- Liu, S., Baker, J. C., Andrews, P. C. & Roche, T. E. (1995) Recombinant Expression and Evaluation of the Lipoyl Domains of the Dihydrolipoyl Acetyltransferase Component of the Human Pyruvate Dehydrogenase Complex. *Arch. Biochem. Biophys.* **316**, 926-940.
- Liu, S., Baker, J. C. & Roche, T. E. (1995b) Binding of the Pyruvate Dehydrogenase Kinase to Recombinant Constructs Containing the Inner Lipoyl Domain of the Dihydrolipoyl Acetyltransferase Component. *J. Biol. Chem.* **270**, 793-800.
- Liu, T-C., Korotchkina, L.G., Hyatt, S.L., Vettakorumakankav, N.N. & Patel, M.S. (1995c) Spectroscopic studies of the characterisation of recombinant human dihydrolipoamide dehydrogenase and its site-directed mutants. *J. Biol. Chem.* **270**, 15545-15550.

- Liu, T. C., Hong, Y. S., Korotchkina, L. G., Vettakkorumakankav, N. N. & Patel, M. S. (1999) Site-Directed Mutagenesis of Human Dihydrolipoamide Dehydrogenase: Role of Lysine-54 and Glutamate-192 in Stabilizing the Thiolate-FAD Intermediate. *Protein Expression and Purification* **16**, 27-39.
- Maas, E. & Bisswanger, H. (1990) Localisation of the 2-Oxoacid Dehydrogenase Multienzyme Complexes Within the Mitochondrion. *FEBS Lett.* **277**, 189-190.
- Maeng, C. Y., Yazdi, M. A., Niu, X. D., Lee, H. Y. & Reed, L. J. (1994) Expression, Purification, and Characterization of the Dihydrolipoamide Dehydrogenase-Binding Protein of the Pyruvate Dehydrogenase Complex From *Saccharomyces Cerevisiae*. *Biochemistry* **33**, 13801-13807.
- Maeng, C. Y., Yazdi, M. A. & Reed, L. J. (1996) Stoichiometry of Binding of Mature and Truncated Forms of the Dihydrolipoamide Dehydrogenase-Binding Protein to the Dihydrolipoamide Acetyltransferase Core of Pyruvate Dehydrogenase Complex From *Saccharomyces Cerevisiae*. *Biochemistry* **35**, 5879-5882.
- Mande, S. S., Sarfaty, S., Allen, M. D., Perham, R. N. & Hol, W. G. (1996) Protein-Protein Interactions in the Pyruvate Dehydrogenase Multienzyme Complex: Dihydrolipoamide Dehydrogenase Complexed With the Binding Domain of Dihydrolipoamide Acetyltransferase. *Structure*. **4**, 277-286.
- Marsac, C., Stansbie, D., Bonne, G., Cousin, J., Jehenson, P., Benelli, C., Leroux, J.-P. & Lindsay, G. (1993) Defect in the Lipoyl-Bearing Protein X Subunit of the Pyruvate

- Dehydrogenase Complex in Two Patients With Encephalomyelopathy. *J. Pediatr.* **123**, 915-920.
- Mattevi, A., Schierbeek, A. J. & Hol, W. G. J. (1991) Refined Crystal Structure of Lipoamide Dehydrogenase From *Azotobacter Vinelandii* at 2.2Å Resolution. A Comparison With the Structure of Glutathione Reductase. *J. Mol. Biol.* **220**, 975-994.
- Mattevi, A., Obmolova, G., Schulze, E., Kalk, K. H., Westphal, A. H., de Kok, A. & Hol, W. G. J. (1992) Atomic structure of the cubic core of the pyruvate dehydrogenase multienzyme complex. *Science* **255**, 1544-1550
- Mattevi, A., Obmolova, G., Kalk, K. H., Westphal, A. H., de Kok, A. & Hol, W. G. J. (1993) Refined crystal structure of the catalytic domain of dihydrolipoyl transacetylase (E2p) from *Azotobacter vinelandii* at 2.6Å resolution. *J.Mol.Biol.* **230**, 1183-1199
- Mattevi, A., Obmolova, G., Kalk, K. H., Teplyakov, A. & Hol, W. G. (1993b) Crystallographic Analysis of Substrate Binding and Catalysis in Dihydrolipoyl Transacetylase (E2p). *Biochemistry* **32**, 3887-3901.
- Mayhew, M., da Silva, A. C. R., Martin, J., Erdjument-Bromage, H., Tempst, P. & Hartl, F. U. (1996) Protein folding in the central cavity of the GroEL-GroES chaperonin complex. *Nature* **379**, 420-426.
- McCartney, R. G., Sanderson, S. J. & Lindsay, J. G. (1997) Refolding and Reconstitution Studies on the Transacetylase-Protein X (E2/X) Subcomplex of the Mammalian Pyruvate

Dehydrogenase Complex: Evidence for Specific Binding of the Dihydrolipoamide

Dehydrogenase Component to Sites on Reassembled E2. *Biochemistry* **36**, 6819-6826.

McCartney, R.G. (1998) PhD thesis

L

De' a

Miles, J. S., Guest, J. R., Radford, S. E. & Perham, R. N. (1988) Investigation of the Mechanism of Active Site Coupling in the Pyruvate Dehydrogenase Multienzyme Complex of *Escherichia Coli* by Protein Engineering. *J. Mol. Biol.* **202**, 97-106.

Miller, J. R., Busby, R. W., Jordan, S. W., Cheek, J., Henshaw, T. F., Ashley, G. W., Broderick, J. B., Cronan, Jr. J. E. & Marletta, M. A. (2000) *Escherichia coli* LipA is a lipoyl synthase: In vitro biosynthesis of lipoylated pyruvate dehydrogenase complex from octanoyl-acyl carrier protein. *Biochemistry* **39**, 15166-15178.

Misawa, S. & Kumagai, I. (1999) Refolding of therapeutic proteins produced in *Escherichia coli* as inclusion bodies. *Biopolymers* **51**, 297-307.

Morris, T. W., Reed, K. E. & Cronan, J. E., Jr. (1994) Identification of the Gene Encoding Lipoate-Protein Ligase A of *Escherichia Coli*. *J. Biol. Chem.* **269**, 16091-19100.

Morris, T. W., Reed, K. E. & Cronan, J. E., Jr. (1995) Lipoic Acid Metabolism in *Escherichia Coli*: the LplA and LipB Genes Define Redundant Pathways for Ligation of Lipoyl Groups to Apoproteins. *J. Bacteriol.* **177**, 1-10.

Neupert, W. (1997) Protein Import into Mitochondria. *Annu. Rev. Biochem.* **66**, 863-917.

- Otulakowski, G. & Robinson, B. H. (1987) Isolation and sequence determination of cDNA clones for porcine and human lipoamide dehydrogenase. *J. Biol. Chem.* **262**, 17313-17318.
- Pai, E. F. & Schulz, G. E. (1983) The Catalytic Mechanism of Glutathione Reductase As Derived From X-Ray Diffraction Analyses of Reaction Intermediates. *J. Biol. Chem.* **258**, 1752-1757.
- Palmer, J. A., Madhusudhan, K. T., Hatter, K. & Sokatch, J. R. (1991) Cloning, sequence and transcriptional analysis of the structural gene for LPD-3, the third lipoamide dehydrogenase of *Pseudomonas putida*. *Eur. J. Biochem.* **202**, 231-240.
- Palmer, J. M., Jones, D. E., Quinn, J., McHugh, A. & Yeaman, S. J. (1999) Characterization of the Autoantibody Responses to Recombinant E3 Binding Protein (Protein X) of Pyruvate Dehydrogenase in Primary Biliary Cirrhosis. *Hepatology* **30**, 21-26.
- Patel, M. S., Naik, S., Wexler, I. D. & Kerr, D. S. (1995) Gene Regulation and Genetic Defects in the Pyruvate Dehydrogenase Complex. *J. Nutr.* **125**, 1753S-1757S.
- Patel, M. S. & Harris, R. A. (1995) Alpha-Keto Acid Dehydrogenase Complexes: Nutrient Control, Gene Regulation and Genetic Defects. Overview. *J. Nutr.* **125**, 1744S-1745S.
- Perham, R. N., Duckworth, H. W. & Roberts, G. C. K. (1981) Mobility of Polypeptide Chain in the Pyruvate Dehydrogenase Complex Revealed by Proton NMR. *Nature* **292**, 474-477.

- Perham, R. N. & Reche, P. A. (1998) Swinging Arms in Multifunctional Enzymes and the Specificity of Post- Translational Modification. *Biochem. Soc. Trans.* **26**, 299-303.
- Perham, R.N. (2000) Swinging arms and swinging domains in multifunctional enzymes: Catalytic machines for multistep reactions. *Annu. Rev. Biochem.* **69**, 961-1004.
- Pettit, F. H., Pelley, J. W. & Reed, L. J. (1975) Regulation of pyruvate dehydrogenase kinase and phosphatase by acetyl-CoA/CoA and NADH/NAD ratios. *Biochem. Biophys. Res. Commun.* **65**, 575-582.
- Pierce, M. M., Raman, C. S. & Nall, B. T. (1999) Isothermal titration calorimetry of protein-protein interactions. *Methods* **19**, 213-221.
- Pons, G., Raefsky-Estrin, C., Carothers, D.J., Pepin, R.A., Javed, A.A., Jesse, B.W., Ganapathi, M.K., Samols, D. & Patel, M.S. (1988) Cloning and cDNA sequence of the dihydrolipoamide dehydrogenase component of human  $\alpha$ -ketoacid dehydrogenase complexes. *Proc. Natl. Acad. Sci. USA.* **85**, 1422-1426.
- Potter, K. N., Thomson, R. K., Hamblin, A., Richards, S. D., Lindsay, J. G. & Stevenson, F. K. (2001) Immunogenetic Analysis Reveals That Epitope Shifting Occurs During B-Cell Affinity Maturation in Primary Biliary Cirrhosis. *J. Mol. Biol.* **306**, 37-46.
- Quinn, J., Diamond, A. G., Masters, A. K., Brookfield, D. E., Wallis, N. G. & Yeaman, S. J. (1993) Expression and Lipoylation in *Escherichia Coli* of the Inner Lipoyl Domain of the E2 Component of the Human Pyruvate Dehydrogenase Complex. *Biochem. J.* **289**, 81-85.

- Radford, S. E., Laue, E. D., Perham, R. N., Martin, S. R. & Appella, E. (1989) Conformational Flexibility and Folding of Synthetic Peptides Representing an Interdomain Segment of Polypeptide Chain in the Pyruvate Dehydrogenase Multienzyme Complex of *Escherichia Coli*. *J. Biol. Chem.* **264**, 767-775.
- Ravindran, S., Radke, G. A., Guest, J. R. & Roche, T. E. (1996) Lipoyl Domain-Based Mechanism for the Integrated Feedback Control of the Pyruvate Dehydrogenase Complex by Enhancement of Pyruvate Dehydrogenase Kinase Activity. *J. Biol. Chem.* **271**, 653-662.
- Reed, K. E. & Cronan, J. E., Jr.(1993) Lipoic Acid Metabolism in *Escherichia Coli*: Sequencing and Functional Characterisation of the LipA and LipB Genes. *J. Bacteriol.* **175**, 1325-1336.
- Reed, L. J. (1974) Multienzyme Complexes. *Acc. Chem. Res.* **7**, 40-46.
- Richards, S.D. (1999) PhD thesis
- Richarme, G. (1989) Purification of a new dihydrolipoamide dehydrogenase from *Escherichia coli*. *J. Bacteriol.* **171**, 6580-6585.
- Robinson, B. H., MacKay, N., Petrova-Benedict, R., Ozalp, I., Coskun, T. & Stacpoole, P. W. (1990) Defects in the E2 Lipoyl Transacetylase and the X-Lipoyl Containing Component of the Pyruvate Dehydrogenase Complex in Patients With Lactic Acidemia. *J. Clin. Invest.* **85**, 1821-1824.

Roche, T. E., Powers-Greenwood, S. L., Shi, W. F., Zhang, W. B., Ren, S. Z., Roche, E. D., Cox, D. J. & Sorensen, C. M. (1993) Sizing of Bovine Heart and Kidney Pyruvate Dehydrogenase Complex and Dihydrolipoyl Transacetylase Core by Quasielastic Light Scattering. *Biochemistry*, **32**, 5629-5637.

Rodger, A. & Ismail, M. A. (2000) Introduction to circular dichroism. Edited by Michael G. Gore. Spectrophotometry and Spectrofluorimetry. A Practical Approach. 99-139. Oxford University Press.

Rowles, J., Scherer, S. W., Xi, T., Majer, M., Nickle, D. C., Rommens, J. M., Popov, K. M., Harris, R. A., Riebow, N. L., Xia, J., Tsui, L. C., Bogardus, C. & Prochazka, M. (1996) Cloning and Characterization of PDK4 on 7q21.3 Encoding a Fourth Pyruvate Dehydrogenase Kinase Isoenzyme in Human. *J. Biol. Chem.* **271**, 22376-22382.

Russell, G. C. & Guest, J. R. (1991) Sequence Similarities Within the Family of Dihydrolipoamide Acyltransferases and Discovery of a Previously Unidentified Fungal Enzyme. *Biochim. Biophys. Acta*, **1076**, 225-232.

Saijo, T., Naito, E., Ito, M., Yokota, I., Matsuda, J. & Kuroda, Y. (1996) Stable Restoration of Pyruvate Dehydrogenase Complex in E1-Defective Human Lymphoblastoid Cells: Evidence That Three C-Terminal Amino Acids of E1 Alpha Are Essential for the Structural Integrity of Heterotetrameric E1. *Biochem. Biophys. Res. Commun.* **228**, 446-451.

- Sanderson, S. J., Khan, S. S., McCartney, R. G., Miller, C. & Lindsay, J. G. (1996a) Reconstitution of Mammalian Pyruvate Dehydrogenase and 2-Oxoglutarate Dehydrogenase Complexes: Analysis of Protein X Involvement and Interaction of Homologous and Heterologous Dihydrolipoamide Dehydrogenases. *Biochem. J.* **319**, 109-116.
- Sanderson, S. J., Miller, C. & Lindsay, J. G. (1996b) Stoichiometry, Organisation and Catalytic Function of Protein X of the Pyruvate Dehydrogenase Complex From Bovine Heart. *Eur. J. Biochem.* **236**, 68-77.
- Schatz, G. & Dobberstein, B. (1996) Common Principles of Protein Translocation Across Membranes. *Science*, **271**, 1519-1527.
- Schein, C. H. (1989) Production of Soluble Recombinant Proteins in Bacteria. *BioTechnology*, **7**, 1141-1149.
- Schierbeek, A. J., Swarte, M. B. A., Dijkstra, B. W., Vriend, G., Read, R. J., Hol, W. G. J., Drenth, J. & Betzel, C. (1989) X-Ray Structure of Lipoamide Dehydrogenase From *Azotobacter Vinelandii* Determined by a Combination of Molecular and Isomorphous Replacement Techniques. *J. Mol. Biol.*, **206**, 365-379.
- Schulze, R., Benen, J. A. E., Westphal, A. H. & de Kok, A. (1991) Interaction of Lipoamide Dehydrogenase With the Dihydrolipoyl Transacetylase Component of the Pyruvate Dehydrogenase Complex From *Azotobacter Vinelandii*. *Eur. J. Biochem.*, **200**, 29-34.

- Seyda, A. & Robinson, B. H. (2000) Expression and Functional Characterization of Human Protein X Variants in SV40-Immortalized Protein X-Deficient and E2-Deficient Human Skin Fibroblasts. *Arch. Biochem. Biophys.*, **382**, 219-223.
- Shany, E., Saada, A., Landau, D., Shaag, A., HersHKovitz, E. & Elpeleg, O. N. (1999) Lipoamide Dehydrogenase Deficiency Due to a Novel Mutation in the Interface Domain. *Biochem. Biophys. Res. Commun.* **262**, 163-166.
- Sheu, K. F., Cooper, A. J. L., Koike, K., Koike, M., Lindsay, J. G. & Blass, J. P. (1994) Abnormality of the  $\alpha$ -Ketoglutarate Dehydrogenase Complex in Fibroblasts From Familial Alzheimer's Disease. *Ann. Neurol.*, **35**, 312-318.
- Sheu, K. F. & Blass, J. P. (1999) The  $\alpha$ -Ketoglutarate Dehydrogenase Complex. *Ann. N. Y. Acad. Sci.* **893**, 61-78.
- Spector, S., Kuhlman, B., Fairman, R., Wong, E., Boice, J. A. & Raleigh, D. P. (1998) Cooperative Folding of a Protein Mini Domain: the Peripheral Subunit- Binding Domain of the Pyruvate Dehydrogenase Multienzyme Complex. *J. Mol. Biol.* **276**, 479-489.
- Sreerama, N. & Woody, R. W. (1993) A self-consistent method for the analysis of protein secondary structure from circular dichroism. *Anal. Biochem.* **209**, 32-44.
- Stanley, C. & Perham, R. N. (1980) Purification of 2-Oxo Acid Dehydrogenase Multienzyme Complexes From Ox Heart by a New Method. *Biochem. J.* **191**, 147-154.
- Stepp, L. R., Pettit, F. H., Yeaman, S. J. & Reed, L. J. (1983) Purification and Properties of Pyruvate Dehydrogenase Kinase From Bovine Kidney. *J. Biol. Chem.* **258**, 9454-9458.

- Stoops, J. K., Baker, T. S., Schroeter, J. P., Kolodziej, S. J., Niu, X. D. & Reed, L. J. (1992) Three-Dimensional Structure of the Truncated Core of the *Saccharomyces Cerevisiae* Pyruvate Dehydrogenase Complex Determined From Negative Stain and Cryoelectron Microscopy Images. *J. Biol. Chem.* **267**, 24769-24775.
- Stoops, J. K., Cheng, R. H., Yazdi, M. A., Maeng, C. Y., Schroeter, J. P., Klueppelberg, U., Kolodziej, S. J., Baker, T. S. & Reed, L. J. (1997) On the Unique Structural Organization of the *Saccharomyces Cerevisiae* Pyruvate Dehydrogenase Complex. *J. Biol. Chem.* **272**, 5757-5764.
- Surh, C.D., Roche, T.E., Danner, D.J., Ansari, A., Coppel, R.L., Prindiville, T., Dickson, E.R. & Gershwin, M.E. (1989) Antimitochondrial autoantibodies in primary biliary cirrhosis recognise cross-reactive epitope(s) on protein X and dihydrolipoamide acetyltransferase of pyruvate dehydrogenase complex. *Hepatology.* **10**, 127-133.
- Szabo, P., Sheu, K. F., Robinson, R. M., Grzeschik, K. H. & Blass, J. P. (1990) The Gene for the Alpha Polypeptide of Pyruvate Dehydrogenase Is X-Linked in Humans. *Am. J. Hum. Genet.* **46**, 874-878.
- Thieme, R., Pai, E. F., Schirmer, R. H. & Schulz, G. E. (1981) Three-dimensional structure of glutathione reductase as 2Å resolution. *J. Mol. Biol.* **152**, 763-782.
- Todd, M.J., Viitanen, P.V. & Lorimer, G.H. (1994) Dynamics of the chaperonin ATPase cycle: Implications for facilitated protein folding. *Science.* **265**, 659-666.

- Toyoda, T., Kobayashi, R., Sekiguchi, T., Koike, K., Koike, M. & Takenaka, A. (1998b) Crystallization and Preliminary X-Ray Analysis of Pig E3, Lipoamide Dehydrogenase. *Acta Crystallogr. D. Biol. Crystallogr.* **54**, 982-985.
- Toyoda, T., Suzuki, K., Sekiguchi, T., Reed, L. J. & Takenaka, A. (1998) Crystal Structure of Eucaryotic E3, Lipoamide Dehydrogenase From Yeast. *J. Biochem.* **123**, 668-674.
- Tsunoda, J. N. & Yasunobu, K. T. (1967) Mammalian Lipoic Acid Activating Enzyme. *Arch. Biochem. Biophys.* **118**, 395-401.
- Van de Water, J., Fregeau, D. D. P., Ansari, A., Danner, D., Leung, P., Coppel, R. & Gershwin, M. E. (1988) Autoantibodies of primary biliary cirrhosis recognise dihydrolipoamide acetyltransferase and inhibit enzyme function. *J. Immunol.* **141**, 2321-2324.
- Wagenknecht, T., Grassucci, R., Radke, G. A. & Roche, T. E. (1991) Cryoelectron Microscopy of Mammalian Pyruvate Dehydrogenase Complex. *J. Biol. Chem.*, **266**, 24650-24656.
- Wallis, N. G. & Perham, R. N. (1994) Structural Dependence of Post-Translational Modification and Reductive Acetylation of the Lipoyl Domain of the Pyruvate Dehydrogenase Multienzyme Complex. *J. Mol. Biol.*, **236**, 209-216.
- Wallis, N. G., Allen, M. D., Broadhurst, R. W., Lessard, I. A. & Perham, R. N. (1996) Recognition of a Surface Loop of the Lipoyl Domain Underlies Substrate Channelling in the Pyruvate Dehydrogenase Multienzyme Complex. *J. Mol. Biol.*, **263**, 463-474.

- West, S. M., Rice, J. E., Beaumont, E. S., Kelly, S. M., Price, N. C. & Lindsay, J. G. (1995) Dissociation and Unfolding of the Pyruvate Dehydrogenase Complex by Guanidinium Chloride. *Biochem. J.* **308**, 1025-1029.
- Wu, T. & Reed, L. J. (1984) Subunit binding in the pyruvate dehydrogenase complex from bovine kidney and heart. *Biochemistry* **23**, 221-226.
- Wynn, R. M., Davies, J. R., Cox, R. P. & Chuang, D. T. (1992) Chaperonins GroEL and GroES promote assembly of heterotetramers ( $\alpha_2\beta_2$ ) of mammalian mitochondrial branched-chain  $\alpha$ -ketoacid decarboxylase in *Escherichia coli*. *J. Biol. Chem.* **267**, 12400-12403.
- Xu, Z., Horwich, A. L. & Sigler, P. B. (1997) The crystal structure of the asymmetric GroEL-GroES-(ADP) sub 7 chaperonin complex. *Nature* **388**, 741-750.
- Yang, D., Song, J., Wagenknecht, T. & Roche, T. E. (1997) Assembly and Full Functionality of Recombinantly Expressed Dihydrolipoyl Acetyltransferase Component of the Human Pyruvate Dehydrogenase Complex. *J. Biol. Chem.* **272**, 6361-6369.
- Yeaman, S. J., Hutcheson, E. T., Roche, T. E., Pettit, F. H., Brown, J. R., Reed, L. J., Watson, D. C. & Dixon, G. H. (1978) Sites of Phosphorylation on Pyruvate Dehydrogenase From Bovine Kidney and Heart. *Biochemistry* **17**, 2364-2370.
- Yeaman, S. J., Fussey, S. P., Danner, D. J., James, O. F., Mutimer, D. J. & Bassendine, M. F. (1988) Primary Biliary Cirrhosis: Identification of Two Major M2 Mitochondrial Autoantigens. *Lancet*, **1**, 1067-1070.

Yi, J.; Nemeria, N.; McNally, A.; Jordan, F.; Machado, R. S.; Guest, J. R. (1996) Effect of Substitutions in the Thiamin Diphosphate-Magnesium Fold on the Activation of the Pyruvate Dehydrogenase Complex From *Escherichia Coli* by Cofactors and Substrate. *J. Biol. Chem.*, **271**, 33192-33200.

Zhou, Z. H., Liao, W., Cheng, R. H., Lawson, J. E., McCarthy, D. B., Reed, L. J. & Stoops, J. K. (2001) Direct Evidence for the Size and Conformational Variability of the Pyruvate Dehydrogenase Complex Revealed by Three-Dimensional Electron Microscopy. The "Breathing" Core and Its Functional Relationship to Protein Dynamics. *J. Biol. Chem.*, **276**, 21704-21713.

Zhou, Z.H., McCarthy, D.B., O'Connor, C.M., Reed, L.J. & Stoops, J.K. (2001b) The remarkable structural and functional organization of the eukaryotic pyruvate dehydrogenase complexes. *Proc. Natl. Acad. Sci. USA*. **98**, 14802-14807.

